POLYMERIC NANOMATERIALS

By

ROBERT LEE SHERMAN JR.

Bachelor of Science
Southern Illinois University
Carbondale, IL
1997

Master of Science
Southern Illinois University
Carbondale, IL
2000

Submitted to the Faculty of the
Graduate College of the
Oklahoma State University
in partial fulfillment of
the requirements for
the Degree of
DOCTOR OF PHILOSOPHY
December, 2004

POLYMERIC NANOMATERIALS

Thesis Approved:

Dr. Warren T. Ford

_____

Thesis Advisor

Dr. Richard A. Bunce

_____

Dr. K. Darrell Berlin

_____

Dr. Legrande M. Slaughter

_____

Dr. Martin S. High

_____

Dr. Gordon Emslie

_____

Dean of the Graduate College

PREFACE

Nanomaterials have dimensions best described in nanometers (one-billionth of a meter). These materials have many interesting properties that vary from that of bulk materials due to their small uniform size. Polymers, large molecules composed of many smaller molecules, have been used to stabilize or compose these nanometer-sized materials.

Some semiconductor nanoparticles, which have diameters less than 10 nm, emit light. They have been made by many different methods throughout the literature. However to stabilize the surface of these nanometer-sized particles, the surface must be stabilized with organic molecules. To increase the efficiency of these surface covering molecules, a polymer of the natural amino acid cysteine, poly(cysteine acrylamide) has been formed. This new coating allows semiconductor nanoparticles to be dispersed in water at a wide range of pHs and in a highly pure form. This new polymeric ligand increases the overall utility of nanoparticles in water.

Nanoparticle/latex composites combine the light emission of nanoparticles with the size and stability of latexes. These organic/inorganic composites are between 80 and 300 nm in diameter. We have synthesized these composites in three different ways. From each synthesis method, nanoparticle/latex composites performed well and had properties specific to each synthetic method. These materials have been shown to be excellent optical tracking materials for fluorescence microscopy.

Core/shell polystyrene/poly(methyl methacrylate) latexes were made using 70 nm polystyrene cores and 530 nm thick poly(methyl methacrylate) shells. This difference in diameter (1:7.5) amounts to a 1:420 difference in volume. Since poly(methyl methacrylate) has a lower refractive index than polystyrene, light scattering experiments can be devised to scatter light only off the cores. Under these conditions highly concentrated core/shell particle solutions will appear to be 420 times more dilute than they actually are.

Dendrimers are a class of highly branched polymers with hollow spherical shape. Chemical reactions with the nitrogen atoms on the dendrimer results in positively charged quaternary ammonium dendrimers. When long oil-like chains were used to quaternized small dendrimers, excellent unimolecular phase-transfer catalysts were formed. These catalysts were used for simple decarboxylation reactions and were most active when 8 dodecyl chains were used for the reaction; this produced the best results for decarboxylation by a dendrimer in the current literature. These materials were also found to be soap-like with low aggregation concentrations, and they formed foamy aqueous solutions when agitated.

ACKNOWLEDGEMENTS

I would like to thank Dr. Warren Ford for being an outstanding advisor. His guidance, patience and work ethic along with the structure of his research group have allowed me to obtain a good overall education. I would also like to thank Dr. Ford for allowing me to be a research assistant through most of my stay and for allowing me to be independent and solve my own research related problems.

I would also like to thank my research committee: Dr. Richard Bunce, Dr. Darrell Berlin, Dr. Martin High, Dr. LeGrande Slaughter and Dr. Nicholas Kotov, for their patience, time and assistance with my thesis and research proposal. I also thank the following people for instrumental and research assistance: Dr. Margaret Eastman, Phoebe Doss, Terry Colberg, Dr. Penger Tong, Dr. Bret Flanders, Birol Ozturk, Dr. Dale Teeters and Dr. Nicholas Kotov's group.

I must thank the Ford Group for the conversations, food and memories. I must specifically thank: Dr. Yiyan Chen, Dr. Susheng Tan, Dr. Jason Kreider, Dr. Egambaram Murugan, Dr. Zushen Xu, Drs. Dongqi and Shuhui Qin and Young Hie Kim for research assistance during my stay.

I would also like to thank my wife Crystal for her support and patience through all my college experience. Without her I would have never gotten this far. I would also like to thank my parents for instilling in me a good work ethic and appreciation of education.

I would also like to thank the National Science foundation and Oklahoma EPSCor for financial assistance.

TABLE OF CONTENTS

LIST OF FIGURES

Chapter II

Chapter III

Chapter IV

Chapter V

Figure .....Page

LIST OF SCHEMES

Chapter II

Chapter III

Chapter IV

Chapter V

LIST OF TABLES

Chapter II

Chapter III

Chapter IV

Chapter V

Chapter I

POLYMERS AND THEIR INFLUENCE ON NANOSTRUCTURED MATERIALS

Introduction

Nanostructured materials are submicron sized materials whose dimensions are often described using nanometers instead of micrometers or angstroms. Nanomaterials typically range from 1-100's of nanometers depending on the individual nanomaterial's composition, which ultimately dictates the particle's size.[1-7] These materials are of great interest to chemists, physicists and engineers because of their potential applications and their interesting chemical and physical properties.[1-7] These properties are often influenced by the extremely high surface area to volume ratio that occurs at such low dimensions. The nanometer size can lead to phenomena such as quantum confinement, which leads to new properties for pure substances, and extremely reactive materials due to the high number of exposed atoms on the surface of the materials.[2-6] Since the size of nanomaterials can result in different physical and chemical properties, relative to bulk materials, these materials are often studied because they bridge the gap between the quantum chemistry of atoms, and bulk chemistry and engineering.

Certain naturally occurring materials may be classified as nanomaterials. Complex materials such as red blood cells, ribosomes, DNA and viruses are all

nanostructures. Synthetic nanomaterials include materials such as Fullerenes,[8] carbon nanotubes,[9,10] nanoparticles, surfactant micelles,[11,12] dendrimers,[1] latexes[7] and zeolites.[13]

Artificial nanomaterials are of interest to science because of their small size, high surface area, quantum confinement, and other physical and chemical properties.[1-6] Some physical and chemical properties for materials which are commonly thought to be inherent properties to that material regardless of size, are in fact size dependent at the nanoscale. For example gold nanoparticles are not gold in color. Their color is dependent upon the size of the individual particles. Since these materials have new properties, they have potential uses as new materials such as catalysts,[4] nano-computers,[14,15] nano-machines,[16] fluorescent materials,[3] mechanical reinforcing materials,[9] photonic materials and drug delivery materials.[17-19]

Polymers are important in nanomaterial chemistry. Polymers have been used as nanomaterials such as polymer brushes,[20] triblock copolymer tarsus[21] and diblock copolymer films.[22] Polymers have also been also been used as oppositely charged layers in layer-by-layer deposition.[23] They have been used to disperse and stabilize insoluble nanomaterials.[10] Polymers are important because of their unlimited functionality, wide range of solubilities and synthetic reactions that can occur with them or their respective monomers, when the appropriate chemistry is applied.[24] Properties that make polymers important for nanochemistry include their size, shape, melting point, glass-transition temperature, morphology, crystallinity, functionality, availability and cost.[24] The important physical and chemical properties of polymers and monomers that have proven valuable in the development of nanomaterials include use as stabilizers,[10] layer-by-layer architectures,[23] ligands and surface coatings. Other important polymeric materials that

have played important roles in nanomaterials include latexes, dendrimers and block and random copolymers.

The research that will be discussed in this thesis used polymers on the nanoscale. The use of quaternary ammonium dendrimers as unimolecular phase transfer catalysts has been partially published in another form.[25] The synthesis of polydentate ligands as nanoparticle stabilizers from ligand monomers has been published in another form.[26] The use of latexes with diameters of 100-300 nm as supports for fluorescent nanoparticles has been partially published in a different form.[27] High volume, low apparent volume, latexes have been synthesized as tracer materials for light scattering experiments.

References

(1) Newkome, G. R.; Moorefield, C. N.; Vogtle, F. *Dendrimers, 2nd Edition*, 2001.

(2) Rossetti, R.; Brus, L. *J. Phys. Chem.* **1982**, *86*, 4470-4472.

(3) Brus, L. *Appl. Phys. A* **1991**, *A53*, 465-474.

(4) Roucoux, A.; Schulz, J.; Patin, H. *Chem. Rev.* **2002**, *102*, 3757-3778.

(5) Kodama, R. H. *J. Magn. Magn. Mater.* **1999**, *200*, 359-372.

(6) Klabunde, K. J.; Editor *Nanoscale Materials in Chemistry*, 2001.

(7) Lovell, P., A.; Al-Aasser, M., S. *Emulsion Polymerization and Emulsion Polymers*; Wiley: Chichester, 1997.

(8) Kraetschmer, W.; Lamb, L. D.; Fostiropoulos, K.; Huffman, D. R. *Nature* **1990**, *347*, 354-358.

(9) Baughman, R. H.; Zakhidov, A. A.; de Heer, W. A. *Science* **2002**, *297*, 787-792.

(10) Qin, S.; Qin, D.; Ford, W. T.; Herrera, J. E.; Resasco, D. E.; Bachilo, S. M.; Weisman, R. B. *Macromolecules* **2004**, *37*, 3965-3967.

(11) Zana, R. *Adv. Colloid Interface Sci.* **2002**, *97*, 205-253.

(12) Gradzielski, M. *Current Opinion in Colloid & Interface Science* **2003**, *8*, 337-345.

(13) Stein, A. *Adv. Mater.* **2003**, *15*, 763-775.

(14) Tseng, G. Y.; Ellenbogen, J. C. *Science* **2001**, *294*, 1293-1294.

(15) Tour, J. M. *Abstracts of Papers, 223rd ACS National Meeting, Orlando, FL, United States, April 7-11, 2002* **2002**, PHYS-151.

(16) Shirai, Y.; Zhao, Y.; Osgood, A. J.; Chiu, Y.-H.; Yao, Y.; Yang, H.; Saudan, L.; Kelly, K. F.; Tour, J. M. *Abstracts of Papers, 228th ACS National Meeting, Philadelphia, PA, United States, August 22-26, 2004* **2004**, ORGN-174.

(17) Baker, J. R., Jr.; Quintana, A.; Piehler, L.; Banazak-Holl, M.; Tomalia, D.; Raczka, E. *Biomedical Microdevices* **2001**, *3*, 61-69.

(18) Esfand, R.; Tomalia, D. A. *Drug Discovery Today* **2001**, *6*, 427-436.

(19) Liu, M.; Kono, K.; Frechet, J. M. J. *Journal of Controlled Release* **2000**, *65*, 121-131.

(20) Milner, S. T. *Science* **1991**, *251*, 905-914.

(21) Pochan, D. J.; Chen, Z.; Cui, H.; Hales, K.; Qi, K.; Wooley, K. L. *Science* **2004**, *306*, 94-97.

(22) Xu, T.; Hawker, C. J.; Russell, T. P. *Macromolecules* **2003**, *36*, 6178-6182.

(23) Fendler, J. H. *Chemistry of Materials* **1996**, *8*, 1616-1624.

(24) Rudin, A. *The Elements of Polymer Science and Engineering*; Second ed.; Academic Press: San Diego, 1999.

(25) Murugan, E.; Sherman, R. L., Jr.; Spivey, H. O.; Ford, W. T. *Langmuir* **2004**, *20*, 8307-8312.

(26) Sherman, R. L., Jr.; Chen, Y.; Ford, W. T. *J. Nanosci. Nanotech.* **2004**, 4, 1032-1038.

(27) Sherman, R. L., Jr.; Ford, W. T. *Polymer Preprints (American Chemical Society, Division of Polymer Chemistry)* **2003**, *44*, 1136-1137.

CHAPTER II

STABILIZATION OF CADMIUM SULFIDE AND CADMIUM SELENIDE/CADMIUM SULFIDE CORE/SHELL NANOPARTICLES WITH POLY(CYSTEINE ACRYLAMIDE)

Abstract

The water-soluble polymerizable thiol ligand, cysteine acrylamide (*N*-acroloyl L-cysteine), can be used for synthesis of nanoparticles or for the replacement of weaker ligands on previously synthesized nanoparticles. Use of polymeric ligands on the surface allows for surface stabilization without excess ligand in solution. Stable tunable CdS nanoparticles have been formed in the presence of cysteine acrylamide. Citrate ligand has also been displaced by cysteine acrylamide on CdSe and CdSe/CdS core/shell nanoparticles. Once cysteine acrylamide is on the surface of the nanoparticles the acrylamide double bond can be polymerized with heat to form a polydentate ligand. The polymer-coated nanoparticle dispersions are colloidally stable even after removal of low molecular weight solutes by dialysis. Emission quantum yields (φ) of the polymer-coated CdSe and CdSe/CdS samples were 0.9% and 2.6% respectively after aging the samples in light. CdSe/CdS coated with poly(cysteine acrylamide) is colloidally stable for at least 2 years in the dark at 5 ^{o}C.

Introduction

Nanoparticles or quantum dots have been studied for the last 20 years.[1,2] Because of their small size, their optical,[3] magnetic[4] and catalytic properties[5] vary greatly from their respective bulk materials. These variations are due to quantum confinement of electrons and the high number of exposed surface atoms.[1,3,5-7] These new properties make nanoparticles some of the most promising nanomaterials being studied as catalysts and fluorescent materials.[3,7-9]

Nanoparticles typically are composed of semiconducting materials,[3,10,11] metals,[5,12] metal oxides,[13] organic polymers[14-16] or magnetic materials.[4] Synthesis of nanoparticles has been carried out using many methods including: chemical reactions inside polymers,[17,18] xerogels,[19] and reverse micelles,[20] and from gas phase reactants by molecular beam epitaxy,[3] single-molecule decomposition,[21] and chemical vapor (gas phase) deposition.[22] Once formed the nanoparticles must be stabilized to prevent aggregation and formation of bulk material. Typically ligands including amines, thiols, carboxylic acids, and phosphine oxides are used to passivate the surface of the materials and to allow the nanoparticles to be dispersed into a solvent.[23]

The passivation of the surface is usually done with monomeric ligands or low molecular weight polymers. Very little research has been done on polymerization from the surface to form stabilizers. Typically the polymer shells that have been formed on the surface of nanoparticles greatly exceed the thickness of monomeric ligands and can affect colloidal stability and physical properties of the particles.

Other methods of stabilization include core/shell materials, in which a second layer of material such as ZnS,[24,25] CdS[26,27] or SiO_2[28-30] is applied to isolate the core from the surrounding environment. This often is accompanied by an enhancement of the physical properties of the core nanoparticle due to environmental isolation.[24-27,31-33] However, these materials typically still need ligands to stabilize the surface and allow for dispersion into solvent.

Nanoparticles have been used recently for many different purposes.[34-37] Catalysts composed of Pt, Pd and other metals have shown promising catalytic properties.[5] Since some semiconductor nanoparticles have high quantum yields, emission tunability, and resistance to photobleaching,[9,10,33,38-41] nanoparticles can be used in place of fluorescent organic tags, which bleach rapidly.[36,42-45] Attachment of antigens to the surface of nanoparticles has allowed for various biological binding and screening methods.[36,46-49] Composite materials composed of latex polymers coated with luminescent nanoparticles have been shown to be micron sized luminescent materials with optical properties of the nanoparticles.[15,41,50-53]

Despite the great potential, nanoparticles have many limitations. Most synthetic conditions to form nanoparticles include extremely toxic chemicals,[32,41] pyrophoric materials,[32] high temperatures,[32] and the need for ligand exchange to transform organic-soluble nanoparticles to water-soluble nanoparticles.[12,32,42,54] Many of these methods are not practical for industrial synthesis. It is also of note that the ligands that solubilize and passivate the surface of nanoparticles are often weakly bound monodentate ligands. Purification of most nanoparticles via dialysis or other purification techniques removes excess stabilizer in the solution and disrupts the equilibrium between attached and

dissolved ligand as shown in Scheme 1. This change in equilibrium results in aggregation and precipitation of the nanoparticles. This lack of stability renders most nanoparticles useless for biological applications where small doses of nanoparticles are diluted by the natural fluids of a living organism.

Scheme 1. Dialysis of Nanoparticles

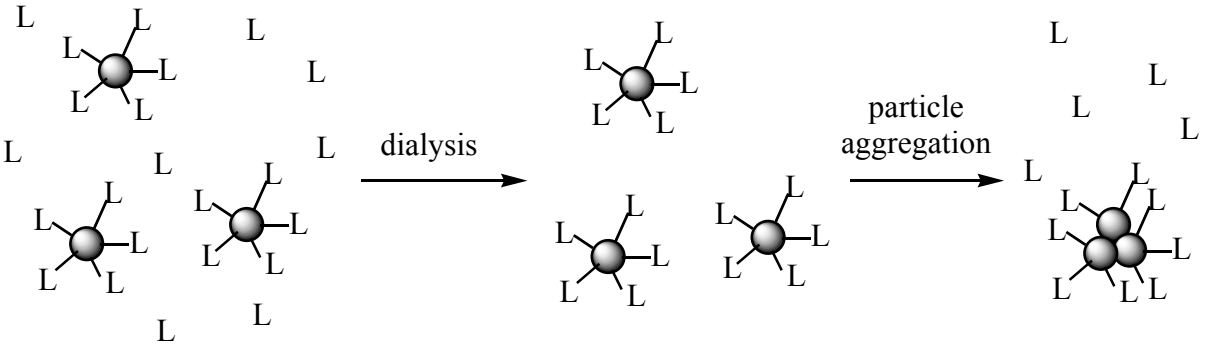

L= ligand

One natural ligand that has been used to stabilize water-soluble nanoparticles is the amino acid L-cysteine[55-57] (**1**). Cysteine has also been used as part of copolypeptides for binding to nanoparticles.[58-60] These methods take advantage of cysteine's water solubility combined with a thiol functionality for ligating. Monomeric L-cysteine as a ligand has a major drawback in that its isoelectric point in water is 5.07.[61] Uncharged nanoparticles aggregate and precipitate from water.[56] For this reason the pH must be kept basic for colloidal stability.

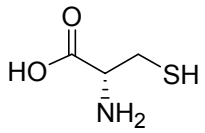

1

In this research L-cysteine's amine functionality is converted to a thermally polymerizable acrylamide group. The amide prevents formation of an uncharged zwitterion, and allows for polymerization to form a polydentate ligand without the need for peptide synthesis. Once polymerized on the surface of the nanoparticle, the polydentate thiol attachment prevents equilibration of the ligand between the adsorbed state and the solution. Since no free ligand is necessary for stabilization, the nanoparticles exist in a free state devoid of any equilibrating ligand in solution.

Results and Discussion

L-Cysteine Acrylamide (5). Cysteine acrylamide was an ideal choice for a polymerizable stabilizer for several reasons. It is water soluble. The methyl ester of cystine, the disulfide of cysteine, is commercially available, making it a well protected starting reagent, which is easily converted to cysteine acrylamide. Acrylamide groups readily polymerize. The thiol group of cysteine is a strong ligand for cadmium and will stabilize the surface of CdS and CdSe nanoparticles. The carboxylate group, which allows for water solubility, can allow further chemical or electrostatic functionalization of the nanoparticle surface.[9,49,62] L-cysteine is a naturally occurring amino acid and is biologically compatible.

Our group has developed the water-soluble polymerizable thiol ligand, cysteine acrylamide, **5**. This ligand can be used for synthesis of nanoparticles or for the replacement of weak ligands on previously synthesized nanoparticles. Using a polymerizable ligand allows for the synthesis of a polydentate thiol ligand so that no additional ligand is needed in solution. Cysteine acrylamide, N-acryloyl L-cysteine, was synthesized by amidation of L-cystine dimethyl ester followed by reduction of the disulfide bond and deprotection of the carboxylate group by ester hydrolysis as shown in Scheme 2.

Scheme 2. Cysteine Acrylamide Synthesis

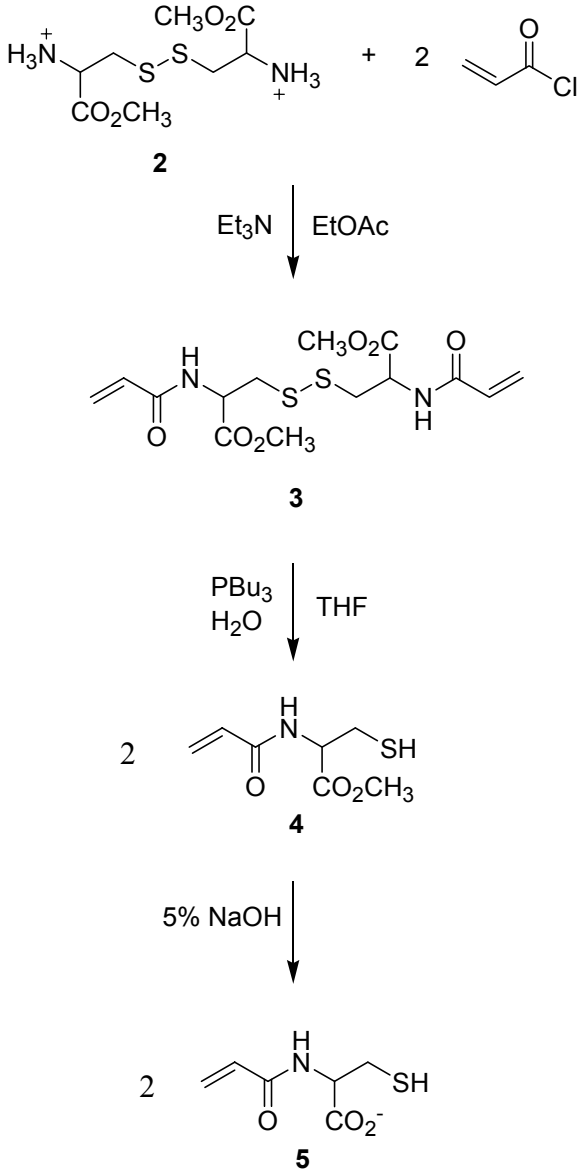

Compound **3**, cystine dimethyl ester diacrylamide, can be stored as a dry white powder for up to a year. When nanoparticle synthesis or ligand exchange is needed, compound **5** can be synthesized from **3** in less than 24 hours and stored for up to a week before use.

Once attached to nanoparticles, **5** can be polymerized to form a polydentate thiol ligand. Analysis by ^{1}H NMR has shown that after heating for 6 hours at 70 ^{o}C no double bonds were present, but a broad polymer peak appeared at 0.5-4.5 ppm. Polymerization was further demonstrated by the high stability of the heat treated nanoparticles after dialysis. Dialysis for greater than 4 days, with more than 20 water changes, which typically destroys weakly ligated nanoparticles and nanoparticles stabilized with non-heat treated **5**, did not harm colloidal stability or the absorption and emission spectra. Dialysis shown in Scheme 3, removed some of the excess ligand and salts as seen by the conductivity measurements in Table 1. As expected samples stabilized with **5** had lower conductivities than citrate stabilized samples due to reduced dissociation of **5** from the stabilized nanoparticle surface. It was also seen that polymerized **5** had lower conductivities than non-polymerized **5** due to the lesser degree of dissociation of polymer than of monomer.

Scheme 3. Nanoparticle Heat Treatment

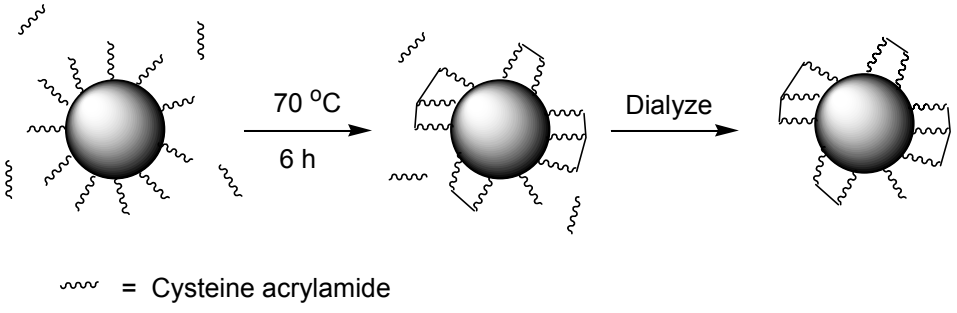

Table 1. Conductivities of CdSe and CdSe/CdS Core/Shell Nanoparticle Dispersions

sample	conductivity (μmhos)
CdSe Citrate[a]	2000
CdSe **5**[b]	650
CdSe **5** Poly[b]	570
CdSe/CdS Citrate[a]	2300
CdSe/CdS **5**[b]	620
CdSe/CdS **5** Poly[b]	550

[a] Dialyzed for 8 hours and diluted by one half. [b] Dialyzed for 8 hours and then 24 hours.

The degree of polymerization that occurred on the surface of the nanoparticles probably was low, but analysis to determine the actual molecular weight and polydispersity of the polymer was not attempted. Molecular weight analysis would require removing poly-**5** from the nanoparticles and then capping the thiol groups to avoid formation of disulfide bonds between polymer chains, which would result in erroneous results.

One further feature of the cysteine acrylamide stabilizer is the carboxylate solubilizing group. The carboxylate group is a reactive functionality that can be used for chemistry. Attachment of groups such as antibodies, fluorescent dyes or other useful groups through an ester or amide linkage may provide utility to these materials. This

would be very useful for dilute long term in vitro/in vivo studies at neutral pH where previous nanoparticles could not perform for long periods of time.

Cadmium Sulfide Nanoparticle Synthesis. Cadmium sulfide nanoparticles were synthesized in the presence of cysteine acrylamide with no other ligands present as shown in Scheme 4.

Scheme 4. Cadmium Sulfide Nanoparticle Synthesis

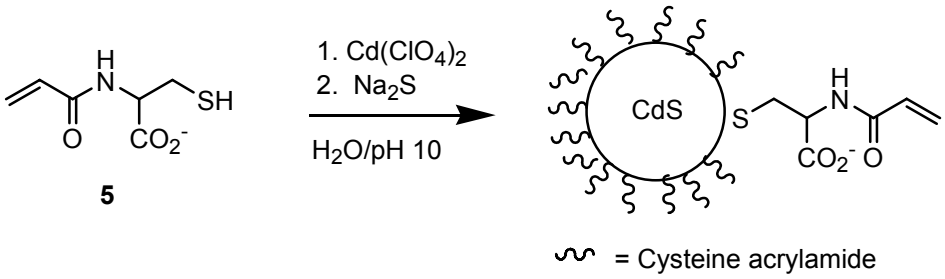

Synthesis begins with deprotonation of the ligand, **5**, followed by coordination to Cd^{2+}. Full coordination of **5** to Cd^{2+} was assumed since the strong odor of **5** immediately went away upon addition of Cd^{2+}, even at a pH as low as 5. After rapid addition of Na_2S, nanoparticle synthesis was complete and a yellow odorless solution was formed. Synthesis of the CdS nanoparticles was quick and reproducible. The particles that were formed were crystalline, and the particles were relatively monodisperse as seen in Figures 1 and 2. Typical absorption and emission spectra are in Figure 1.

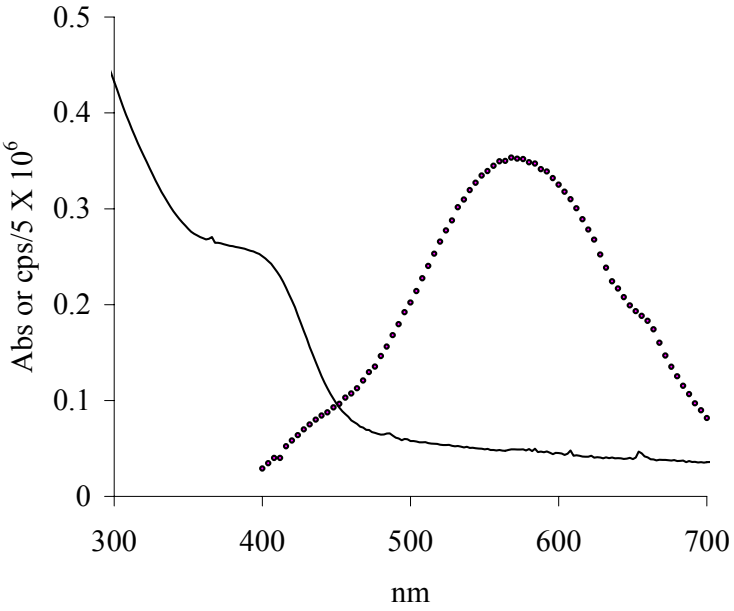

Figure 1. Absorption and emission spectra of CdS nanoparticles stabilized by cysteine acrylamide, (λ_{ex} = 340 nm).

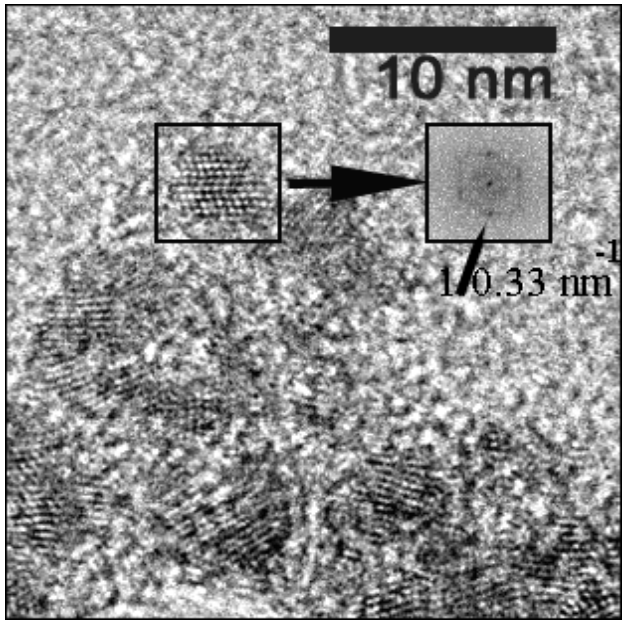

Figure 2. High resolution TEM of cubic CdS nanoparticles prepared as reported in the Experimental Section.

Cadmium sulfide nanoparticles synthesized by this method were stable. Samples that were heated and then dialyzed have been stored, in the dark under nitrogen, for up to two years. These old nanoparticles show similar absorption and emission spectra to their newer counterparts.

The size of the nanoparticles as well as the composition determines the absorption and emission properties of the material. Cadmium sulfide nanoparticles can be synthesized to various sizes. Examples of the tunability of nanoparticles can be seen in Figure 3 and Table 2. The nanoparticles shown in Figure 3 vary only in the ratio of the starting materials. CdS nanoparticles were synthesized with absorption maxima varying

over 380-480 nm. The nanoparticles in Figure 3 have absorption band edges varying over 420-480 nm, corresponding to diameters of 5 to 6.6 nanometers.[63,64]

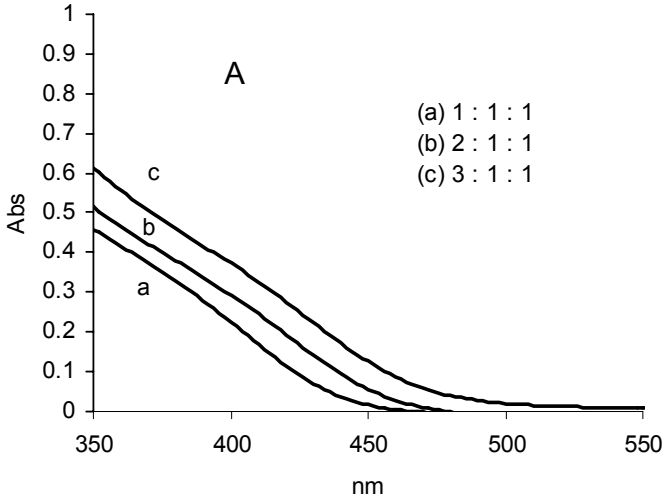

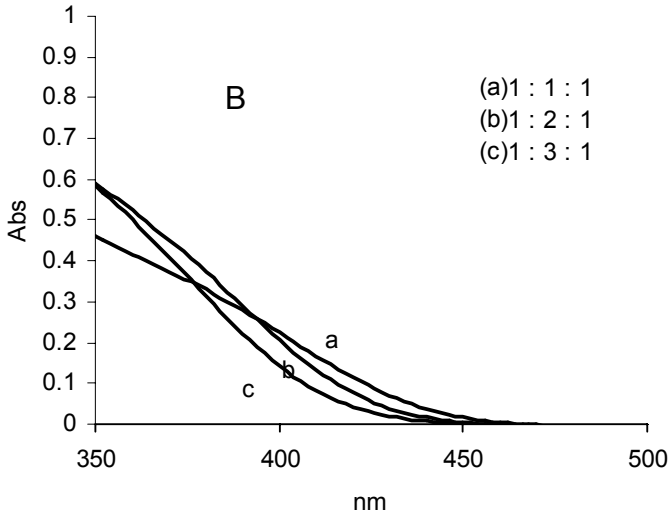

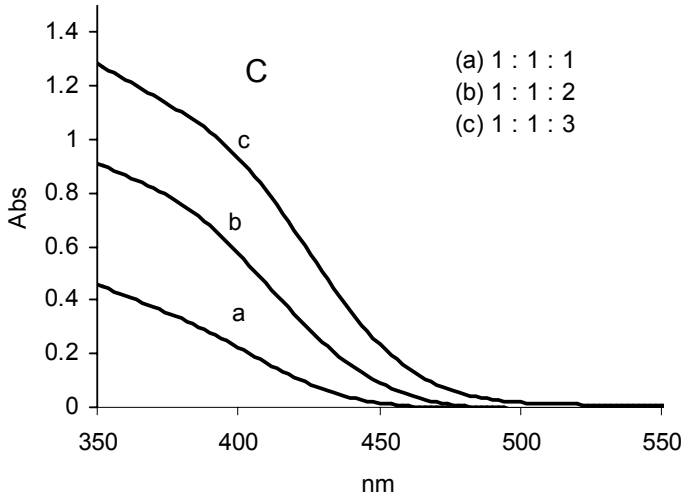

Figure 3. Absorption spectra of CdS nanoparticles synthesized from varied relative molar amounts of $Cd(ClO_4)_2$:**5**:Na_2S. (A) Varied $Cd(ClO_4)_2$ at constant 1:1 **5**:Na_2S. (B) Varied **5** at constant 1:1 $Cd(ClO_4)_2$:Na_2S. (C) Varied Na_2S at constant 1:1 $Cd(ClO_4)_2$:**5** (Note change in Y-axis). The concentration of the equimolar components in all experiments was 1.3 mM.

Table 2. Particle Sizes of CdS Nanoparticles

sample Cd:**5**:S	absorption edge[a] (nm)	radius[b] (nm)
1:1:1	440	2.7
2:1:1	457	2.9
3:1:1	475	3.3
1:2:1	430	2.6
1:3:1	422	2.5
1:1:2	452	2.8
1:1:3	465	3.1

[a]Extrapolated to baseline. [b]Radius determined from absorption edge.[64]

As seen in Figure 3 the amount of Cd^{2+}, **5** and S^{2-} all determined the size of the nanoparticles. When the amount of Cd^{2+} increased (Figure 3A) the particle size also increased as would be predicted with increasing volume. When the amount of **5** was increased (Figure 3B) the size of the particles decreased due to higher surface area. When the amount of S^{2-} increased (Figure 3C) the size increased as expected. The emission also dramatically decreased as the amount of S^{2-} increased. This was accompanied by a dramatic increase in absorption. This phenomenon may be due to having sulfur atoms exposed on the surface and not having a pure cadmium/**5** surface. This would allow for inefficient recombination of electron hole pairs, leading to reduced emission.

Dispersions of nanoparticles in aqueous solutions must be stable to changing pH if they are to be useful. The effect of pH on nanoparticle absorption and stability was determined. Figure 4 shows CdS nanoparticle absorption spectra at various pH values.

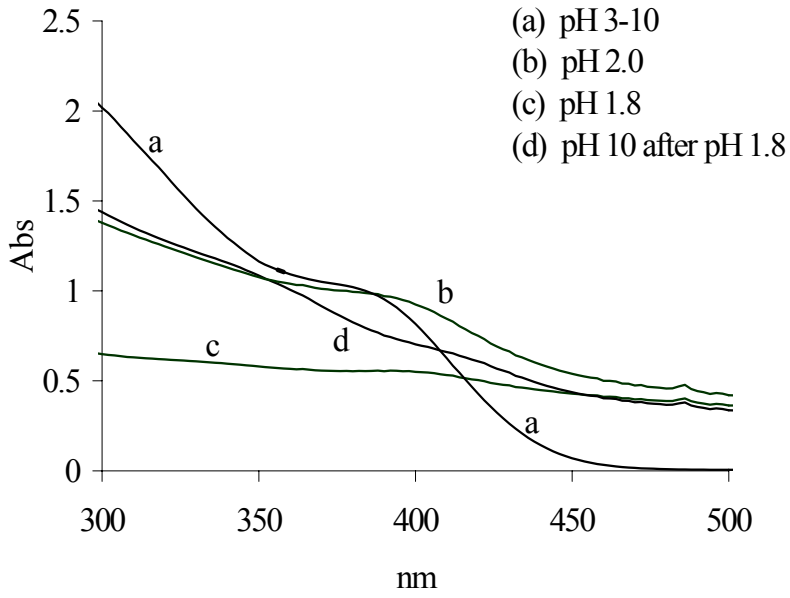

Figure 4. Effect of pH on CdS nanoparticle absorption spectra, showing increasing acid concentration (a,b,c) and reformation of particles by base addition (d).

Cadmium sulfide nanoparticles were found to be stable between pH 3 and 10, over a period of at least a week. Optimum pH values between 6 and 9 allow for extended shelf life of at least a year. At pH lower than 3, the nanoparticles began to deteriorate. The deterioration began with a slight clouding of the dispersion, as seen in the increased absorption above 400 nm, as shown in Figure 4b,c. The clouding may be explained by loss of stabilizer and aggregation of the particles as the carboxylate group was reprotonated. As more acid was added and the pH dropped, slow evolution of $H_2S(g)$

was noticed. Full destruction of the nanoparticles occurred at approximately pH 1.8. After destruction of the nanoparticles was complete, addition of base to raise the pH of the solution resulted in some regeneration of nanoparticles as shown in Figure 4d. These nanoparticles, however, were polydisperse, and loss of H_2S prevented reformation of full nanoparticles.

Cadmium Selenide and Cadmium Sulfide/Cadmium Selenide Nanoparticles. Cadmium selenide and cadmium selenide/cadmium sulfide core/shell nanoparticles have better tunability and quantum yield than cadmium sulfide.[33,65] We have used the method of Kotov et al.,[65] shown in Scheme 5, for aqueous synthesis of CdSe and CdSe/CdS nanoparticles stabilized by citrate. Attempts at forming CdSe in the presence of **5** failed due to the slow mechanism of Se^{2-} release and the higher temperatures of the CdSe synthesis. Since direct synthesis using **5** failed, CdSe and CdSe/CdS nanoparticles stabilized with weakly bound citrate ligands were chosen. Higher quality CdSe and CdSe/CdS particles could be synthesized using the more strongly ligated thioglycerol, but ligand exchange would be much more difficult.

Scheme 5. Cadmium Selenide/Cadmium Sulfide Core/Shell Nanoparticle Synthesis

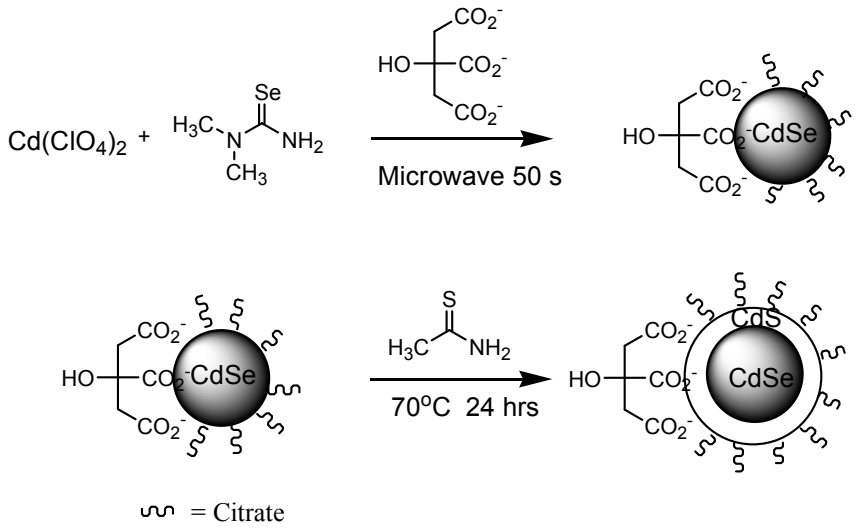

To obtain high quantum yield CdSe and CdSe/CdS nanoparticles, the nanoparticles must be aged[1,66] in the presence of light, in a process called light-induced luminescence activation.[1,66,67] This aging, under continuous light exposure, allows for an increase in quantum yield by a factor of 100 as seen in Table 3. This increase in quantum yield was most dramatic after one week of aging, but after one month the quantum yield began to decrease due to photobleaching. This light-induced luminescence activation was only used for CdSe and CdSe/CdS nanoparticles, since CdS nanoparticles will photobleach and do not show light-induced luminescence activation.

Table 3. Quantum Yields of CdSe and CdSe/CdS Nanoparticle Dispersions

sample[a]	quantum yield aged	quantum yield non-aged
Rhodamine B		100%
CdSe citrate	1.1%	0.01%
CdSe **5** polymerized	0.9%	0.06%
CdSe/CdS citrate	5.1%	0.81%
CdSe/CdS **5** polymerized	2.6%	0.61%

[a] λ_{ex} = 400 nm

Nanoparticles made using the Kotov method contain a citrate to cadmium molar ratio of 2 to 1. The excess in stabilizer produces highly stable nanoparticles. However when dialyzed the nanoparticles deteriorate due to loss of dissociated citrate. To obtain highly luminescent core/shell nanoparticles, the stronger thiol ligand, **5**, was exchanged with the weaker carboxylate ligand of citrate shown in Scheme 6. Typical ligand exchange was carried out for 36 hours. Nanoparticles with better quantum yields were produced when ligand exchange was carried out at 5 ^{o}C in the dark and not carried out at room temperature in the dark. After ligand exchange the cysteine acrylamide was polymerized to obtain highly stable, highly luminescent nanoparticles. Figures 5 and 6

show the absorption and emission spectra of CdSe and CdSe/CdS nanoparticles with citrate and polymerized cysteine acrylamide ligands.

Scheme 6. Ligand Exchange

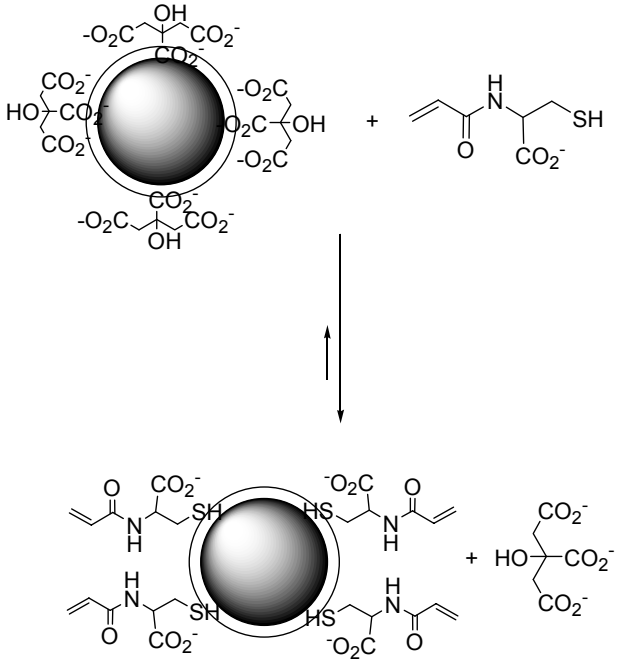

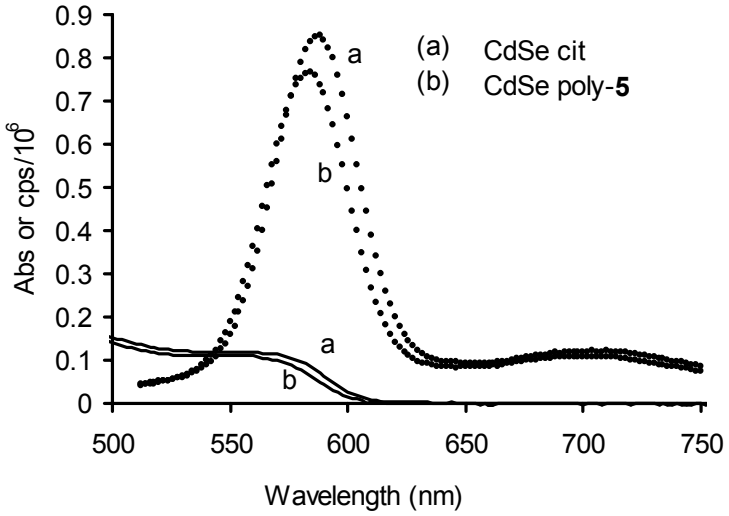

Figure 5. Absorption and emission spectra of aged CdSe nanoparticles (λ_{ex} = 400 nm).

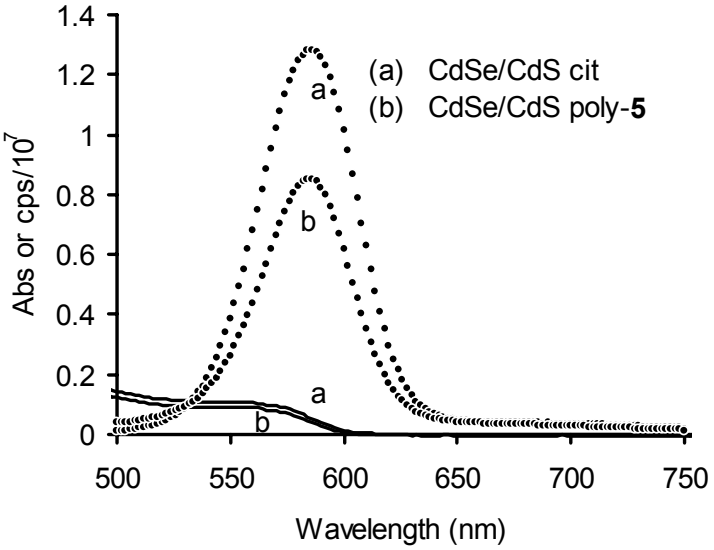

Figure 6. Absorption and emission spectra of CdSe/CdS nanoparticles (λ_{ex} = 400 nm).

Exchange of **5** for citrate on CdSe and heating to polymerize **5** did not affect the absorption spectrum as seen in Figure 5. The fluorescence spectrum of the citrate stabilized CdSe nanoparticles seen in Figure 5 had the usual emission peak at 590 nm and a broad trapped emission band at longer wavelengths. The quantum yields of CdSe/citrate and CdSe/poly-**5** were nearly the same as seen in Table 2. Quantum yields of about 1% at 590 nm are common for aqueous dispersions of CdSe nanoparticles after aging.[65] Quantum yields could not be measured from dialyzed CdSe nanoparticles stabilized with monomeric **5** because of coagulation after aging.

The core/shell CdSe/CdS nanoparticles exhibit less trapped emission and greater luminescence intensity than the CdSe nanoparticles,[26,30,65] as shown in Figure 6 and Table 2. The quantum yield from CdSe/CdS/poly-**5** was about half of the quantum yield from the sample of CdSe/CdS/citrate. Quenching of CdSe luminescence by thiols is well known and is related to hole transfer, from the excited state of the nanoparticles to the thiol.

The CdSe/CdS nanoparticles that have been synthesized were made in 50 mL batches. Our overall goal was to use these materials in large scale synthesis of composite materials, so scale up attempts to 200 mL, to prevent inconsistencies between small batches were made. These scaled up versions resulted in slower heating and therefore slower nanoparticle formation. The resulting nanoparticles were more polydisperse than the nanoparticles from methods that start with only 50 mL of solution. This has shown that to make large quantities of high quality CdSe/CdS nanoparticles, by the method of Kotov, one large batch must be divided into several small batches for heating to produce large quantities of identical particles.

To demonstrate the longevity of our polymerized nanoparticles, a poly-**5** stabilized CdSe/CdS sample was thoroughly dialyzed and allowed to sit for 1.5 years at 5 ^{o}C in the dark. After 1.5 years no precipitate was seen in the thoroughly dialyzed sample, while the parent citrate stabilized sample, which was not dialyzed, had precipitate present. The absorbance and emission spectra were also very strong and not altered after 1.5 years as shown in Figure 7. This helps prove the utility of our polymerized and dialyzed nanoparticle solutions since typical nanoparticle solutions precipitate very rapidly after dialysis and our sample showed no precipitate and retained its optical properties.

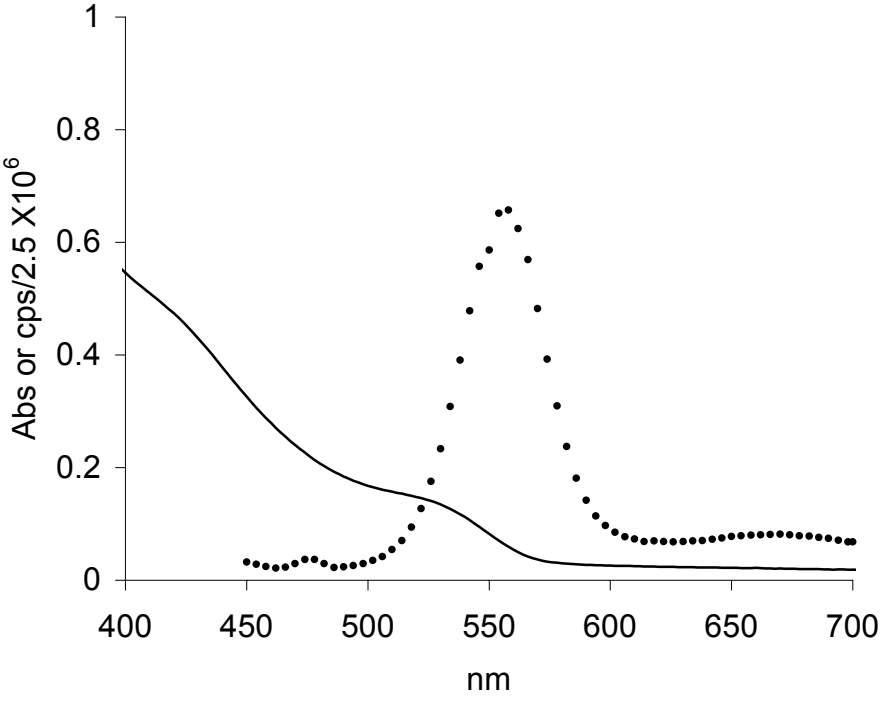

Figure 7. Absorption and emission spectra of 1.5-year-old CdSe/CdS core/shell nanoparticles stabilized with poly(cysteine acrylamide), (λ_{ex} = 400 nm).

Conductivity measurements were carried out to prove that cysteine acrylamide and poly(cysteine acrylamide) stabilized nanoparticles contained little free ligand, since surface attached ligands and polymerized ligands will result in lower conductivities than free ligand in solution. To prove this, citrate stabilized CdSe and CdSe/CdS nanoparticles were lightly dialyzed for 8 hours to remove excess citrate and followed with ligand exchange. After ligand exchange, the **5** and poly-**5** samples were dialyzed for 24 hours and compared to citrate stabilized samples that had 8 hours of dialysis, since 24 hours of dialysis would destroy the citrate stabilized samples. The solutions were then diluted to match the optical density concentration, by UV/Vis. Analysis of CdSe and CdSe/CdS nanoparticles show that citrate stabilized nanoparticles have a much higher conductivity than the cysteine acrylamide stabilized nanoparticles, as expected due to shorter dialysis time. This dilution and dialysis did greatly reduce the conductivity of the parent citrate stabilized nanoparticle solution from 5400 μmhos. It was also shown repeatedly that heat-treated **5** stabilized nanoparticles have lower conductivities than the non heat-treated **5** stabilized nanoparticles. This can be attributed to cysteine acrylamide polymer reducing the amount of ligand equilibrating between the particle surface and the surrounding solution.

Conclusions

We have synthesized a new polymerizable thiol stabilizer, cysteine acrylamide, for the stabilization of aqueous dispersions of CdS, CdSe and CdSe/CdS nanoparticles at neutral and basic pH. By polymerizing the acrylamide double bond of the stabilizer with heat it was possible to cover the surface of a nanoparticle with strong polythiol ligands.

Since the ligand was a polythiol, no excess ligand was needed in solution for stabilization of the particles, and all necessary ligand for surface passivation and solubilization was attached to the nanoparticle surface. Cadmium sulfide nanoparticles were synthesized in the presence of cysteine acrylamide and have been found to be highly stable and size tunable. Ligand exchange with citrate was accomplished with CdSe and CdSe/CdS core/shell nanoparticles. Attachment of cysteine acrylamide produced no change in absorption spectra. Attachment of cysteine acrylamide to CdSe produced a reduction in emission. Core/shell CdSe/CdS nanoparticles stabilized only by polymerized cysteine acrylamide also showed a reduction in emission however, they have been found to be stable for greater than a year with little degradation in optical properties.

Further experiments using cysteine acrylamide-stabilized nanoparticles take advantage of the high stability of these luminescent particles in dilute solutions as seen in Chapter III. Experiments in Chapter III also take advantage of the charged carboxylate group on cysteine acrylamide. Composite materials in Chapter III will be made from these nanoparticles and various polymers.

Future Work

Nanoparticles stabilized by poly(cysteine acrylamide) are more stable than nanoparticles synthesized under standard conditions. This novel method for stabilization can allow for many future experiments outside the field of chemistry. Since poly(cysteine acrylamide)-stabilized nanoparticles are free nanoparticles and exist at many pHs, these materials can be of great use for biological samples.

First **5** should be placed on CdTe nanoparticles. CdTe is a more tunable nanoparticle with much higher quantum yields. Addition of poly-**5** to the surface would increase the utility of these nanoparticles.

Also addition of antibodies to the surface of high quality nanoparticles through an amide or ester linkage would allow for useful studies of these materials as tracers in biological studies.

Experimental Section

General Methods. All reagents were purchased from Aldrich or Fisher and used without purification. Fluorescence was carried out on a Fluorologue 3-Tau-11 fluorometer calibrated with Rhodamine B (quantum yield 100%). UV/Vis spectroscopy was carried out on a Hewlett Packard model 8452A diode array spectrophotometer. ^{1}H NMR spectra were carried out on a Varian Gemini instrument at 300 MHz. Measurements of pH were carried out on a Fischer Scientific Accumet® pH meter with an Orion combination pH electrode 910600. Conductivities were measured with a YSI model 31 conductivity bridge meter using a 1 cm^2 platinum electrode. Microwave heating was done in a General Electric Model JES638WF 700 W microwave oven. Water was purified via a three-column Barnstead e-pure water filtration system to a conductivity of $< 4\ \mu ohm^{-1}cm^{-1}$. Dialysis was done in 1000 MWCO Spectra/Por 7 membrane tubing (sulfur and heavy metal free).

Cystine Dimethyl Ester Diacrylamide (3). Under nitrogen, 1.000 g (2.93 mmol) of L-cystine dimethyl ester dihydrochloride (**2**) was suspended in 200 mL of ethyl acetate by magnetic stirring for 30 min. To the suspension 2.37 g (23.5 mmol) of triethylamine

was added dropwise and stirred for 30 min, and 0.80 g (8.8 mmol) of acryloyl chloride in 50 mL of ethyl acetate was added dropwise. The mixture was stirred overnight while protected from light. Water (50 mL) was added, and any precipitate that formed was dissolved with a few mL of additional water. The aqueous solution was extracted 3 times with 50 mL of ethyl acetate. The combined organic layers were washed 3 times with 100 mL of water, once with 100 mL of $NaHCO_3$ (satd), and 3 more times with 100 mL of water. The ethyl acetate was rotary evaporated. The residue was dissolved in 50 mL of dichloromethane. The dichloromethane solution was washed twice with 50 mL of 2 N HCl, twice with 50 mL of water, twice with 50 mL of $NaHCO_3$, and three times with 50 mL of water, and then dried with $MgSO_4$. The solution was rotary evaporated, and the residual solid was dried under vacuum to leave a white powder (**3**), which was stored under nitrogen at –30 ^{o}C protected from light. Compound **3** was useful for up to 12 months, after which attempted nanoparticle formation was not successful. ^{1}H NMR (300 MHz, $CDCl_3$,) δ 3.2 (2 H, qd, J = 14.4, 5.3 Hz), 3.7 (3 H, s), 4.9 (1 H, m), 5.6 (1 H, dd, J = 10.0, 1.8 Hz), 6.2 (2 H, m), 6.9 (1 H, d, J = 7.2 Hz). ^{13}C NMR (75 MHz, $CDCl_3$) δ 170.8, 165.3, 130.0, 127.7, 52.8, 51.7, 40.7. FTIR (neat, NaCl) 3370, 1741, 1660, 1630, 1541, 1437, 1410, 1215, 1173, 800-600 (br) cm^{-1} .

Cysteine Acrylamide (5). Disulfide **3** (0.050 g, 0.113 mmol) was dissolved in 15 mL of THF under nitrogen, and 0.107 g (0.530 mmol) of tributylphosphine and 1 mL of water were added, by the method of Ayers.[68] The mixture was stirred for at least 3 h in the dark to give *N*-acrylamido-L-cysteine methyl ester (**4**), 10 mL of 5% NaOH was added, and the heterogeneous mixture was stirred for at least 4 h. The THF was removed under vacuum to give about 8 mL of an aqueous dispersion. The dispersion was washed

with 3 x 10 mL of diethyl ether to remove tributylphosphine oxide. The aqueous solution was rotary evaporated to remove ether, and the pH was adjusted to 7 with dilute HCl to give a colorless, odorous solution of **5**. The solution was stored under nitrogen at 5 ^{o}C and was good for nanoparticle stabilization for at least one week.

Cadmium Sulfide Nanoparticles Stabilized with Cysteine Acrylamide. In a 250-mL Erlenmeyer flask under nitrogen, 0.045 g (0.260 mmol) of cysteine acrylamide in 100 mL of water and 0.065 g (0.208 mmol) of $Cd(ClO_4)_2$ hydrate were mixed. The solution was adjusted to pH 10 with NaOH. (If a precipitate forms when the pH exceeds 7 the cystine dimethyl ester diacrylamide is no longer useful). The solution was vigorously stirred with a magnetic stirring bar, and 0.0104 g (0.130 mmol) of fresh Na_2S in 10 mL of water was rapidly added in one batch. The solution is then diluted to 150 mL, and stirred for 10 minutes before storage under nitrogen in the dark.

Dialysis of Nanoparticle Solution. The solution was filled into a dialysis membrane with a 1,000 molecular weight cut-off and suspended in 10-20 x the bag's volume of water. A stream of nitrogen gas was bubbled through the water. The water was changed 4-5 times per day, with typical dialysis lasting for 48 hours. UV/Vis analysis of the non-polymerized CdS nanoparticles showed only slight dilution at all wavelengths.

Polymerizing 5 on the Nanoparticle Surface. In a 120-mL glass bottle wrapped in aluminum foil, 100 mL of the CdS nanoparticle solution was added. The headspace was replaced with nitrogen. The vial was suspended in a 75 ^{o}C oil bath and kept for 6 h. Stirring the solution did not affect the outcome based on UV/Vis analysis. It was further noted that dialysis of the nanoparticles prior to heating did not affect the final product.

^{1}H NMR (D_2O, 300 MHz) after concentrating the solution under vacuum, showed broad polymer peaks at δ 0.5-4.5, with no peaks past δ 5.0. Solutions were further dialyzed as described before using the nanoparticle solution.

pH Adjustment and Spectra of CdS Nanoparticles. A 50-mL sample of stock CdS nanoparticle solution was placed in a 200-mL round-bottomed flask equipped with a stirring bar and a pH electrode. The pH of the solution was adjusted using 0.05 M HCl and 0.05 M NaOH solutions. The pH was adjusted initially to 10 with NaOH. The sample was acidified with HCl and measurements taken at pHs: 10.0, 9.0, 7.0, 5.0, 3.5, 3.0, 2.5, 2.0, 1.8, and 10.0. After 10 minutes of equilibration at each point UV spectra were taken. At a pH of 1.8 the nanoparticles were destroyed. NaOH was added to bring the pH of the solution back to 10, and a final UV spectrum was taken after the nanoparticles were partially regenerated.

CdSe/Citrate Nanoparticles.[65] A 4 x 10^{-2} M $Cd(ClO_4)_2$ solution (2.0 mL) was added to a solution of 40 mL of water and 50 mg of sodium citrate. The solution was adjusted to pH 9.0 with 0.05 M NaOH, and 1.0 x 10^{-2} M and 1,1-dimethyl-2-selenourea solution (2.0 mL) was added. The solution was heated to the boiling point quickly in a microwave oven (55 s at 700 W), left standing to cool to room temperature, and stored overnight at 5 ^oC.

An attempt to synthesize the CdSe nanoparticles on a scale of 200 mL instead of 50 mL using the same concentrations of reagents resulted in slower heating in the microwave oven, slower nanoparticle formation, and a more polydisperse product.

CdSe/CdS/Citrate Nanoparticles. To the CdSe/citrate nanoparticle solution, 0.5 mL of 4 x 10^{-2} M thioacetamide was added, and the solution was heated at 70 ^{o}C for 20 h to give CdSe/CdS/citrate.

Ligand Exchange. The citrate-stabilized nanoparticles were dialyzed for 8 h with one change of water to remove excess citrate, cadmium and other salts. To the solution was added 0.12 mmol of **5** (1.5 mol per mol of Cd^{+2}). The headspace was filled with nitrogen, and the solution was stirred for 36 h at 25 ^{o}C. The solution was dialyzed overnight with one change of water, a 50% increase in volume was noted. The CdSe nanoparticles stabilized with **5** were heated to 70 ^{o}C for 6 h, cooled to room temperature, and dialyzed for 48 h with 10 changes of water to give CdSe/poly-**5**.

Aging CdSe and CdSe/CdS Nanoparticles. Prior to absorption and emission analysis, the CdSe and CdSe/CdS samples were aged under continuous exposure to laboratory fluorescent light at 25 ^{o}C. After 1 week, the emission quantum yields increased by as much as one hundred times, and nearly maximum emission intensity was achieved. Exposure to light for more than one month resulted in some photobleaching. After aging, the samples were stored in the dark at 5 ^{o}C under nitrogen. After storage of a CdSe/CdS-poly-**5** stabilized sample that was 1.3 mM in Cd for two years at 5 ^{o}C in the dark, there was no precipitate and no change of the absorption or emission spectrum.

Quantum Yields.[65] Absorption spectra were obtained for nanoparticle dispersions and for Rhodamine B standard solutions (100% quantum yield) to determine absorption peaks. A common absorption peak of 400 nm was chosen and the samples were then diluted to an absorbance of 0.05 absorption units at that wavelength, optical density. Fluorescence spectra were then obtained using 400 nm as the excitation

wavelength, and the peak area of the emission peak was calculated for each sample. Quantum yields were then calculated using the following equation, $\varphi_{np} = \varphi_s(I_{np}/I_s)(OD_s/OD_{np})$, where φ, I, OD, np, and s stand for quantum yield, emission intensity, optical density, nanoparticle sample and standard sample respectively.

References

(1) Rossetti, R.; Brus, L. *J. Phys. Chem.* **1982**, *86*, 4470-4472.

(2) Rossetti, R.; Nakahara, S.; Brus, L. E. *J. Chem. Phys.* **1983**, *79*, 1086-1088.

(3) Brus, L. *Appl. Phys. A* **1991**, *A53*, 465-474.

(4) Bader, S. D. *Surf. Sci.* **2002**, *500*, 172-188.

(5) Roucoux, A.; Schulz, J.; Patin, H. *Chem. Rev.* **2002**, *102*, 3757-3778.

(6) Kodama, R. H. *J. Magn. Magn. Mater.* **1999**, *200*, 359-372.

(7) Klabunde, K. J.; Editor *Nanoscale Materials in Chemistry*, 2001.

(8) Rao, C. N. R.; Cheetham, A. K. *J. Mater. Chem.* **2001**, *11*, 2887-2894.

(9) Pathak, S.; Choi, S.-K.; Arnheim, N.; Thompson, M. E. *J. Am. Chem. Soc.* **2001**, *123*, 4103-4104.

(10) Alivisatos, A. P. *Science* **1996**, *271*, 933-937.

(11) Talapin, D. V.; Rogach, A. L.; Shevchenko, E. V.; Kornowski, A.; Haase, M.; Weller, H. *J. Am. Chem. Soc.* **2002**, *124*, 5782-5790.

(12) Gittins, D. I.; Caruso, F. *Chem. Phys. Chem.* **2002**, *3*, 110-113.

(13) Suzdalev, I. P. *Russ. J. Gen. Chem.* **2002**, *72*, 551-568.

(14) Horn, D.; Rieger, J. *Angew. Chem., Int. Ed. Engl.* **2001**, *40*, 4330-4361.

(15) Zhang, J.; Coombs, N.; Kumacheva, E. *J. Am. Chem. Soc.* **2002**, *124*, 14512-14513.

(16) Landfester, K.; Montenegro, R.; Scherf, U.; Guntner, R.; Asawapirom, U.; Patil, S.; Neher, D.; Kietzke, T. *Adv. Mater.* **2002**, *14*, 651-655.

(17) Bekiari, V.; Lianos, P. *Langmuir* **2000**, *16*, 3561-3563.

(18) Qi, L.; Coelfen, H.; Antonietti, M. *Nano Lett.* **2001**, *1*, 61-65.

(19) Rao, A. P.; Rao, A. V. *Mater. Chem. Phys.* **2001**, *68*, 260-265.

(20) Quinlan, F. T.; Kuther, J.; Tremel, W.; Knoll, W.; Risbud, S.; Stroeve, P. *Langmuir* **2000**, *16*, 4049-4051.

(21) Pickett, N. L.; O'Brien, P. *Chemical Record* **2001**, *1*, 467-479.

(22) Brus, L. E.; Szajowski, P. F.; Wilson, W. L.; Harris, T. D.; Schuppler, S.; Citrin, P. H. *J. Am. Chem. Soc.* **1995**, *117*, 2915-2922.

(23) Nagesha, D. K.; Liang, X.; Mamedov, A. A.; Gainer, G.; Eastman, M. A.; Giersig, M.; Song, J.-J.; Ni, T.; Kotov, N. A. *J. Phys. Chem. B* **2001**, *105*, 7490-7498.

(24) Kuno, M.; Lee, J. K.; Dabbousi, B. O.; Mikulec, F. V.; Bawendi, M. G. *J. Chem. Phys.* **1997**, *106*, 9869-9882.

(25) Hines, M. A.; Guyot-Sionnest, P. *J. Phys. Chem.* **1996**, *100*, 468-471.

(26) Peng, X.; Schlamp, M. C.; Kadavanich, A. V.; Alivisatos, A. P. *J. Am. Chem. Soc.* **1997**, *119*, 7019-7029.

(27) Hao, E.; Sun, H.; Zhou, Z.; Liu, J.; Yang, B.; Shen, J. *Chem. Mater.* **1999**, *11*, 3096-3102.

(28) Mulvaney, P.; Liz-Marzan, L. M.; Giersig, M.; Ung, T. *J. Mater. Chem.* **2000**, *10*, 1259-1270.

(29) Chang, S.-Y.; Liu, L.; Asher, S. A. *J. Am. Chem. Soc.* **1994**, *116*, 6739-6744.

(30) Rogach, A. L.; Kornowski, A.; Gao, M.; Eychmueller, A.; Weller, H. *J. Phys. Chem. B* **1999**, *103*, 3065-3069.

(31) Gorer, S.; Penner, R. M. *J. Phys. Chem. B* **1999**, *103*, 5750-5753.

(32) Dabbousi, B. O.; Rodriguez-Viejo, J.; Mikulec, F. V.; Heine, J. R.; Mattoussi, H.; Ober, R.; Jensen, K. F.; Bawendi, M. G. *J. Phys. Chem. B* **1997**, *101*, 9463-9475.

(33) Nirmal, M.; Brus, L. *Acc. Chem. Res.* **1999**, *32*, 407-414.

(34) Pinna, N.; Weiss, K.; Sack-Kongehl, H.; Vogel, W.; Urban, J.; Pileni, M. P. *Langmuir* **2001**, *17*, 7982-7987.

(35) Lin, Y.; Skaff, H.; Emrick, T.; Dinsmore, A. D.; Russell, T. P. *Science* **2003**, *299*, 226-229.

(36) Han, M.; Gao, X.; Su, J. Z.; Nie, S. *Nature Biotech.* **2001**, *19*, 631-635.

(37) Chen, C.-C.; Yet, C.-P.; Wang, H.-N.; Chao, C.-Y. *Langmuir* **1999**, *15*, 6845-6850.

(38) Lee, J.; Sundar, V. C.; Heine, J. R.; Bawendi, M. G.; Jensen, K. F. *Adv. Mater.* **2000**, *12*, 1102-1105.

(39) Mamedov, A. A.; Belov, A.; Giersig, M.; Mamedova, N. N.; Kotov, N. A. *J. Am. Chem. Soc.* **2001**, *123*, 7738-7739.

(40) Hu, J.; Li, L.-s.; Yang, W.; Manna, L.; Wang, L.-w.; Alivisatos, A. P. *Science* **2001**, *292*, 2060-2063.

(41) Talapin, D. V.; Haubold, S.; Rogach, A. L.; Kornowski, A.; Haase, M.; Weller, H. *J. Phys. Chem. B* **2001**, *105*, 2260-2263.

(42) Bruchez, M., Jr.; Moronne, M.; Gin, P.; Weiss, S.; Alivisatos, A. P. *Science* **1998**, *281*, 2013-2016.

(43) Maxwell, D. J.; Taylor, J. R.; Nie, S. *J. Am. Chem. Soc.* **2002**, *124*, 9606-9612.

(44) Gerion, D.; Pinaud, F.; Williams, S. C.; Parak, W. J.; Zanchet, D.; Weiss, S.; Alivisatos, A. P. *J. Phys. Chem. B* **2001**, *105*, 8861-8871.

(45) Parak, W. J.; Gerion, D.; Zanchet, D.; Woerz, A. S.; Pellegrino, T.; Micheel, C.; Williams, S. C.; Seitz, M.; Bruehl, R. E.; Bryant, Z.; Bustamante, C.; Bertozzi, C. R.; Alivisatos, A. P. *Chem. Mater.* **2002**, *14*, 2113-2119.

(46) Dubertret, B.; Skourides, P.; Norris, D. J.; Noireaux, V.; Brivanlou, A. H.; Libchaber, A. *Science* **2002**, *298*, 1759-1762.

(47) Wang, S.; Mamedova, N.; Kotov, N. A.; Chen, W.; Studer, J. *Nano Lett.* **2002**, *2*, 817-822.

(48) Wang, D.; Rogach, A. L.; Caruso, F. *Nano Lett.* **2002**, *2*, 857-861.

(49) Bangs, L. B. *Pure Appl. Chem.* **1996**, *68*, 1873-1879.

(50) Liang, Z.; Susha, A. S.; Caruso, F. *Adv. Mater.* **2002**, *14*, 1160-1164.

(51) Zhang, J.; Coombs, N.; Kumacheva, E.; Lin, Y.; Sargent, E. H. *Adv. Mater.* **2002**, *14*, 1756-1759.

(52) Lin, Y.; Zhang, J.; Sargent, E. H.; Kumacheva, E. *Appl. Phys. Lett.* **2002**, *81*, 3134-3136.

(53) Hirai, T.; Saito, T.; Komasawa, I. *J. Phys. Chem. B* **2001**, *105*, 9711-9714.

(54) Aldana, J.; Wang, Y. A.; Peng, X. *J. Am. Chem. Soc.*, *123*, 8844-8850.

(55) Liang, X.; Kotov, N. A. *Abstracts of Papers, 224th ACS National Meeting, Boston, MA, United States, August 18-22, 2002* **2002**, PHYS-260.

(56) Mandal, S.; Gole, A.; Lala, N.; Gonnade, R.; Ganvir, V.; Sastry, M. *Langmuir* **2001**, *17*, 6262-6268.

(57) Bae, W.; Abdullah, R.; Mehra, R. K. *Chemosphere* **1998**, *37*, 363-385.

(58) Wong, M. S.; Cha, J. N.; Choi, K.-S.; Deming, T. J.; Stucky, G. D. *Nano Lett.* **2002**, *2*, 583-587.

(59) Nguyen, L.; Kho, R.; Bae, W.; Mehra, R. K. *Chemosphere* **1998**, *38*, 155-173.

(60) Bae, W.; Mehra, R. K. *J. Inorg. Biochem.* **1998**, *70*, 125-135.

(61) Lide, D. R. *Handbook of Chemistry and Physics, 73rd Edition*, 1993.

(62) Wang, Y. A.; Li, J. J.; Chen, H.; Peng, X. *J. Am. Chem. Soc.* **2002**, *124*, 2293-2298.

(63) Rockenberger, J.; Troeger, L.; Kornowski, A.; Vossmeyer, T.; Eychmueller, A.; Feldhaus, J.; Weller, H. *J. Phys. Chem. B* **1997**, *101*, 2691-2701.

(64) Weller, H.; Schmidt, H. M.; Koch, U.; Fojtik, A.; Baral, S.; Henglein, A.; Kunath, W.; Weiss, K.; Dieman, E. *Chem. Phys. Lett.* **1986**, *124*, 557-560.

(65) Rogach, A. L.; Nagesha, D.; Ostrander, J. W.; Giersig, M.; Kotov, N. A. *Chem. Mater.* **2000**, *12*, 2676-2685.

(66) Wageh, S.; Shu-Man, L.; Xu-Rong, X. *Physica E* **2003**, *16*, 269.

(67) Wang, Y.; Tang, Z.; Correa-Duarte, M. A.; Liz-Marzan, L. M.; Kotov, N. A. *J. Am. Chem. Soc.* **2003**, *125*, 2830-2831.

(68) Ayers, J. T.; Anderson, S. R. *Synth. Commun.* **1999**, *29*, 351-358.

CHAPTER III

SEMICONDUCTOR NANOPARTICLE/POLYSTYRENE LATEX COMPOSITE MATERIALS

Abstract

Cadmium sulfide (CdS) and cadmium selenide/cadmium sulfide (CdSe/CdS) core/shell nanoparticles, stabilized with poly(cysteine acrylamide), have been attached to polystyrene latexes (PS) to form composite materials. First, anionic 5 nm CdS nanoparticles were electrostatically attached to 130 nm surfactant-free cationic PS latexes to form stable dispersions at less than 10% of a calculated monolayer of coverage and at greater than a monolayer of coverage. Filtration of samples with one monolayer of coverage, through a 100 nm membrane, gave no nanoparticles in the filtrate. Transmission electron microscopy (TEM) showed nanoparticles attached to the surface of the latex particles. Second, monodisperse anionic surfactant-free PS latexes were also synthesized in the presence of CdS and CdSe/CdS nanoparticles, and TEM showed monodisperse latex composites (<250 nm diameter) with trapped nanoparticles. Third, surfactant stabilized latexes were synthesized with vinylbenzyl(trimethyl)ammonium chloride electrostatically bound to the CdSe/CdS nanoparticle surface. The motion and emission color of these various composites was detected by fluorescence microscopy.

Introduction

Composites are materials composed of two or more different materials. The goal of making a composite material is to combine the physical and chemical properties of the individual materials into a new material that has overall properties superior to the individual materials. Composites can be combinations of organic/organic,[1-7] organic/inorganic[8-21] or inorganic/inorganic[13,14,22] materials. One specific type of organic/inorganic composite material involves organic polymers combined with non-polymeric materials such as metals, semiconductors or other inorganic materials. These composites takes advantage of the useful physical and chemical properties of the inorganic material, and the size, moldability, chemical resistance and low cost of polymeric materials.[23] Typical examples of these composites include fiberglass reinforced plastics and metal catalysts supported on polymers. In this research we combine the size tunability and water dispersability of latexes particles[24] with the photoluminescence and reduced photo bleaching of semiconductor nanoparticles.[25-30]

Latex particles are submicron sized polymer spheres that are stabilized sterically or electrostatically in water.[24] They are most often formed by emulsion polymerization techniques. In a typical emulsion polymerization[23,24] experiment a water insoluble monomer is agitated in water to form monomer droplets and a small quantity of dissolved monomer as shown in Scheme 1. This dispersion of monomer in water is heated to the polymerization temperature and a radical initiator is added. Typically a charged monomer or surfactant will also be incorporated into the mixture to give stability, however charged initiator alone can provide the stabilizing groups on the particle surface.

Once polymerization begins, small polymer chains begin to form in the aqueous phase until they reach a size that is too large to be soluble. These chains then aggregate to from primary particles. These primary particles are colloidally unstable and will aggregate to form mature particles. The mature particles will continue to grow by monomer swelling from the aqueous phase and polymerization will continue due to entrance of growing radical chains from solution. Emulsion polymerization results in highly monodisperse particles, because the swelling of monomer into the latex is a thermodynamic process, and continued polymerization by entrance of radicals from the aqueous phase is dependent on the surface area of the individual particles,

Scheme 1. Latex Synthesis Mechanism

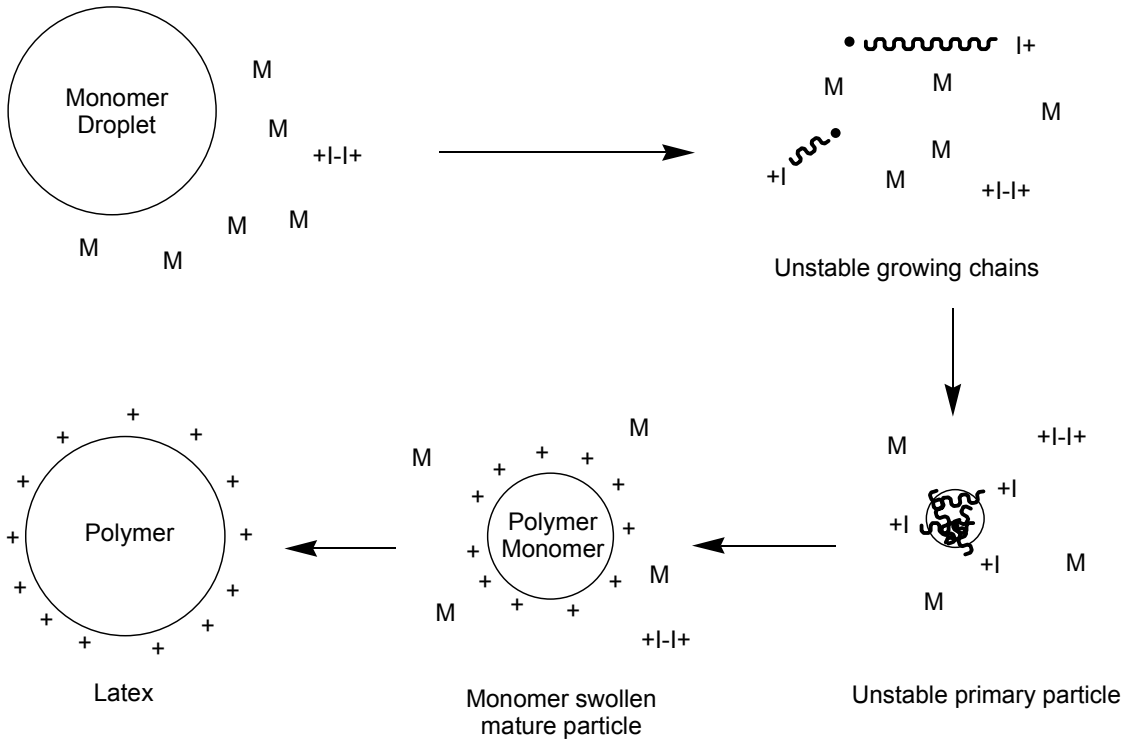

In this research we wish to take advantage of the high monodispersity of polymer latexes for the purpose of making uniform submicron sized fluorescent particles. The latexes used were composed of glassy polystyrene (**2**) and contain either a positive or negative charge, that is introduced by comonomers and/or initiators. The size of these particles can easily be controlled between 50 nm and 1000 nm.[24]

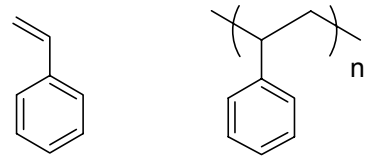

styrene **1** polystyrene **2**

Submicron sized fluorescent particles have been previously synthesized by many different methods.[1-4,6,7] Typically emulsion or dispersion polymerization is carried out using either a polymerizable fluorescent dye or an oil soluble dye that is not soluble in the solvent,[1-4,6] or a dye that is added to the latex dispersion and absorbed into the polymer. These composites provide extremely high quantum yield materials, but these organic dyes photobleach very rapidly.[2] These materials are not only important for academic research, but they are also commercially available.[31] Nanoparticles have been used by several groups instead of dyes.[8,9,19-21] This reduces the rate of photobleaching, but also reduces the overall quantum yield. Nanoparticles have been attached to polymer particles electrostatically,[8,9,15] by ligand exchange[18] and by trapping during solvent swelling.[19]

Nanoparticles have been synthesized on the surface of polymer particles,[20] and recently nanoparticles have been captured from solution during polymer particle synthesis.[11]

We have combined latexes with premade semiconductor nanoparticles in several different ways. However latex dispersions are very susceptible to aggregation in the presence of salts. This is a problem when working with nanoparticle dispersions, since most aqueous synthesized nanoparticles contain large quantities of dissociated ligand and soluble salts and may have a high pH.[22] These problems are overcome by using poly(cysteine acrylamide) stabilized nanoparticles as described in Chapter II. Poly(cysteine acrylamide) stabilized nanoparticles are thoroughly dialyzed to remove salts, and the thiols that ligate the nanoparticle surface cannot dissociate from the nanoparticle to act as chain-transfer agents during free-radical polymerization. This allows us to take advantage of the negative charge of the free carboxylate group of the cysteine and potentially take advantage of non-polymerized acrylamide double bonds, without the problem of added ligands, salts or high pH.

The goal of this research is to produce water dispersable polystyrene/semiconductor nanoparticle composites that are 100-300 nm in diameter and have easily visible fluorescence by optical microscopy as seen in Scheme 2. In an experiment the particles will be excited using a laser or other intense wavelength specific light source and then all wavelengths at or shorter than the excitation wavelength will be filtered out as seen in Scheme 3. This filtering will result in a black background with glowing points of light, since fluorescence results in emission of light that is at a wavelength longer than the excitation wavelength.

Scheme 2. Nanoparticle/Latex Composite

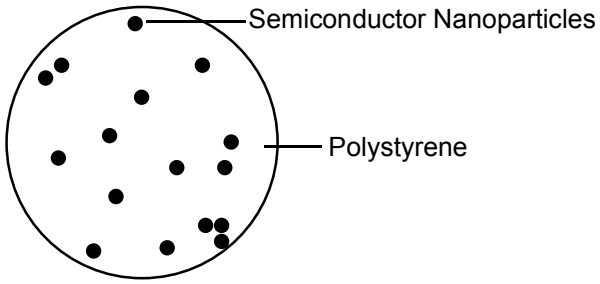

Scheme 3. Fluorescence Microscopy Experiment

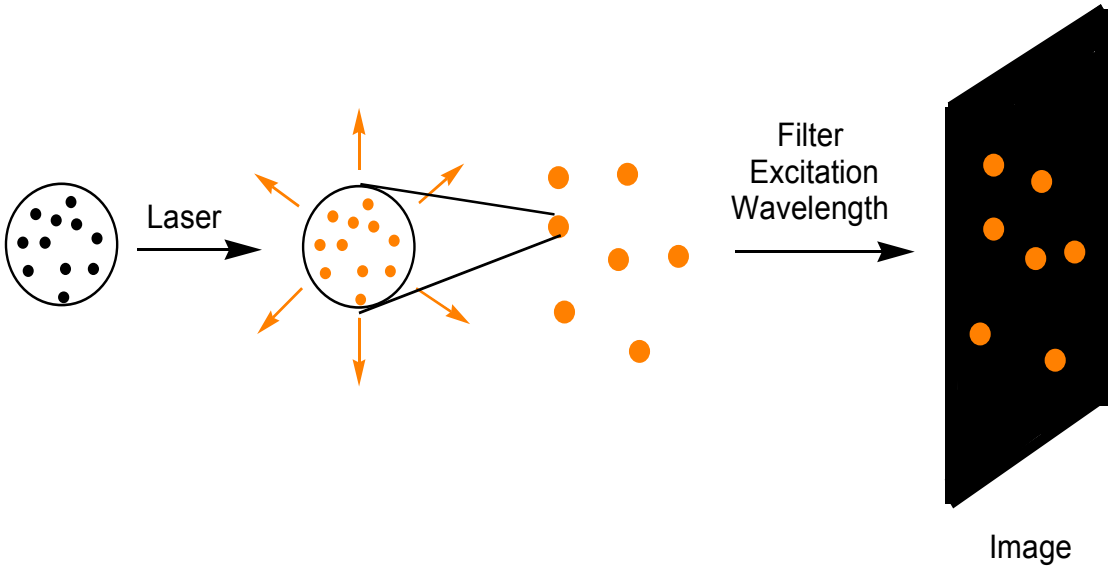

A typical particle motion measurement that can be tracked by optical microscopy are seen in Scheme 4. This type of motion will be studied by Dr. Penger Tong's group at Hong Kong University of Science and Technology. The motion that can be studied with these particles, and that is of particular interest to Dr. Tong, is the motion of particles at

the air/water interface or at an water/oil interface. This will be used to help explain forces that attract and repel particles at an interface.

Scheme 4. Interface Aggregation of Composite Particles

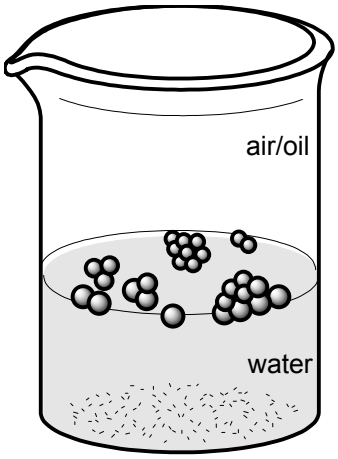

In this research we have attached nanoparticles to latexes in several different ways including electrostatic, covalent and trapping mechanisms. Our goal is to produce robust composites that fluoresce strongly and evenly, do not photobleach readily and are colloidally stable with the nanoparticles irreversibly bound to the latex particle.

Results and Discussion

The following cadmium sulfide and cadmium selenide/cadmium sulfide core/shell nanoparticles were prepared for use in composites (Table 1).

Table 1. Semiconductor Nanoparticles used for Composites

sample (ID)	abs. cutoff (nm)	em. max (nm)	diameter (nm)
CdS (**236**)	430	-	5.2[32,33]
CdS (**288**)	435	-	5.3[32,33]
CdS (**496**)	415	-	4.9[32,33]
CdSe/CdS (**239**)	600	585	approx. 5[22]
CdSe/CdS (**333**)	597	580	approx. 5[22]
CdSe/CdS (**359**)	605	600	approx. 5[22]

The following cationic polystyrene latexes have been prepared for use in composites (Table 2).

Table 2. Cationic Polystyrene Latexes used for Composites

Sample	Diameter TEM (nm)	PDI[a]	Diameter DLS (nm)
(+) Latex (**230**)	117	1.01	167
(+) Latex (**345**)	271	1.01	250

[a]Polydispersity index

Electrostatic Attachment of Nanoparticles to Oppositely Charged Latexes. To form latex/semiconductor nanoparticle composite materials with a core/shell structure,

CdS nanoparticles have been attached to cationic latex particles as shown in Scheme 5. Cadmium sulfide and cadmium selenide/cadmium sulfide core/shell nanoparticles stabilized with poly(cysteine acrylamide) (poly-**3**) have a net negative charge. This negative charge is due to the carboxylate group of the cysteine acrylamide stabilizer at a pH >7. The negative charge of the nanoparticles makes attachment/association, due to charge, possible for formation of composite materials.

Scheme 5. Electrostatic Attachment of Nanoparticles to Latexes

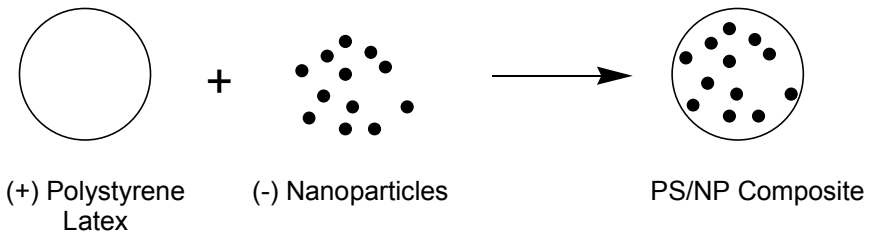

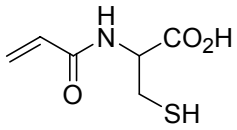

3

Coating the cationic latex with CdS was shown using TEM as shown in Figure 1, and by dynamic light scattering (DLS) measurements shown in Table 3. The amount of CdS that could be used to stably coat the cationic latex was limited to less than 10% of a monolayer, sample **242**, or greater than a monolayer, sample **262**. Quantities of CdS between 10 and 100% of a monolayer of coverage, samples **240** and **246**, resulted in aggregation and precipitation of a yellow powder leaving a colorless supernatant. This

was caused by reaching charge neutrality or by reducing the charge density enough that charged particles can bridge two larger particles of opposite charge. Further addition of CdS with agitation failed to redisperse the yellow precipitate. This showed that the CdS was attaching itself to the latex and was being pulled out of solution by the unstable latex. This continues until a calculated monolayer of nanoparticles was reached at which point the aggregated particles would not redispersed but a transparent yellow solution of nanoparticles was formed.

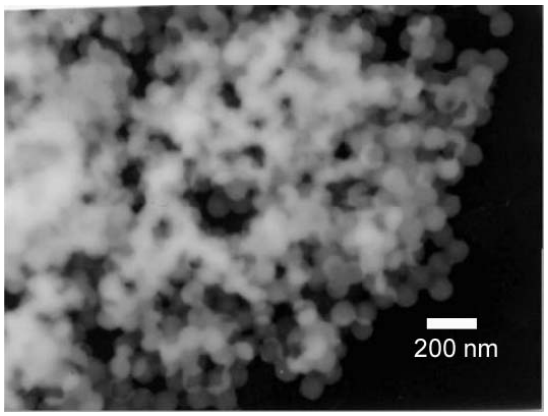

(a)

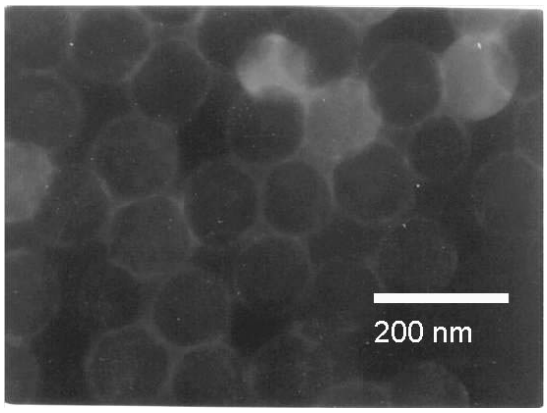

(b)

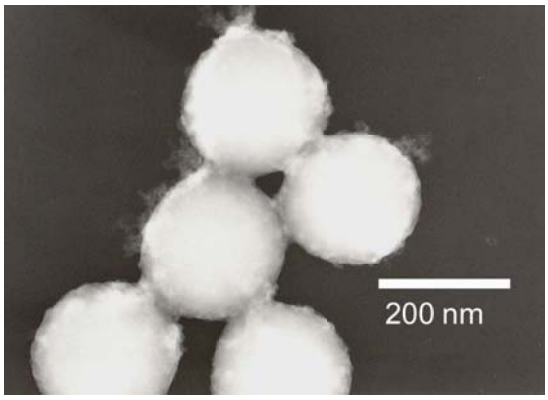

(c)

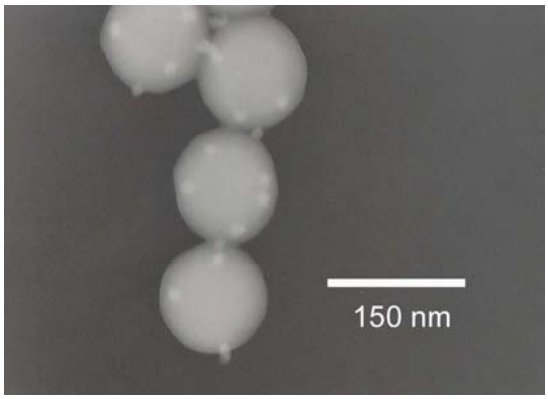

(d)

Figure 1. TEM of composite materials: (a) (**240**) 50% of one monolayer CdS on 120 nm latex, (b) (**246**) one monolayer CdS on 120 nm latex, (c) (**262**) greater than one monolayer of CdS on 220 nm latex, (d) (**337A**) 50 % of a monolayer CdSe/CdS on 120 nm latex.

Table 3. Latex/ CdS Nanoparticle Composite Mixtures

sample	composition[a]	diameter (nm)	appearance (color)
242	(+) Latex (**230**) 1/10 CdS (**236)**	186[b]	Stable dispersion (milky yellow)
240	(+) Latex (**230**) 1/2 CdS (**236)**	ppt	Rapidly aggregates (yellow ppt)
246	(+) Latex (**230**) mono CdS (**236)**	924[b]	Slowly aggregates (yellow ppt)
262	(+) Latex (**230**) > mono CdS (**236)**	178[b]	Stable dispersion (milky yellow)
337B	(+) Latex (**345**) > mono CdS (**236)**	-	Stable dispersion (milky yellow)
337A	(+) Latex (**230**) CdSe/CdS (**239)**	-	Stable dispersion (milky orange)

[a]Sample numbers are in parentheses. [b]Size by dynamic light scattering.

TEM analysis showed CdS nanoparticles attached to the cationic latex as seen in Figure 1. Treatment of the material with 50% of a calculated monolayer of CdS (**240**) results in Figure 1a. This sample was found to aggregate immediately and form large

nearly millimeter-sized clumps. Analysis of the TEM image shows a highly aggregated system with CdS covering the particles as seen by the bright fuzzy layer on the surface of the latex spheres. Figure 1b (**246**) shows the effect of a calculated monolayer of CdS on the cationic latex. This sample was stable for three days before precipitation began. After precipitation the sample could be redispersed, but only for a few hours. In this monolayer sample, TEM showed a much smaller, more 2-dimensional, aggregate (Figure 1b) with nearly complete coverage of the latex with CdS. The larger degree of coverage of CdS led to more stable and less aggregated composites. Sample **262** that had more than a monolayer of coverage was also prepared using latex sample **230**. No aggregated material was detected by DLS. A TEM image was also taken of a larger cationic latex (**345**) with greater than a monolayer of coverage (**337B**) as seen in Figure 1, and no aggregates were seen. However as the amount of CdS approached two monolayers of coverage CdS NPs were seen in the background on the TEM grid.

Dynamic light scattering experiments shown in Table 1, show the effects of CdS on the solution size of the materials. Addition of 10% of a monolayer of CdS (sample **236**, Table 1) results in a 15 nm growth in the particles (sample **242**, Table 3). This is larger than the expected value of <10 nm. Addition of of a monolayer of CdS (sample **236**, Table 1) resulted in some aggregation as seen in the large value for the monolayer sample **246**. More than a monolayer of coverage of CdS (sample **236**, Table 1) resulted in a 10 nm increase in diameter (sample **262**). This value was expected for the addition of 5 nm particles around the entire sample. The 10 nm increase in sample **262** showed that this sample was stable and was not aggregated.

To determine if the CdS was attached to the latex, the material was filtered. To filter the composite material, several milliliters of the monolayer CdS composite (**246**) was forced through a 100 nm cutoff syringe filter. This resulted in retention of a yellow solid and colorless filtrate, showing that the latex and CdS were trapped in the filter. As a control experiment, a CdS nanoparticle solution (sample **236**, Table 1) was filtered through the same size filters; no solid was obtained and only a yellow filtrate was present. The filtrates were then analyzed by absorption spectroscopy. The yellow nanoparticle filtrate retained the original nanoparticle spectrum as expected, and the colorless composite filtrate had no spectrum, as expected for a water sample.

CdSe/CdS nanoparticles (sample **239**, Table 1) were also attached to cationic latex **230**. This composite latex (**337A**) did not show behavior similar to the CdS/latex composites. This was due to the size of the CdSe/CdS nanoparticle samples. The CdSe/CdS nanoparticles form monodisperse aggregates that were approximately 18 nm in diameter, as reported in literature.[34,35] Analysis of various cationic latex/CdSe/CdS nanoparticle composite samples has shown that these composites do not aggregate for any ratio of CdSe/CdS nanoparticles to cationic latex. This was because the attachment of nanoparticles to the latex was not strong. TEM analysis has shown that most of the CdSe/CdS nanoparticles (smaller bright spots in Figure 1d) were associated with the latex; however, some were not associated with latex. This observation of composites and free nanoparticles was never seen in the CdS/latex composites.

Fluorescence studies were carried out on composite latex samples. CdSe/CdS coated latexes, shown in Figure 2, fluoresce with no shift in emission wavelength. Emission studies from CdS coated latexes were more difficult. CdS nanoparticles

fluoresce best when the excitation wavelength is below 400 nm. This was a problem for nanoparticle dispersions because they scatter light. Scattering and absorption of light was found to be strong below 400 nm, meaning that a wavelength above 400 nm was necessary for absorption of light by the nanoparticles. Since CdS nanoparticles had absorption cutoffs of approximately 420 nm, an excitation wavelength of 400 nm was chosen. This choice of excitation wavelength close to the absorption cutoff resulted in Rayleigh and especially Raman scattered light interference in the emission spectra, so a decent spectrum was not acquired.

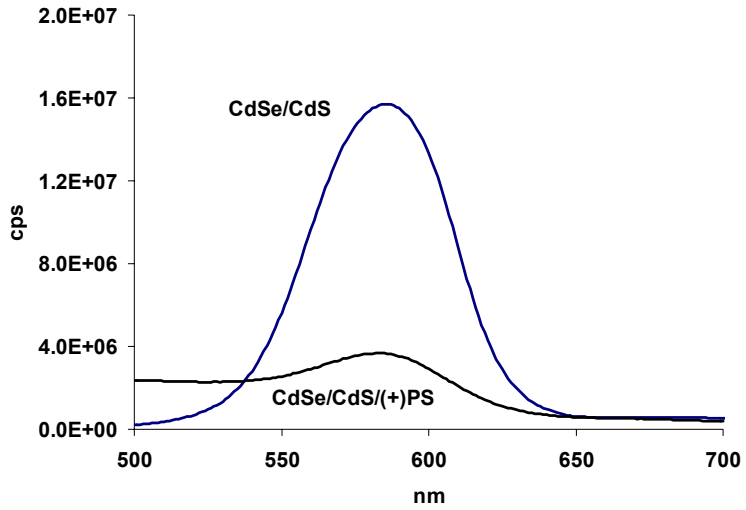

Figure 2. Emission spectrum of CdSe/CdS nanoparticles (**239**) and CdSe/CdS/polystyrene composite (**337A**).

Electrostatic attachment of CdS to cationic latexes was shown to be promising. However during further experiments with the stable composite materials it was found that under certain conditions the CdS could be easily removed from the latex. These

conditions were when cationic surfactants, cationic initiators or cationic monomers were introduced to the dispersion. Under these conditions the nanoparticles rapidly aggregated into a yellow oil leaving behind a white latex dispersion. This has led to the need for a stronger more permanent method of attachment for nanoparticles.

A new method for covalently attaching the electrostatically attached nanoparticles to the latex was investigated (sample **307**). In the experiment, a 10% coverage CdS composite with non-polymerized CdS NPs was slightly swollen with styrene monomer and polymerized as shown in Scheme 6.

Scheme 6. Polymerization of Nanoparticles to a Latex Surface

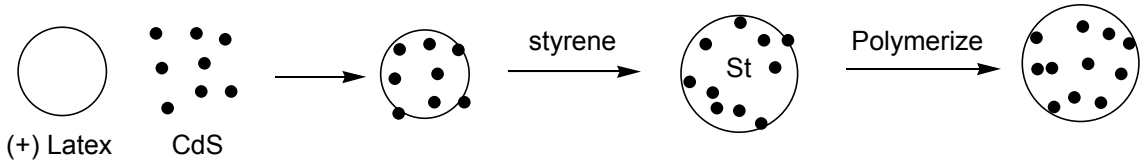

These experiments resulted in stable dispersions that retain most of their color. However, not all the nanoparticles were attached to the surface of the latex as shown by a precipitate of nanoparticles. This set of experiments did lead to one important discovery. As expected, the thiols of the cysteine acrylamide were thoroughly attached to the surface of the nanoparticles. This was determined by the fact that the nanoparticles did not aggregate or fade during or after polymerization. Since poly(cysteine acrylamide) nanoparticles did not interfere with the polymerization reaction, newer more robust latexes were investigated.

Formation of Polystyrene Latexes That Contain CdS Nanoparticles. Previous attempts at covalent or electrostatic attachment of CdS NPs to preformed polystyrene latexes (Table 1) proved ineffective for future plans of growing large poly(methyl methacrylate) shell on the surface of the particles, so formation of polystyrene latexes made in the presence of nanoparticles was investigated. By combining standard surfactant-free emulsion polymerization conditions for anionic latex[24,36] formation with a modified shot growth polymerization technique,[37,38] latexes were produced as shown in Scheme 7. Non-polymerized CdS nanoparticle solutions were substituted for water during the first shot of the shot growth polymerization. In this shot growth polymerization the majority of the monomer is first polymerized to form a latex, but before the polymerization is complete the remainder of the monomer is added to both increase the size of the latex and the monodispersity. This two-step addition allows for capture of the nanoparticles in the first stage of the polymerization and then allows for further latex growth during the second shot of monomer. Conditions for synthesis are shown in Table 4 and respective TEMs are shown in Figure 3.

Scheme 7. Capture of Nanoparticles during Latex Formation

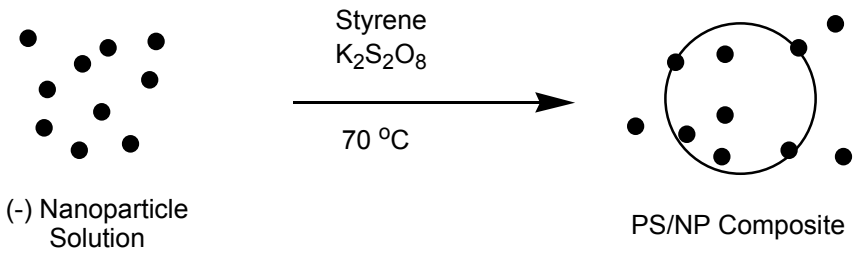

Table 4. Trapping Nanoparticles during Two Step Shot Growth Emulsion Polymerization

sample	H_2O (mL)	styrene (mg)	NaSS[a] (mg)	$K_2S_2O_8$ (mg)	T (^oC)	diameter (nm)	PDI
292	30 (CdS **288**)[b,c]	5.0	26	33	75	177[d]	1.00
	6	1.0	17	7			
316	20 (CdS **288**)[b,c]	2.0	16	15	60	166[d]	1.01
	10	0.5[e]	10	5			
317	20 (CdS **288**)[b,f]	2.0	16	15	60	140[d]	1.21
	10	0.5[e]	10	5			
374	30 (CdSe/CdS **355**)[b,c]	2.5	15	15	60	121[d]	1.01
497	60 (CdS **496**)[b,c]	10	50	66	75	195[g]	-
	12	1.0	30	14			

[a]Sodium 4-styrenesulfonate. [b]Approximately 0.8 mg of nanoparticles/mL. [c]Non-polymerized CdS. [d]Size from TEM. [e]MMA used in place of styrene. [f]Polymerized CdS. [g]Size from DLS.

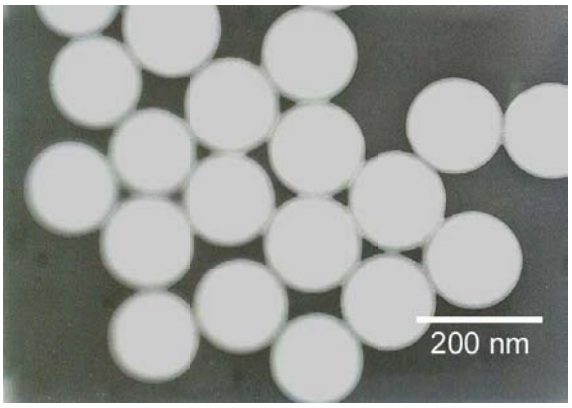

(a)

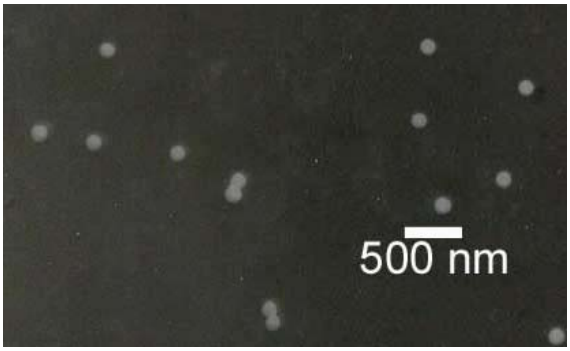

(b)

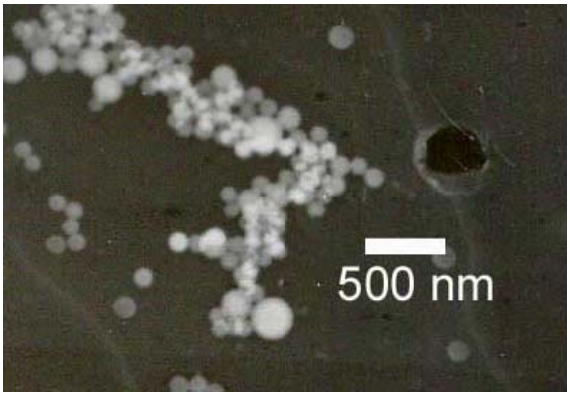

(c)

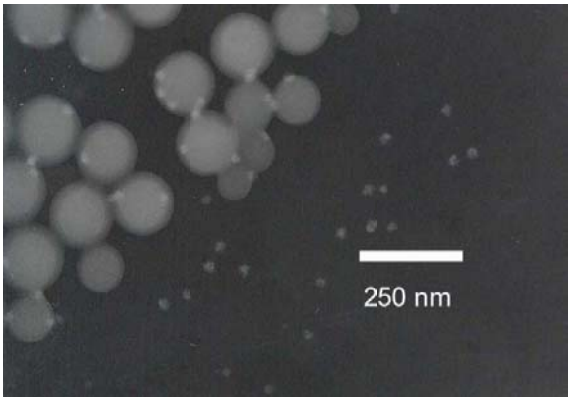

(d)

Figure 3. TEM images of composites: (a) non-polymerized CdS (**292)**, (b) non-polymerized CdS (**316**), (c) polymerized CdS (**317**), (d) non-polymerized CdSe/CdS (**374**).

Sample **292** was analyzed by TEM and DLS and determined to have a diameter of 178 nm and 226 nm respectively with high monodispersity as seen in Figure 3. This sample was stable for greater than 2 years with no precipitate and no loss of nanoparticle

color. The method was also found to be reproducible as seen in the duplicate sample **497**. Samples **316** and **317** were attempts at integrating MMA into the latex. These materials were stable solutions that retained the yellow CdS color. Sample **316** was formed using non-polymerized CdS NPs and **317** used polymerized CdS. Using non-polymerized CdS resulted in better uptake of the nanoparticles during emulsion polymerization while the polymerized NPs resulted in a more random distribution between solution NPs and NPs trapped in the latex spheres. Also seen in Figure 3b and 3c, sample **316** with non-polymerized nanoparticles produced a monodisperse latex, while **317** was polydisperse. This was also seen in samples similar to **292** where polymerized nanoparticles resulted in polydisperse samples, unstable dispersions or nanoparticle precipitate. It is of note that sample **317** had domains of PMMA as seen in the TEM images. PMMA was seen as the low contrast spots on the PS latexes in Figure 3c.

Sample **374** was an attempt at integrating CdSe/CdS nanoparticles into latexes. Figure 3d shows the TEM that proves that some of the nanoparticles are taken up into the latex while others are excluded. Fluorescence spectra were also taken and show the strong fluorescence of the latex composite as shown in Figure 4.

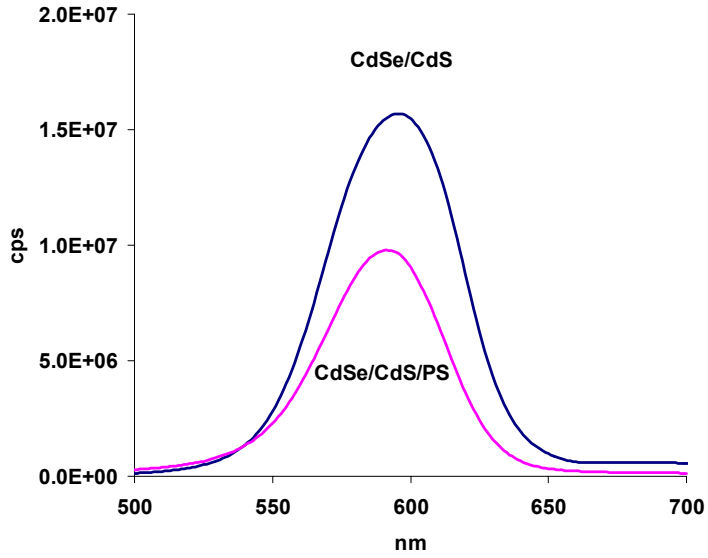

Figure 4. Emission spectra of CdSe/CdS nanoparticles (**355**) and CdSe/CdS/PS composite sample **374**.

Fluorescence microscopy of **497** was taken to determine the utility of these materials as optical tracking devices. Figure 5 shows five frames from a movie of these particles undergoing Brownian motion. As seen various particles are moving in random directions. Motion of these particles was determined using fluorescence microscopy under conditions similar to that of Dr. Tong's experiments. It was noted that during the microscopy experiment the particles did not photobleach even after nearly 45 minutes of analysis.

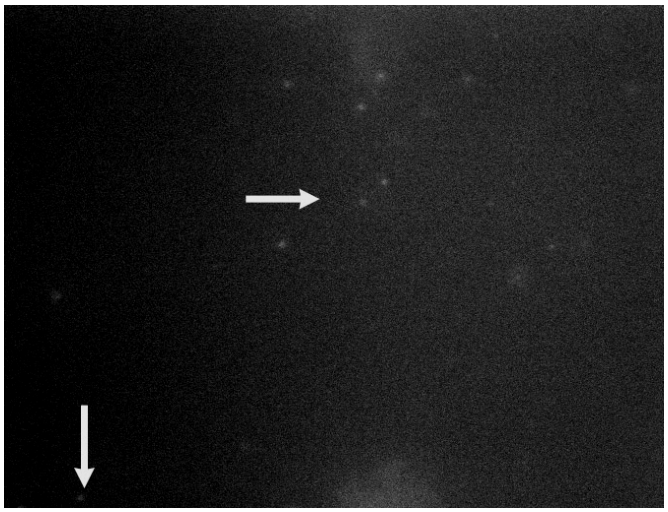

(a)

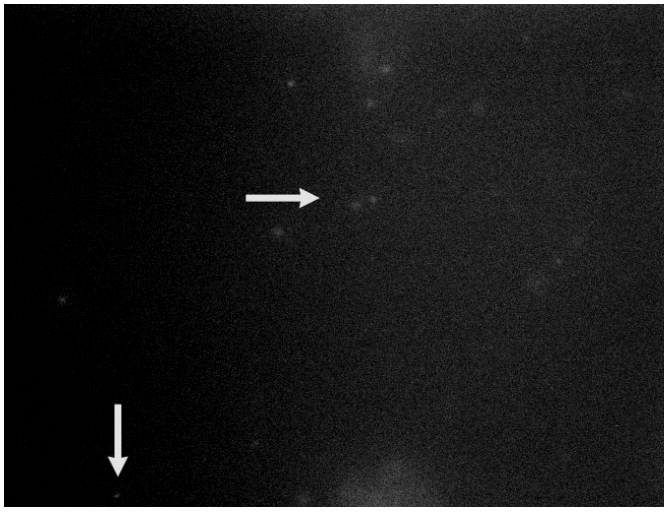

(b)

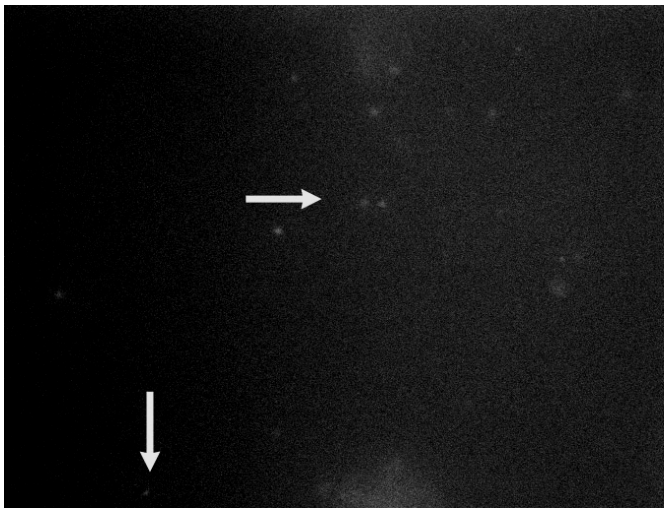

(c)

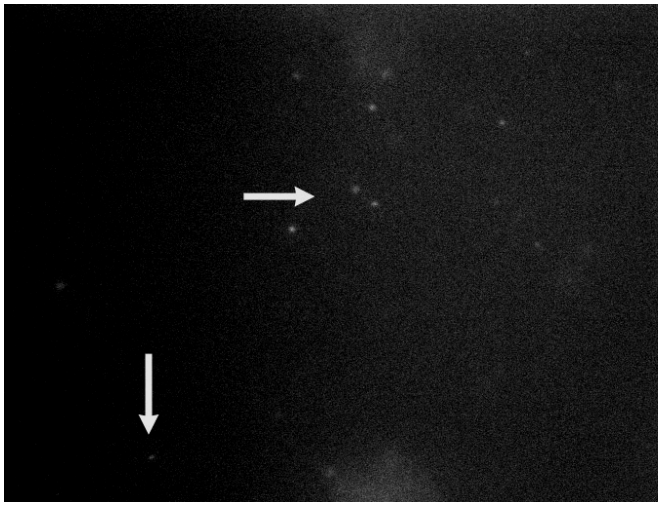

(d)

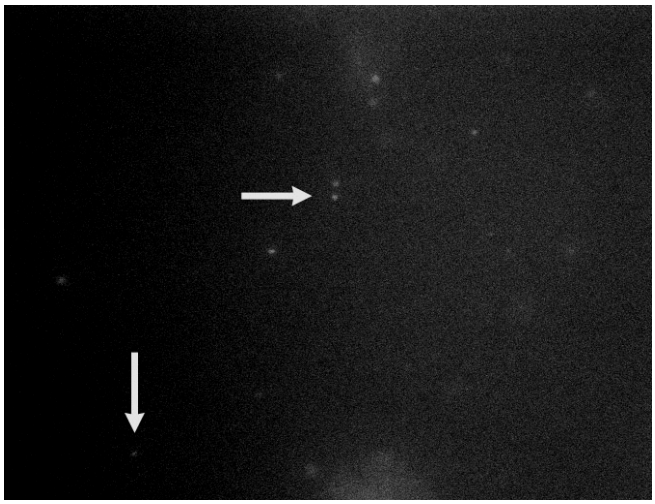

(e)

Figure 5. Fluorescence microscopy images of sample **497**, taken at 1 second intervals.

These composite materials were very simple to synthesize and they formed stable dispersions. The nanoparticles appear to be well trapped and those nanoparticles that were not trapped were easily removed by ultrafiltration. However not all nanoparticles were taken up into the latex in sample **374**, and not all latex particles in **374** appear to contain nanoparticles. These assumptions were not applied to the CdS nanoparticle

samples whose diameters were approximately 5 nm versus CdSe/CdS samples whose diameters were approximately 18 nm. Thus CdS samples were several times more concentrated on a particle basis. To obtain better uptake of the large CdSe/CdS nanoparticle aggregates, the nanoparticles need to be less hydrophilic.

Formation of Polystyrene Latexes using CdSe/CdS Nanoparticles with Vinylbenzyl(trimethyl)ammonium Counter Ions. Since anionic NPs attract quaternary ammonium groups, we have formed a nonionic PS latex where charged monomer was pre-bound to CdSe/CdS NPs. In this method CdSe/CdS was titrated with vinylbenzyl(trimethyl)ammonium chloride to 1/10 the concentration needed to qualitatively precipitate the nanoparticles. This reduced the hydrophilic nature of the nanoparticles and provided vinylbenzyl groups for polymerization from the nanoparticle surface while retaining water solubility. This complex was then introduced into an emulsion polymerization using sodium dodecylsulfate (SDS) as a stabilizer as seen in Scheme 8. This method is similar to molecular imprinting,[39,40] where various monomers are electrostatically or covalently attached to the surface of a target molecule and then polymerized. After polymerization and removal of the target molecules, future addition of target molecules will result in binding. The method in use here is similar, except the target nanoparticles are not removed.

Scheme 8. Nanoparticle Capture via Monomer Coordination

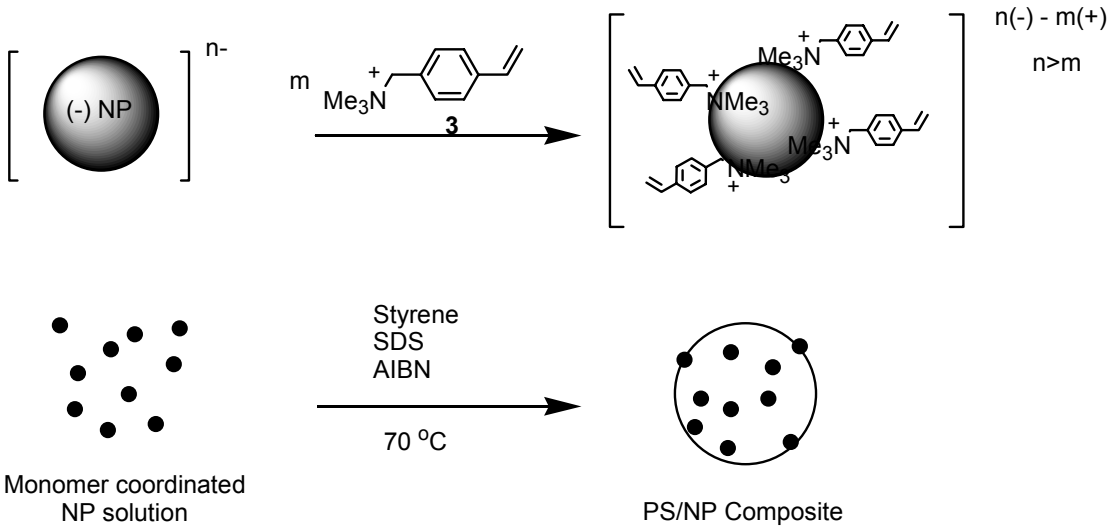

Latex synthesis was successful using this method as seen in Table 5 and Figure 6. The particles were colloidally stable and showed strong emission. One interesting phenomenon that did occur to the samples in Table 5 was that during the polymerization process the orange colored nanoparticles changed from orange to purple, and finally after 30 minutes reaction time, became milky pink. The resulting latexes were milky pink in color and showed good fluorescence as seen in Figure 7. This change in color resulted in a 25 nm blue shift in emission. Blue shifts in nanoparticles are very rare and indicate that the band gap is getting larger.[25-30] In other words the nanoparticles were getting smaller. This change was significant, since the CdSe/CdS nanoparticles were coated in a non-removable layer of poly(cysteine acrylamide) and a layer of CdS. To get smaller, both the poly(cysteine acrylamide) and the CdS layer would have to be removed and the amount of CdSe removed would have to be very small and uniform. This was very improbable since the composite material retained colloidal stability, and retained

absorption and emission characteristics for greater than a year. This means that some other mechanism was increasing the energy for excitation. One possible explanation may be seen in Figure 6. The TEMs in Figure 6 do not show large high contrast 18 nm CdSe/CdS nanoparticles, compared to Figures 1d and 3d. This may mean that during the emulsion polymerization process, where SDS, AIBN and the vinylbenzyl(trimethyl)ammonium chloride are present, the 18 nm CdSe/CdS nanoparticle aggregates break up into the individual nanoparticles (3-4 nm).[35,41] This could explain an increase in bandgap, since two nanoparticles that are touching could give up excited state energy to the adjacent nanoparticle and thus have reduced the apparent bandgaps. In control experiments, mixing and heating CdSe/CdS nanoparticles with each individual reactant, and combinations of the reactants did not result in a change in color. Only when all the reactants were present did the color shift occur.

TABLE 5. Latex Synthesis using Precoordinated Nanoparticles

sample	CdSe/CdS[a] (mg)	H_2O (mL)	**3**[b] (mg)	styrene (mL)	SDS (mg)	AIBN (mg)	T (^oC)	diameter (nm)	PDI[c]
336	32	45[d]	100	4.3	250	49	70	80[e]	1.2
365	16	20[f]	50	3.0	120	20	60	94[d]	1.4
366	16	20[f]	50	3.0	60	20	60	ppt	-
367	16	20[f]	50	3.0	90	20	60	119[e]	1.1
375	20	30[f]	0	3.0	80	70[g]	60	132[h]	-
380	8	15[f]	200	1.5	90	20	70	74[h]	-

[a]Approximate mg of nanoparticles used. [b]Vinylbenzyl(trimethyl)ammonium chloride. [c]Polydispersity index. [d]CdSe/CdS (**333**), [e]TEM. [f]CdSe/CdS (**342**). [g]2,2'azobis[2-(2-imidazolin-2-yl)propane] dihydrochloride (VA-044) cationic initiator. [h]DLS.

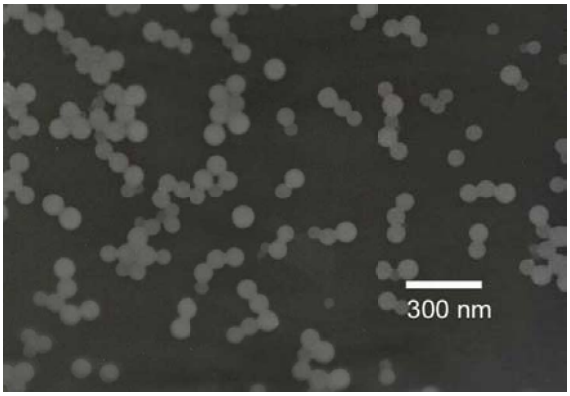

(a)

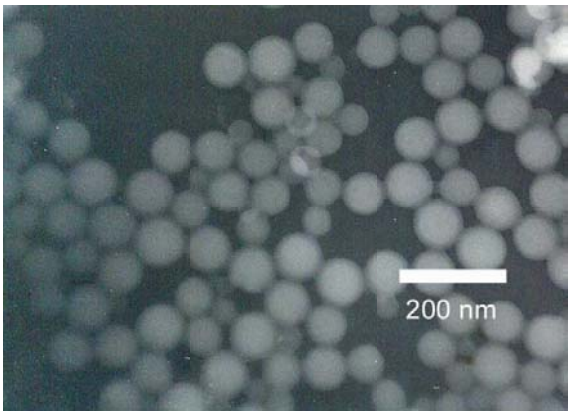

(b)

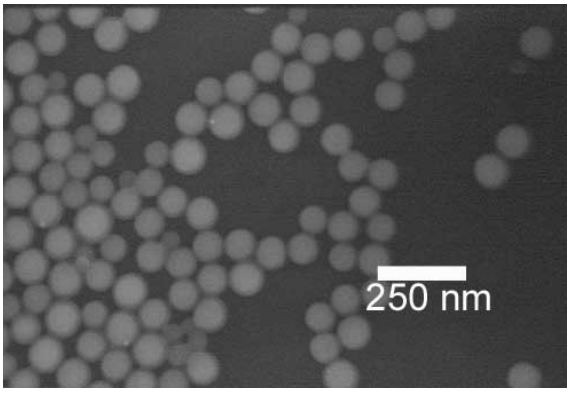

(c)

Figure 6. TEM image of composites (a) **336**, (b) **365**, (c) **367**.

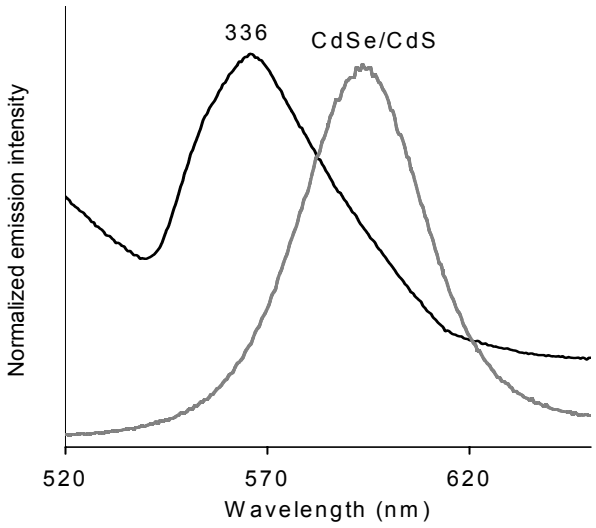

Figure 7. Fluorescence spectra of CdSe/CdS (**333**) and composite latex **336**.

The latexes reported in Table 5 all showed good emission and colloidal stability. Sample **336** was found to be a small latex, 80 nm, and found to be relatively monodisperse. Samples **365-367** were attempts at increasing the size of these latexes. As expected, as the relative amount of surfactant was decreased, the size of the latex increased. However, sample **366**, which had the least SDS, was not colloidally stable. Sample **375** was an attempt at using cationic initiator to coordinate the nanoparticles. This resulted in larger particles that were stable. Sample **380** was an attempt at using a large quantity of cationic monomer **3**. This was done near the precipitation point of the nanoparticles. These latexes were smaller than the composites made with less **3**, but these were colloidally stable. All latexes had reasonable monodispersity for small surfactant stabilized latexes, but were not as monodisperse as the other latexes from this research.

Conclusions

Nanoparticle/polystyrene latex composite materials have been synthesized in three ways. (1) Electrostatic attachment of CdS nanoparticles to preformed cationic latexes proved to be simple and effective. The range for colloidal stability for these electrostatically attached composites was less than 10% of a calculated monolayer and greater than a monolayer. Concentrations between 10% and a full monolayer resulted in aggregation and precipitation. It was found that the attachment of the nanoparticles to the latex surface was weak, and cationic molecules could remove the nanoparicles from the latex. These materials were not suitable for particle tracking by microscopy, due to the low coverage materials being too dim and the higher coverage having a slightly glowing background. (2) Attachment of the non-polymerized CdS nanoparticles to latexes by entrapment during anionic latex formation proved to be simple and effective. Several different latexes were formed and the size of the latexes was found to be easily tunable over the range of 120 to 195 nm. Unfortunately not all the nanoparticles were integrated into the new latexes. This means that random distributions of nanoparticles may exist and in some instances such as the CdSe/CdS nanoparticle composite latex **374**, some of the latex particles did not appear to contain nanoparticles. Only the CdS nanoparticle/latex composite samples were useful for tracking by fluorescence microscopy. (3) Vinylbenzyl(trimethyl)ammonium chloride was electrostatically attached to the surface of CdSe/CdS nanoparticles. This resulted in good uptake of nanoparticles during emulsion polymerization and good emission. An unexpected blue

shift in emission occurred during polymerization and is attributed to the break up of CdSe/CdS nanoparticle aggregates. These materials have potential for tracking experiments since they have strong fluorescence. However, the size of these particles is approximately 100 nm, making them too small for the intended fluorescence microscopy experiments.

Future Work

Nanoparticle/polystyrene composite latexes have been shown to be easily synthesized. Since poly(cysteine acrylamide)-stabilized nanoparticles were found to not interfere with free-radical emulsion polymerization, further experiments should be easily achieved.

Polystyrene/poly(methyl methacrylate) random copolymers should be used for the synthesis of NP/latex composites. This would allow for their use as a core for core/shell latexes, as discussed in Chapter IV.

CdSe/CdS nanoparticles synthesized as described in Chapter II are aggregates of 3-4 nm nanoparticles with an overall diameter of 18 nm. This is very large. If a layer-by-layer or a starved semi-batch emulsion polymerization approach can be taken, a shell of polymer could be grown on the surface. A layer of polymer could allow for seed growth of these materials. If this is possible then a highly fluorescent core of 18 nm and a thick polymer shell could be formed, similar to the methods seen in Chapter IV.

Experimental

General Methods. All reagents were purchased from Aldrich or Fisher and used without purification. VA-044 was purchased from Waco Specialty Chemicals. Styrene and methyl methacrylate were purified by passing the monomers down a column of basic alumina to remove inhibitors. Water was purified via a three column Barnstead e-pure water filtration systystem to a conductivity of < 4 μohm^{-1} cm^{-1}. Fluorescence was carried out on a Fluorologue 3-Tau-11 fluorometer. Syringe filtration was carried out using 20 nm polypropylene Whatman filters lot #01643C, and 100 nm Millipore filters, lot #H6DM07113. Ultrafiltration was carried out using 0.1 μm cellulose acetate/nitrate membrane from Millipore, lot #66434. Dynamic light scattering sizes were determined using a Malvern HPPS 5001 high performance particle sizer with 1 cm quartz cuvettes at 20 ^{o}C. Transmission electron microscope images were measured using a JEOL 100 keV microscope with samples dispersed at less than a monolayer on Formvar coated nickel grids. Average particle diameters and polydispersity indexes were calculated from measurement of 50 or more particles using a calibrated stage.

Nanoparticle Preparation. Nanoparticles were prepared as described in Chapter II.[42] CdS samples used were **236, 288** and **496**, with absorption cutoff at 430, 435 and 415 nm which correspond with diameters of 5.2, 5.3 and 4.9 nm respectively. CdSe/CdS samples used were **239, 333,** and **359** with emission maxima at 585, 580 and 600 nm respectively.

Cationic Latex Spheres. Method VBC1HY[37] produced particles (**230**) with diameter of 117 nm (PDI 1.01) by TEM, 167 by DLS, 5.1 mol % chloride by titration[43] and were diluted to 10% solids after ultrafiltration. A second larger latex (**345**)[44] was made based on a similar method using 5.00 mL of styrene, 1.0 mL of vinybenzyl chloride, 75 mL of water, and 0.012 g of VA-044 initiator. The second addition included 1.00 mL of styrene, 5 mg of vinylbenzyl(trimethyl)ammonium chloride, 5 mL of water, and 20 mg of VA-044. The latex containing chloromethyl groups was quaternized with 20 mL of 30% $N(CH_3)_3$ for 2 days at 70 ^oC, and the latex was ultrafiltered for a week to purify the latex. A diameter of 271 nm (PDI 1.01) was obtained by TEM, 250 nm by DLS, 11.3 mol % chloride by titration[43] and were diluted to 10% solids after ultrafiltration.

Coating Latexes with Cadmium Sulfide (262). In a 4-oz bottle. 22 mL of a CdS NP solution (0.63 mg/mL of 4 nm particles, 12.6 nm^2 cross-sectional area/particle and 4.64 x 10^{15} particles/mL) was stirred vigorously with fast addition of 6 mL of cationic latex (0.050 g/mL of 117 nm particles, 4.23 x 10^4 nm^2 surface area/particle and 5.68 x 10^{13} particles/mL). The solution was stirred for 10 min, sonicated for 5 min, and stirred again under nitrogen for 10 min. The dispersion was stored at 4 ^oC in the dark until needed.

Polymerizing CdS NPs on the Surface of Latexes (307). In a round-bottomed flask under N_2 protection, 2 mL of latex **230** (0.144 g), 10 mL of water, 0.144 g of styrene and 10 mg of AIBN were stirred overnight. After equilibration, 5 mL of CdS **288** was added and stirred for 2 h at 70 ^oC. The final product produced yellow coagulum that coated the walls of the flask, and had a slightly milky yellow dispersion.

Capturing CdS NPs During Latex Formation (292). In a round-bottomed flask under N_2 protection, 5.0 mL of styrene and 30 mL of CdS NP dispersion (**288**) were stirred vigorously in a 75 ^oC oil bath. After 25 min, 26 mg of sodium 4-styrenesulfonate, 13 mg of sodium bicarbonate, and 33 mg of potassium persulfate were added. One hour after addition of the initiator a second shot containing 1.0 mL of styrene, 17 mg of sodium 4-styrenesulfonate, 7 mg of potassium persulfate, 4 mg of sodium bicarbonate and 6 mL of water were added. The reaction was carried out for an additional 2 h, and the beige dispersion was filtered through cotton. Final TEM size analysis showed 178 nm particles, while DLS showed 226 nm.

Coordinating Vinylbenzyl(trimethyl)ammonium Chloride to Nanoparticles for Composite Latex Formation (336). In a round-bottomed flask under N_2 protection, 20 mL of CdSe/CdS NP (**333**) solution (approximately 10 mmol cysteine acrylamide) was stirred while 0.100 g (0.477 mmol) of vinylbenzyl(trimethyl)ammonium chloride in 15 mL of water was slowly added. The flask was submerged in a 70 ^oC oil bath and 4.3 mL of styrene and 250 mg of SDS were added with rapid stirring. The polymerization was initiated with 49 mg of AIBN. After 1 h, the second shot, which contained 0.5 mL of styrene and 10 mg of AIBN, was added and the reaction continued heating for 6 h. The final product was pink in color with TEM showing a diameter of 70 nm with a PDI of 1.02.

Fluorescence Measurements. Samples were placed in a 1 cm fluorescence cuvet and measured at either a 90^o angle or head-on depending on the transparency of the solution. All samples were examined under various excitation wavelengths to determine

optimum excitation wavelength and to determine which peaks corresponded to Rayleigh and Raman scattering.

References

(1) Jardine, R. S.; Bartlett, P. *Colloids Surf., A: Physicochemical and Engineering Aspects* **2002**, *211*, 127-132.

(2) Hu, H.; Larson, R. G. *Langmuir* **2004**, *20*, 7436-7443.

(3) Bosma, G.; Pathmamanoharan, C.; de Hoog, E. H. A.; Kegel, W. K.; van Blaaderen, A.; Lekkerkerker, H. N. W. *J. Colloid Interface Sci.* **2002**, *245*, 292-300.

(4) Pham, H. H.; Gourevich, I.; Oh, J. K.; Jonkman, J. E. N.; Kumacheva, E. *Adv. Mater.* **2004**, *16*, 516-520.

(5) Harley, S.; Thompson, D. W.; Vincent, B. *Colloids Surf.* **1992**, *62*, 163-176.

(6) Bradley, M.; Ashokkumar, M.; Grieser, F. *J. Am. Chem. Soc.* **2003**, *125*, 525-529.

(7) Radtchenko, I. L.; Sukhorukov, G. B.; Gaponik, N.; Kornowski, A.; Rogach, A. L.; Mohwald, H. *Adv. Mater.* **2001**, *13*, 1684-1687.

(8) Susha, A. S.; Caruso, F.; Rogach, A. L.; Sukhorukov, G. B.; Kornowski, A.; Mohwald, H.; Giersig, M.; Eychmuller, A.; Weller, H. *Colloids and Surfaces, A: Physicochemical and Engineering Aspects* **2000**, *163*, 39-44.

(9) Rogach, A.; Susha, A.; Caruso, F.; Sukhorukov, G.; Kornowski, A.; Kershaw, S.; Mohwald, H.; Eychmuller, A.; Weller, H. *Adv. Mater.* **2000**, *12*, 333-337.

(10) Uricanu, V.; Eastman, J. R.; Vincent, B. *J. Colloid Interface Sci.* **2001**, *233*, 1-11.

(11) Yang, X.; Zhang, Y. *Langmuir* **2004**, *20*, 6071-6073.

(12) Furusawa, K.; Anzai, C. *Colloids Surf.* **1992**, *63*, 103-111.

(13) Rajeshwar, K.; de Tacconi, N. R.; Chenthamarakshan, C. R. *Chem. Mater.* **2001**, *13*, 2765-2782.

(14) Rogach, A. L.; Kotov, N. A.; Koktysh, D. S.; Susha, A. S.; Caruso, F. *Colloids and Surfaces, A: Physicochemical and Engineering Aspects* **2002**, *202*, 135-144.

(15) Caruso, F.; Lichtenfeld, H.; Giersig, M.; Moehwald, H. *J. Am. Chem. Soc.* **1998**, *120*, 8523-8524.

(16) Percy, M. J.; Armes, S. P. *Langmuir* **2002**, *18*, 4562-4565.

(17) Wang, D.; Caruso, F. *Chem. Mater.* **2002**, *14*, 1909-1913.

(18) Hirai, T.; Saito, T.; Komasawa, I. *Journal of Physical Chemistry B* **2001**, *105*, 9711-9714.

(19) Han, M.; Gao, X.; Su, J. Z.; Nie, S. *Nature Biotech.* **2001**, *19*, 631-635.

(20) Zhang, J.; Coombs, N.; Kumacheva, E. *J. Am. Chem. Soc.* **2002**, *124*, 14512-14513.

(21) Farmer, S. C.; Patten, T. E. *Chem. Mater.* **2001**, *13*, 3920-3926.

(22) Rogach, A. L.; Nagesha, D.; Ostrander, J. W.; Giersig, M.; Kotov, N. A. *Chem. Mater.* **2000**, *12*, 2676-2685.

(23) Rudin, A. *The Elements of Polymer Science and Engineering*; Second ed.; Academic Press: San Diego, 1999.

(24) Lovell, P., A.; Al-Aasser, M., S. *Emulsion Polymerization and Emulsion Polymers*; Wiley: Chichester, 1997.

(25) Pathak, S.; Choi, S.-K.; Arnheim, N.; Thompson, M. E. *Journal of the American Chemical Society* **2001**, *123*, 4103-4104.

(26) Alivisatos, A. P. *Science* **1996**, *271*, 933-937.

(27) Nirmal, M.; Brus, L. *Acc. Chem. Res.* **1999**, *32*, 407-414.

(28) Lee, J.; Sundar, V. C.; Heine, J. R.; Bawendi, M. G.; Jensen, K. F. *Adv. Mater.* **2000**, *12*, 1102-1105.

(29) Mamedov, A. A.; Belov, A.; Giersig, M.; Mamedova, N. N.; Kotov, N. A. *J. Am. Chem. Soc.* **2001**, *123*, 7738-7739.

(30) Hu, J.; Li, L.-s.; Yang, W.; Manna, L.; Wang, L.-w.; Alivisatos, A. P. *Science* **2001**, *292*, 2060-2063.

(31) Bangs Laboratories, I.: www.bangslabs.com, 2004.

(32) Rockenberger, J.; Troeger, L.; Kornowski, A.; Vossmeyer, T.; Eychmueller, A.; Feldhaus, J.; Weller, H. *J. Phys. Chem. B* **1997**, *101*, 2691-2701.

(33) Weller, H.; Schmidt, H. M.; Koch, U.; Fojtik, A.; Baral, S.; Henglein, A.; Kunath, W.; Weiss, K.; Dieman, E. *Chem. Phys. Lett.* **1986**, *124*, 557-560.

(34) Ji, T.; Fang, J. *Abstracts of Papers, 225th ACS National Meeting, New Orleans, LA, United States, March 23-27, 2003* **2003**, INOR-241.

(35) Yan, Y.-l.; Li, Y.; Qian, X.-f.; Yin, J.; Zhu, Z.-k. *Mater. Sci. Eng., B* **2003**, *B103*, 202-206.

(36) Sunkara, H. B.; Jethmalani, J. M.; Ford, W. T. *J. Polym. Sci., Part A: Polym. Chem.* **1994**, *32*, 1431-1435.

(37) Ford, W. T.; Yu, H.; Lee, J. J.; El-Hamshary, H. *Langmuir* **1993**, *9*, 1698-1703.

(38) Kim, J. H.; Chainey, M.; El-Aasser, M. S.; Vanderhoff, J. W. *J. Polym. Sci., Part A: Polym. Chem.* **1989**, *27*, 3187-3199.

(39) Bures, P.; Huang, Y.; Oral, E.; Peppas, N. A. *Journal of controlled release* **2001**, *72*, 25-33.

(40) Batra, D.; Shea, K. J. *Current Opinion in Chemical Biology* **2003**, *7*, 434-442.

(41) Underwood, S.; Mulvaney, P. *Langmuir* **1994**, *10*, 3427-3430.

(42) Sherman, R. L., Jr.; Chen, Y.; Ford, W. T. *J. Nanosci. Nanotech.* **2004**, 4, 1032-1038.

(43) Kreider, J. L.; Ford, W. T. *J. Polym. Sci., Part A: Polym. Chem.* **2001**, *39*, 821-832.

(44) Tan, S.; Sherman, R. L., Jr.; Ford, W. T. *Langmuir* **2004**, *20*, 7015-7020.

Chapter IV

CORE/SHELL POLYSTYRENE/POLY(METHYL METHACRYLATE) LATEXES

Abstract

Cationic core/shell polystyrene/poly(methyl methacrylate) latexes (PS/PMMA) have been produced with a core:shell diameter ratio of 1:7.5 and a core:shell volume ratio of 1:420. These particles were produced using starved semi-continuous emulsion polymerization, in three successive growth steps. The cross-linked 80% polystyrene/20% poly(methyl methacrylate) seed (70 nm) was grown to approximately double the original diameter three times to give 160, 300 and 530 nm particles respectively. Dynamic light scattering (DLS) and scanning electron microscopy (SEM) were used to determine particle sizes while stained microtomed samples were inspected internally by transmission electron microscopy (TEM). Growth using larger core latexes resulted in growth to 800 nm, but second generation latex particles prevailed after 800 nm.

Introduction

Polystyrene (PS) and poly(methyl methacrylate) (PMMA) are immiscible polymers with different polarities and refractive indexes (n).[1,2] Because these two polymers are immiscible, yet their respective mononomers are soluble in both polymers, various types of composites have been studied.[1] Composites of PS and PMMA have been previously investigated because of their many interesting morphologies, and subsequent physical properties. The morphologies (shape caused by the segregation of two immiscible polymers) of these composites are determined by how the polymers are made or mixed. Specific examples of PS/PMMA composite materials include latex particles,[3-5] dispersion particles,[6,7] block and random copolymers[8] and homopolymer blends.[9] The morphology of these materials can be controlled kinetically or thermodynamically. Under thermodynamic morphology control, core/shell and inverted core/shell structures are formed as seen in Scheme 1.[1,6] Kinetic morphologies, seen in Scheme 1, are a result of restricting an equilibrium structure.[1,6] However, these kinetic structures can be converted to the more thermodynamically stable structure. For example; multiple core latexes can be thermally annealed to give core/shell latexes. The morphologies of these composites are controlled by many factors including: differences in the solubilities of the monomers and the polymers,[1] the viscosity of monomer swollen polymer,[1,3,4,6,10] the rate of radical transport into polymer,[1,3,6] cross-linking,[1,11] the differences in polarity of the monomers and polymers[1,10] and the charge of the initiator.[1] This gives rise to kinetic and thermodynamic control of morphology, depending on many

variables including monomer, polymer and initiator concentrations,[1,3-6,10] temperatures,[12] solvent[4,7] and charge of the molecules used[4,13-15]

Scheme 1. Various Polymer Particle Morphologies

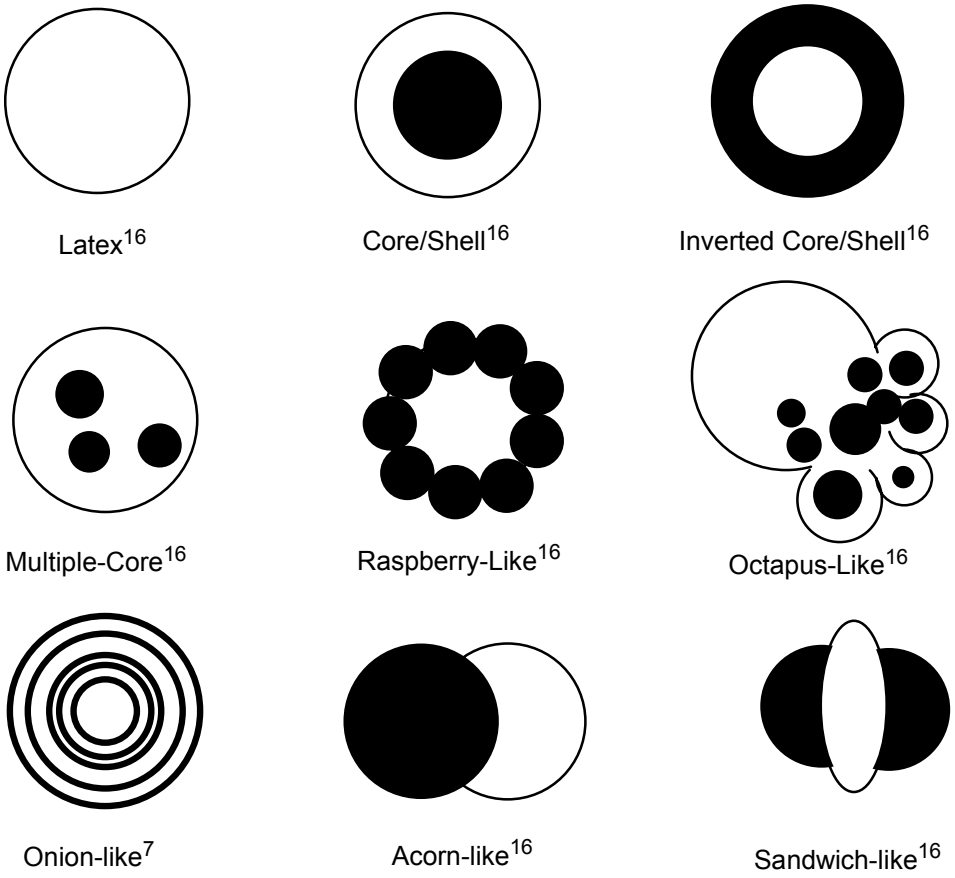

Several methods have been used for forming core/shell PS/PMMA particles including latex seed growth by monomer swelling,[1,4,10,11] batch[1,4,10] and semi-batch[1,3,4,10] polymerization and starved[3,4,10,14] polymerization. Dispersion polymerization has been used to control morphology of large particles[6,7] while other PS/PMMA composites have been formed by heterocoagulation,[8,15] and thermal annealing[12] of preformed PS/PMMA

composite particles. In these methods the many variables used in the synthesis allow for kinetic or thermodynamic control of morphology.[1,6]

The goal of this research is to form micron-sized polymer particles that contain a small core with refractive index much different from the thick shell. This material is to be used for light scattering experiments. To be useful in light scattering experiments, these core/shell latexes must meet several strict conditions. First, the shell must have a lower refractive index than the core, and the shell's refractive index must be relatively low. Second, the core must have a diameter approximately one tenth the size of the shell; large shells are not normally seen in the literature. Third, the polymers used must be immiscible in one another and be glassy, not crystalline. Finally, the particles must be dispersable in water and in a solvent with a refractive index that matches the shell, and that swells neither the shell nor the core. To achieve these goals PS/PMMA core/shell latexes have been chosen and are depicted in Scheme 2. Polystyrene with refractive index 1.59[2] have contrast compared to PMMA's refractive index of 1.49.[2] Refractive index matching solvent *cis*-decahydronaphthalene, n = 1.48,[16,17] can be used to disperse these particles without swelling the PMMA shell.

Scheme 2. PS/PMMA Core/Shell Latex

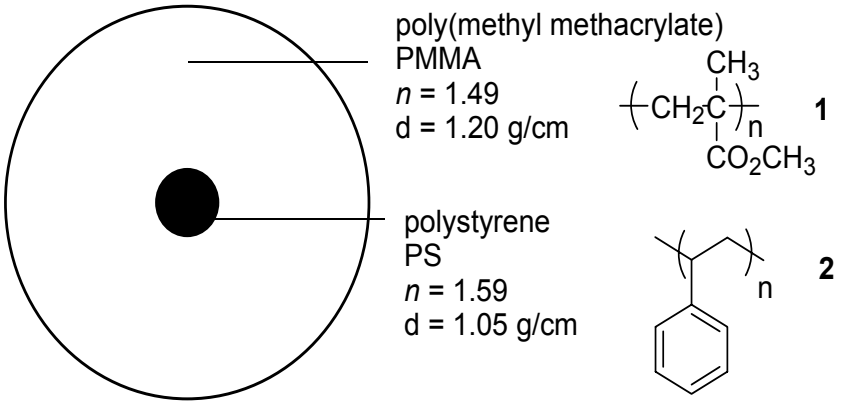

The group of Dr. Penger Tong at the Hong Kong University of Science & Technology, will measure the diffusion coefficients of the particles in concentrated dispersions by light scattering. Since homopolymer latexes scatter light, concentrated dispersions of latexes result in multiply scattered light as shown in Figure 1A. Multiply scattered light is not useful for particle motion studies using dynamic light scattering techniques. The core/shell particles with a 1:10 diameter ratio have a 1:1000 volume ratio. In a refractive index matching solvent, the large shell can not scatter light and only the small core can scatter light. With a 1:1000 difference in volume between the core and shell, the concentrated dispersions appear to be 1000 times more dilute than they actually are. This dilution effect will make particle tracking in concentrated dispersion possible as shown in Figure 1B.

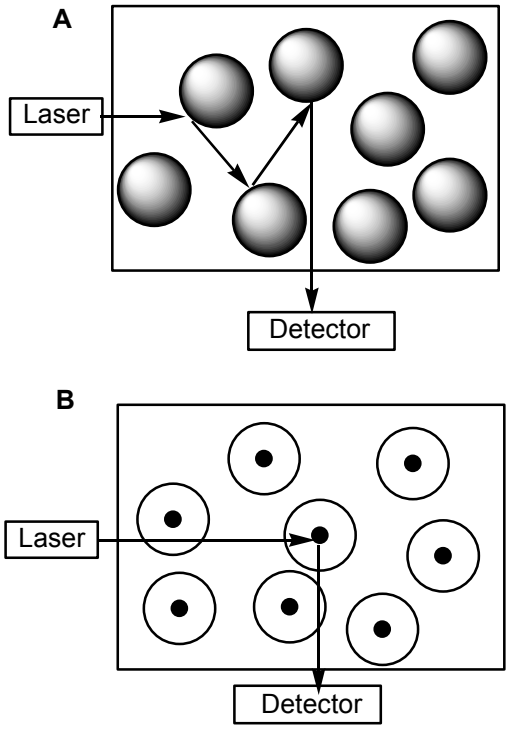

Figure 1. (A) Light scattering by homogeneous particles. (B) Light scattering by core/shell particles with solvent matched to the refractive index of the particles shell.

To obtain core/shell latexes, seeded emulsion polymerization techniques can be used.[3,4] These methods use preformed PS latex cores (seeds) that can have a PMMA shell grown onto the exterior, kinetically or thermodynamically. Since growth of the latexes can result in a 1000 fold increase in volume, the growth of the shell must be done in several steps. Since a 1000-fold difference is desired, three growth steps, with each step increasing the volume by 10 times or $\sqrt[3]{10}$ in diameter, were planned. Without three steps 1 g of seed latex would require 1000 g of MMA monomer and approximately 10 L of solvent as seen in Figure 2A. In the stepwise method, 1 g of seed can be grown to 10 g

of product. Of that 10 g of product, 1 g can be used as seed for the next growth step. In this stepwise method, only 30 g of monomer are consumed as seen in Figure 2B.

A

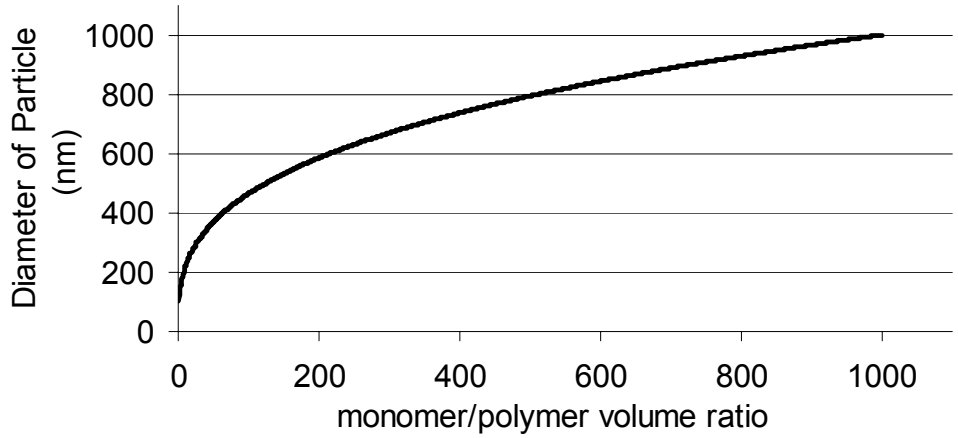

B

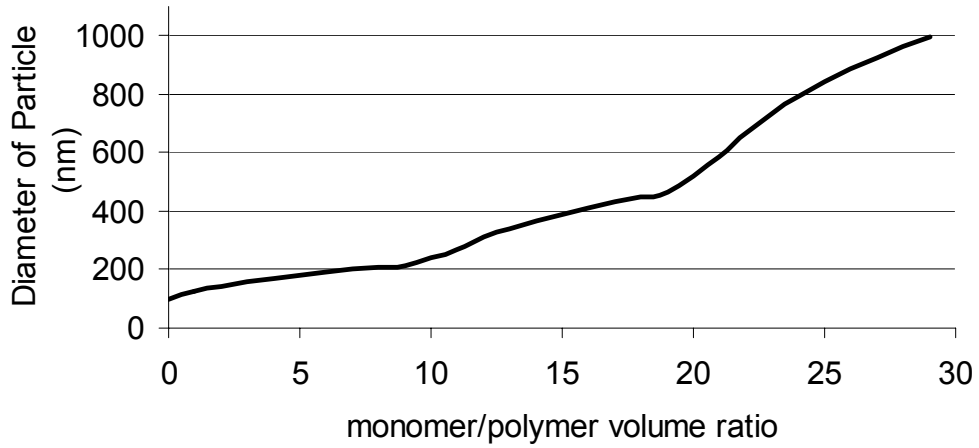

Figure 2. Theoretical growth of 100 nm spheres by two different methods. (A) Ten times diameter growth in one step. (B) Ten times diameter growth in three steps.

Results and Discussion

PMMA Shell Growth by Monomer Swelling. Historically, large scale growth of latex spheres has been accomplished by seeded emulsion polymerization in which a small latex seed is swollen to many times its original diameter with monomer.[11,18-20] This monomer swollen latex seed is then polymerized by conventional free radical polymerization.[21] Typically under these conditions surfactant stabilization is needed and the final latex is composed of only one polymer.[19,20] Since poly(methyl methacrylate) is insoluble in polystyrene, but methyl methacrylate monomer is highly soluble in polystyrene, core/shell latexes were investigated using the seed growth method with monomer swelling to produce a thermodynamically controlled morphology as seen in Scheme 3.

Scheme 3. Core/Shell Latex by Monomer Swelling

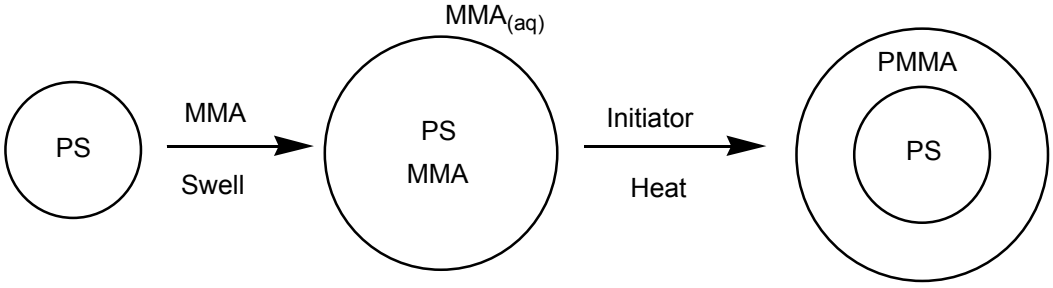

In the growth mechanism shown in Scheme 3, a preformed polystyrene seed latex is swollen with methyl methacrylate monomer over a period of time. After swelling is complete the polymerization is initiated, preferably from the solution. The growing

polymer chains collide with the swollen latex and begin polymerizing the monomer inside. This results in pure PMMA chains. Since polymerization starts outside of the latex, and PMMA is more hydrophilic than polystyrene, a PMMA shell is created.

Results from this set of experiments were not promising. Over 150 separate experiments attempted to use seed swelling to gain a PMMA shell. Typical results gave new small PMMA particles or, in the best cases, PMMA domains on the seed latex. Many different variables were controlled to determine the best method for shell growth including: monomer swelling rates, monomer swelling temperatures, co-monomer charge, initiator charge, polymerization temperatures, agitation methods, surfactant assistance, co-solvents, seed concentration, monomer concentration, seed charge, seed composition, seed cross-linking, and swelling agents. Some surfactants were found to give PMMA domains on the surface. Cationic seeds and initiators worked better than anionic or non-ionic materials. Cross-linked seeds showed no sign of growth. Room temperature swelling with slow addition of monomer prevented particle aggregation. The best results came when hexadecane was introduced to the seed latex before MMA addition, based on the methods of Ugelstad.[19,20] Hexadecane, with the aid of 50% ethanol solvent, was swollen into the polystyrene. Once the swollen latex was purified by ultrafiltration, the hexadecane produced an osmotic pressure that drove MMA into the PS seed. However, an off-center inverted core/shell structure was achieved, resembling a stuffed olive. Since no core/shell materials could be produced, and growth that had been achieved did not meet theoretical values, this method was abandoned.

Shell Growth by Semi-Continuous Seeded Emulsion Polymerization. Since monomer swollen latexes, under thermodynamic control, did not produce core/shell materials, a kinetically controlled method of shell growth was devised.

Törnell showed that a thin uniform polystyrene shell could be formed on PMMA latexes using starved semi-continuous emulsion polymerization.[4,14] In starved semi-continuous emulsion polymerization, monomer is slowly added to the reaction vessel that contains seed latexes and a high concentration of initiator radicals. Since there is a high concentration of radicals in solution, polymerization occurs very rapidly. The growing polymer chains, and possibly primary particles that may form, collide with the high surface area latex seeds, before having the chance to form mature latex particles as shown in Scheme 4.[3,21] This growth of the seed latex was facilitated by some degree of monomer swelling from the solution into the latex seed's surface as shown in Scheme 4. The amount of swelling was kept low due to continuous entrance of growing radical chains, and the slow rate of monomer addition.[1,3,4] The overall morphology of the core/shell particle was kinetically controlled due to the slow diffusion of high molecular weight polymer.[1,3]

Scheme 4. Starved Semi-Continuous Emulsion Polymerization.

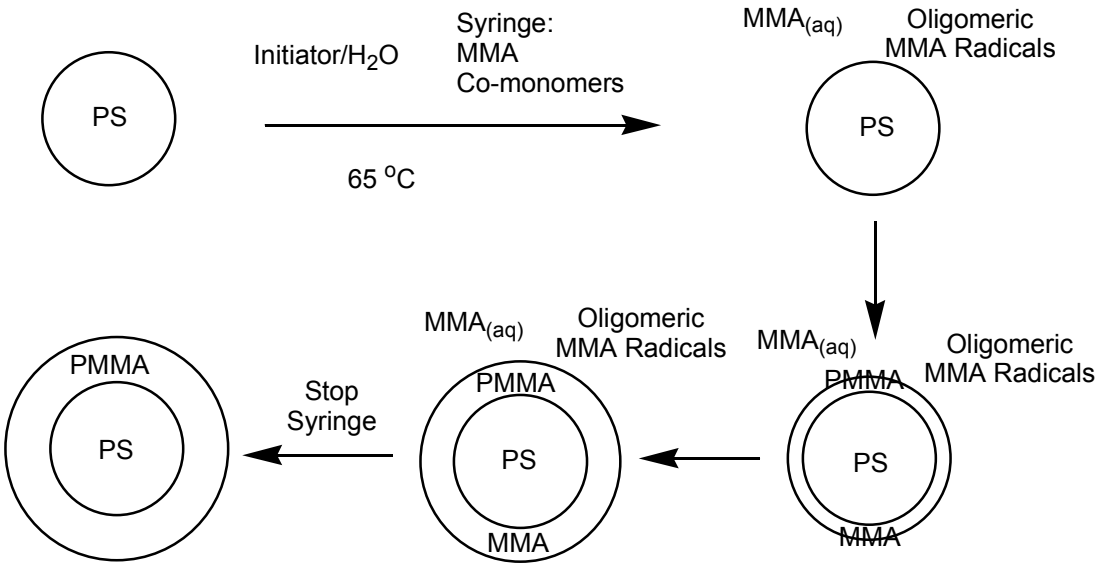

To achieve the high number of aqueous radicals needed to do a starved polymerization reaction, a radical initiator with a short half-life was needed. This was achieved by using the initiator VA-044, (2,2'-azobis[2-(2-imidazolin-2-yl)propane] dihydrochloride, (**3**). This commercially available cationic azo initiator has a 10 hour half life at 44 °C.[22] At a polymerization temperature of 65 °C, a half life of approximately 40 minutes is achieved. Since VA-044 is cationic, cationic core/shell latexes have been synthesized. Very little core/shell research has been done with cationic materials. To aid in the colloidal stability of these latexes extra cationic monomer was added in the form of 2-(dimethylamino)ethyl methacrylate (**4**), and a cross-linking monomer, ethylene glycol dimethacrylate (**5**), was added to help reduce flow of the polymer shell.[1,11] Seeds used for shell growth are seen in Table 1 and results for the starved semi-continuous emulsion polymerization are seen in Table 2.

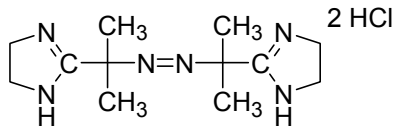

3

2,2'-Azobis[2-(2-imidazolin-2-yl)propane] dihydrochloride

VA-044

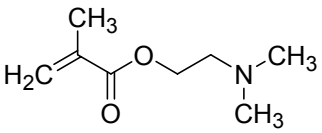

4

2-(dimethylamino)ethyl methacrylate

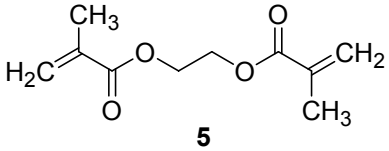

5

ethylene glycol dimethacrylate

Table 1. Seeds used for Shell Growth

sample	MMA (mL)	styrene (mL)	water (mL)	VA-044 (mg)	T (^{o}C)	DLS (nm)	SEM[a] (nm)
446	1.0	3.0	40	20	65	327	320
491	2.0	8.0	100	150	80	50	70

[a]PDI not reported due to uncertainty during particle measurement. [b]0.200 g of vinybenzyl(trimethyl)ammonium chloride and 0.150 g of divinylbenzene comonomers.

Table 2. Shell Growth of Seed Latex by Starved Semi-Continuous Emulsion Polymerization

sample	seed (g)	solution (mL)	VA-044 (mg)	MMA (mL)	MMA Rate (mL/h)	DLS (nm)	SEM (nm)
455	0	10	10	1.0[a]	0.5	330	-
458	**446**[b] (1.0)	110	150	9.0[c]	4.0	780	730
460	**458** (0.15)	10	10	0.15	-	poly	930,270
461	**458** (0.2)	20	15	1.6[d]	0.7	poly	1200,770
492	**491**[e] (1.0)	115	150	9.0[c]	4.0	101	160
493	**492** (1.0)	115	150	9.0[c]	4.0	255	300
494	**493** (1.0)	115	150	9.0[c]	4.0	507	530

[a]10 mg of **4** and 10 mg of **5.** [b]320 nm by SEM. [c]60 mg of **4** and 60 mg of **5**. [d]15 mg of **4** and 15 mg of **5**. [e]70 nm by SEM.

Results from the growth of two different seed particles are given in Table 2. The first entry, **455**, was a control experiment with no seed, entries **458-461** used a 75%/25% PS/PMMA copolymer latex while the last three entries, **492-494**, used an 80%/20% PS/PMMA cross-linked copolymer latex core. Random PS/PMMA core latexes were needed because pure PS latexes resulted in aggregation and no shell growth, of PS or PMMA particles during standard seeded emulsion polymerization. A random PS/PMMA copolymer core is not a problem because the polymer has a refractive index equal to the sum of the products of the percent polymer and its respective refractive index. One

possible reason that a copolymer seed was needed was that during emulsion polymerization the growing PMMA chain needed a compatible polymer to attach to. The PS/PMMA seed used had PMMA rich domains that were formed in the initial stages of the seed polymerization in solution.[21] These PMMA rich domains segregate to the surface of the latex, making future PMMA attachment more probable. Finally PS and PMMA are not soluble in one another. A highly starved polymerization may result in no PMMA growth on a pure PS surface and result in aggregated material.

Growth of the shell was found to work best with slow addition of PMMA. However, the initiator needed to be added in one batch 10 minutes prior to monomer addition. Addition of a second batch of initiator, during the monomer addition process, resulted in second generation particles. Therefore, addition of MMA had to be at a rate such that monomer swelling was not competing with the polymerization reaction, and the amount of initiator at the end of the monomer addition was adequate to carry the polymerization to completion in a starved growth manner. These conditions were found when the last of the monomer was added approximately 2 hours after the addition began, and the oil bath temperature was kept at 70 ^{o}C.

Growth of the 320 nm latex **446,** to give the 730 nm latex **458,** was found to be reproducible and gave monodisperse products shown in Figure 3b. Subsequent growth above 800 nm was not possible due to the formation of second generation particles. Several different methods of growth were attempted, with **460** (swelling method) and **461** (starved semi-continuous growth method) being representative samples as shown in Figure 3c,d and Table 1. This set of experiments was carried out on other seed latexes similar to **446**, with easy growth to 800 nm, but growth above 800 nm was found to

always give polydisperse samples. This was due to the rapidly decreasing surface area, for a given weight of seed, of the latex particles shown in Figure 4. This decrease in surface area per volume increases the chances of the growing chains colliding with one another to form primary particles and the primary particles aggregating to form new mature particles. Since the new mature particles have much higher surface area than the seed latex, growth of the second generation particles will be much faster than the original seed. The growth of second generation particles and the slow growth of the seed latex was seen in Figure 3c and d and Table 1. Attempts at controlling particle concentration, cationic monomer, monomer addition rate and several other variables resulted in the same polydispersity once 800 nm was reached.

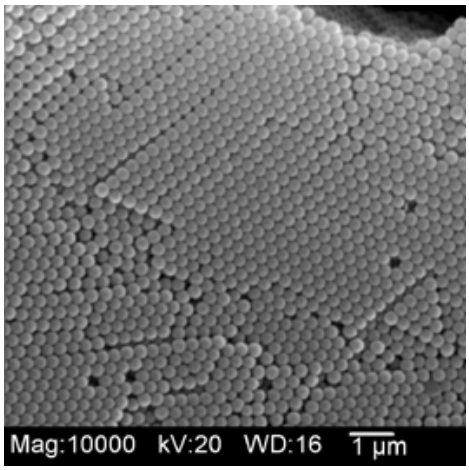
Mag:10000 kV:20 WD:16 1 µm

(a)

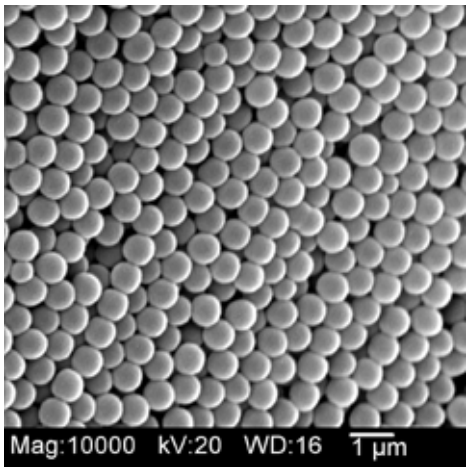
Mag:10000 kV:20 WD:16 1 µm

(b)

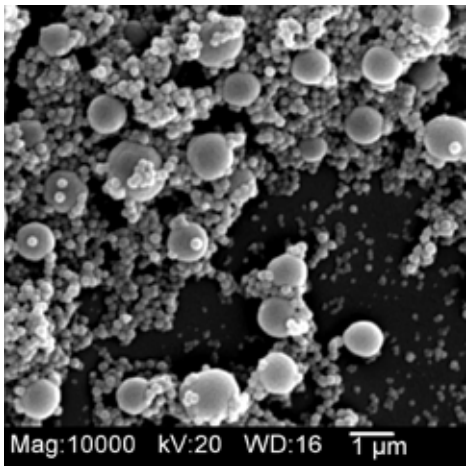
Mag:10000 kV:20 WD:16 1 µm

(c)

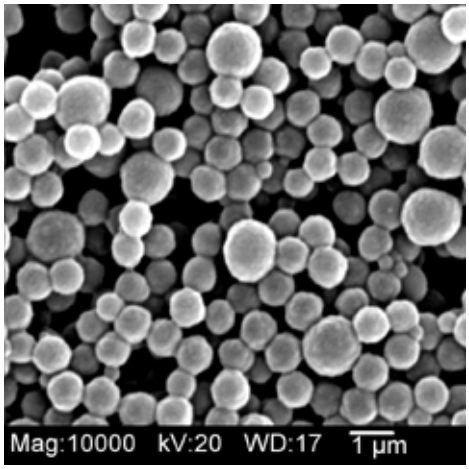

(d)

Figure 3. SEM images of (a) 300 nm 80/20 PS/PMMA core latex **446**, (b) sample **458** from growth step 1, (c) sample **460** from growth by monomer swelling, (d) sample **461** from growth by starved emulsion polymerization.

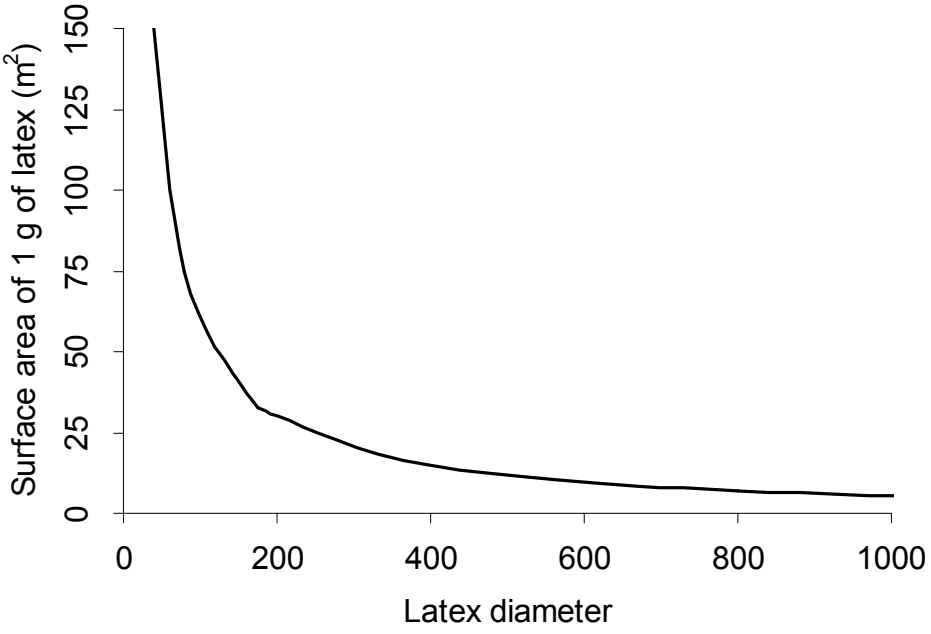

Figure 4. Surface area vs. latex diameter

Since a core/shell diameter ratio of approximately 1/10 was desired, a smaller core was produced such that a 1/10 diameter ratio was achieve before 800 nm was achieved. In addition to having a smaller core, the core was cross-linked to prevent the core from dispersing in the core/shell latex. The new smaller core **491** was cross-linked by 1.5% with divinylbenzene and had a diameter of 50 nm by DLS and 70 nm by SEM and TEM. Growth of seed **491** by an approximate doubling of the diameter in three steps resulted in an increase in diameter from 70 nm to 160, 300 and 530 nm, respectively by SEM, Figure 5. This resulted in a core to shell diameter ratio of 1 to 7.5 or a core to shell volume ratio of 1 to 420. This result was slightly less than the amount expected for three doubling steps where a core to shell diameter ratio of 1 to 8 and a core to shell volume ratio of 512 would be expected. This smaller size can be explained by the higher density of PMMA compared to MMA, 1.2 vs. 0.94 g/cm^3, and inaccuracies in measuring the weight of seed polymer. Further growth to give a full 1:10 diameter ratio could be easily achieved by doubling the mass of the core to give a final diameter of 700 nm.

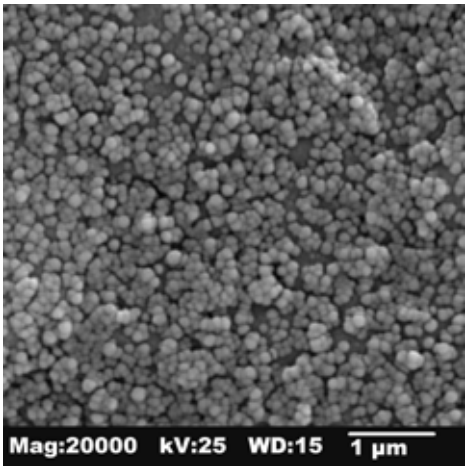

(a)

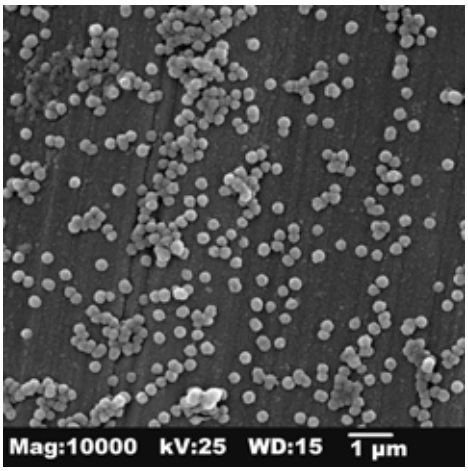

(b)

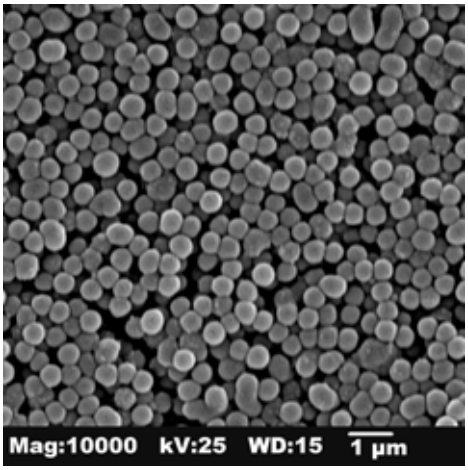

(c)

Figure 5. SEM images of particles from (a) first growth step (**492)**, (b) second growth step (**493)** and (c) third growth step (**494).**

To determine if a true core shell morphology was achieved, the latex particles were dispersed into epoxy resin, the resin was sliced into 70 nm thick slices and the polystyrene was stained with ruthenium tetroxide.[23] Ruthenium tetroxide was used because it is a very reactive molecule that readily sublimes, reacts selectively with aromatic rings but not with epoxy or PMMA and as a metal, with atomic weight of 101,

scatters electrons to give contrast in transmission electron microscopy. This results in dark polystyrene spots and a medium gray epoxy background. The PMMA was not seen in TEM and was represented by the lightest colored spots. This was due to the fact that PMMA depolymerizes under the electron beam. This results in an immediate destruction of the PMMA, as seen by the PMMA evaporating or in some cases boiling or splattering in the TEM.

Negatives of sectioned TEM samples **493** and **494** show light stained polystyrene spots, and **493** and **494** show the dark colored PMMA areas, as seen in Figure 6. Sample **492** was too concentrated in the epoxy, and the electron beam destroyed not only the sample but also the epoxy resin, so no TEM was available. Samples **493** and **494** both show clear core/shell structure. Not all the PMMA spots in Figure 6 are of the same size, this was due to the microtoming process. During microtoming the latex particles were suspended three dimensionally in the epoxy. As the sample was cut, the particles were cut through various areas, so that only the samples cut through the center were of the correct size and contained a core. Those spheres that were cut off center were smaller and contained no core or only a small portion of the core. The location of the core by TEM was also questionable. This was because the destruction of the PMMA might not be uniform or might be violent, which could move or even melt the polystyrene core. Also the microtoming process commonly distorts deformable polymeric materials by shearing them.

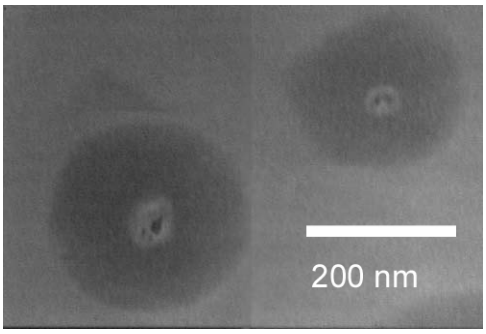

(a)

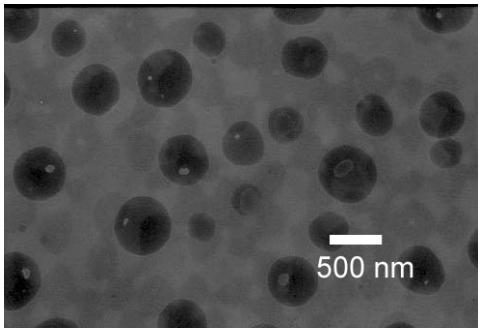

(b)

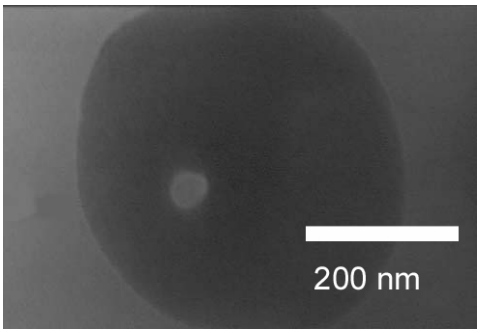

(c)

Figure 6. TEM images of (a) second growth step **493**, (b), third growth step **494,** (c) third growth step **494.**

Conclusions

Core/shell polystyrene/poly(methyl methacrylate) latexes have been synthesized. Methods to produce core/shell latexes by monomer swelling of preformed latexes failed. Starved semi-continuous emulsion polymerization to give PMMA shells only occurred when polystyrene/poly(methyl methacrylate) random copolymer latex cores were used. This method was found to be a quick and easy method when the short half-life cationic initiator VA-044 was used. Core/shell materials starting with 300 nm cores were found to grow to 800 nm, after which subsequent growth resulted in second generation particles. Since our goal of a 200 nm core and with a 2000 nm shell could not be achieved, a smaller 70 nm core was found to be useful for the forming of a thick PMMA shell. The final product had a diameter of 530 nm and a core:shell diameter ratio of 1:7.5. These core/shell particles may still be useful for DLS studies in concentrated dispersions since 70 nm particles are easily resolved by light scattering.

Future Work

The first experiment that needs to be done is the incorporation of nanoparticles or long-lived fluorescent dyes into the polystyrene core. These materials can be used for optical tracking of the core. This can be accomplished by the synthesis of an anionic core/shell material. Using the method of Törnell[4,14] to catalyze the rate of persulfate initiation, or by using an anionic initiator with a short half life such as VA-057 (2,2'-azobis[*N*-(2-carboxyethyl)-2-methylpropionamidine]tetrahydrate) from Wako would allow for rapid initiation. Then, several of the nanoparticle/polystyrene latexes from Chapter III could be used as seeds for fluorescent core/shell materials.

A second experiment that could be attempted is to produce an inverted core/shell material, with a small PMMA core and a thick polystyrene shell. Thin polystyrene shells around PMMA cores are prevalent in the core/shell latex literature, but thick PS shells are not found. This would also allow for better imaging of large latexes since the polystyrene is not damaged by the TEM's electron beam.

Finally, optical studies on colloidal crystals of core/shell materials should be made. Since the cores have tunable sizes and the shell thickness can be tuned, many different colloidal crystal samples can be prepared. These materials may have interesting optical properties compared to the standard homopolymer latexes.

Other methods using the starved semi-continuous emulsion polymerization will be discussed in Chapter V.

Experimental

General Methods. All monomers were purchased from Aldrich or Fisher; VA-044 was purchased from Wako Specialty Chemicals and ruthenium tetroxide was purchased from Polysciences. Divinylbenzene was pure to 55%. Water was purified to a conductance of <4 μohm^{-1} cm^{-1} using a three-column Barnstead e-pure system. Monomers were purified by passing through a basic alumina column to remove inhibitors. Dynamic light scattering sizes were determined using a Malvern HPPS 5001 high performance particle sizer with 1 cm quartz cuvettes at 20 ^{o}C. Transmission electron microscope images were measured using a JEOL 100 keV microscope with Formvar coated nickel grids. Scanning electron microscope images were measured using a JEOL JXM 6400 microscope with samples cast onto aluminum stubs and coated with

Au/Pd. Ultrafiltration was carried out using 100, 220 and 450 nm cellulose acetate/nitrate Millipore filters.

Non-Cross-Linked 300 nm Seed Latex (446). In a 100-mL round-bottomed flask submerged in a 65 ^{o}C oil bath and equipped with a nitrogen purged condenser, 1.0 mL of methyl methacrylate, 3.0 mL of styrene and 40 mL of water were stirred with a 1-inch magnetic stirring bar. After 20 min of heating, 20 mg of VA-044 initiator was added. The polymerization was carried out for 8 h. The final latex was filtered through cotton and then ultrafiltered for 24 h using 100 nm filters with multiple water changes. The final product had particle sizes of 327 nm by DLS and 320 nm by SEM.

Shell Growth (458). In a 250-mL two-necked round-bottomed flask equipped with a nitrogen-purged condenser and a syringe pump, 1.0 g of **446** (10 mL of solution) and 100 mL of water were heated and stirred with a 1.5-inch magnetic stirring bar for 10 min in a 70 ^{o}C oil bath. To the heated mixture, 150 mg of VA-044 was added and heating was continued for 10 min to begin the generation of radicals. The syringe pump was started and 9.0 mL of methyl methacrylate, 60 mg of ethylene glycol dimethacrylate and 60 mg of 2-(dimethylamino)ethyl methacrylate were added at a rate of 4.0 mL/h. After 3 h, the reaction was stopped and filtered through a cotton plug. DLS size of 780 nm and SEM size of 730 nm were observed.

Cross-Linked 70 nm Seed Latex (491). In a 250-mL round-bottomed flask submerged in an 80 ^{o}C oil bath and equipped with a nitrogen-purged condenser, 100 mL of water, 8.0 mL of styrene, 2.0 mL of methyl methacrylate and 0.200 g of vinylbenzyl(trimethyl)ammonium chloride were stirred with a 1.5-inch magnetic stirring bar. After 30 minutes of heating, 0.150 g of VA-044 was added. Once the reaction

mixture became turbid, 0.150 g of divinylbenzene was added as a cross-linking agent. The reaction was carried out for 2 h, after which the latex was filtered through cotton. The product had a final size of 50 nm by DLS and 70 nm by TEM.

Shell Growth (492). Using the method of **458**, 1.0 g of **491** (14 mL of solution), 100 mL of water, 150 mg of VA-044, 9.0 mL of methyl methacrylate, 60 mg of ethylene glycol dimethacrylate and 60 mg of 2-(dimethylamino)ethyl methacrylate produced particles with a DLS size of 101 nm and SEM size of 160 nm.

TEM Preparation of 491-494.[23] Epoxy embedded core/shell materials were prepared by drying latex samples **491-494** and dispersing in ethanol. A small portion of the ethanol dispersion was dispersed into PolyBed 812 epoxy resin. The samples were cured overnight in an oven at 60 ^{o}C. Samples were ultra-microtomed to a thickness of 70 nm, and placed on Formvar coated nickel TEM grids. The grids were placed in a petri dish, and one drop of aqueous 0.5% RuO_4 solution was placed 0.5 cm from each grid. The cover was placed on the dish and the dish was allowed to stand for 30 minutes in the fume hood. The excess RuO_4 was removed by pipette and the stained samples were allowed to stand overnight before TEM analysis.

References

(1) Sundberg, D. C.; Durant, Y. G. *Polymer Reaction Engineering* **2003**, *11*, 379-432.

(2) Mark, J., E., Ed. *Polymer Data Handbook*; Oxford University Press: New York, 1999.

(3) Stubbs, J.; Karlsson, O.; Jonsson, J.-E.; Sundberg, E.; Durant, Y.; Sundberg, D. *Colloids Surf., A: Physicochemical and Engineering Aspects* **1999**, *153*, 255-270.

(4) Joensson, J. E. L.; Hassander, H.; Jansson, L. H.; Toernell, B. *Macromolecules* **1991**, *24*, 126-131.

(5) Joensson, J.-E.; Hassander, H.; Toernell, B. *Macromolecules* **1994**, *27*, 1932-1937.

(6) Okubo, M.; Izumi, J. *Colloids Surf., A: Physicochemical and Engineering Aspects* **1999**, *153*, 297-304.

(7) Okubo, M.; Takekoh, R.; Izumi, J. *Colloid Polym. Sci.* **2001**, *279*, 513-518.

(8) Ito, F.; Ma, G.; Nagai, M.; Omi, S. *Colloids Surf., A: Physicochemical and Engineering Aspects* **2002**, *201*, 131-142.

(9) Tsai, I. Y.; Kimura, M.; Russell, T. P. *Langmuir* **2004**, *20*, 5952-5957.

(10) Karlsson, L. E.; Karlsson, O. J.; Sundberg, D. C. *J. Appl. Polym. Sci.* **2003**, *90*, 905-915.

(11) Durant, Y. G.; Sundberg, E. J.; Sundberg, D. C. *Macromolecules* **1997**, *30*, 1028-1032.

(12) Lee, C.-F. *J. Appl. Polym. Sci.* **2003**, *88*, 312-321.

(13) Wang, Z.; Paine, A. J.; Rudin, A. *J. Colloid Interface Sci.* **1996**, *177*, 602-612.

(14) Joensson, J.-E.; Karlsson, O. J.; Hassander, H.; Toernell, B. *Macromolecules* **2001**, *34*, 1512-1514.

(15) Omi, S.; Fujiwara, K.; Nagai, M.; Ma, G.-H.; Nakano, A. *Colloids Surf., A: Physicochemical and Engineering Aspects* **1999**, *153*, 165-172.

(16) Dullens, R. P. A.; Claesson, M.; Derks, D.; Van Blaaderen, A.; Kegel, W. K. *Langmuir* **2003**, *19*, 5963-5966.

(17) Lide, D. R. *Handbook of Chemistry and Physics, 73rd Edition*; CRC Press, Inc., 1993.

(18) Okubo, M.; Shiozaki, M.; Tsujihiro, M.; Tsukuda, Y. *Colloidd Polym. Sci.* **1991**, *269*, 222-226.

(19) Ugelstad, J. *Makro. Chemie* **1978**, *179*, 815-817.

(20) Ugelstad, J.; Kaggerud, K. H.; Hansen, F. K.; Berge, A. *Makro. Chemie* **1979**, *180*, 737-744.

(21) Lovell, P., A.; Al-Aasser, M., S. *Emulsion Polymerization and Emulsion Polymers*; Wiley: Chichester, 1997.

(22) Wako; http://www.wakousa.com/specialty/index.html, 2004; Vol. 2004.

(23) Lee, S.; Rudin, A. *ACS Symposium Series* **1992**, *492*, 234-254.

CHAPTER V

SYNTHESIS AND CATALYTIC ACTIVITY OF LONG CHAIN QUATERNARY AMMONIUM POLY(PROPYLENEIMINE) DENDRIMERS

Abstract

Quaternary ammonium poly(propylenimine) dendrimers were synthesized from tertiary methylated poly(propylenimine) octaamine, dotriacontamine and tetrahexacontaamine dendrimers (TAM D8, D32 and D64) in DMF using 1-iodobutane, benzyl bromide, 1-bromo-2-ethylhexane, 1-bromooctane, 1-bromododecane and 1-bromohexadecane. The degree of quaternization was controlled by varying the mol ratio of alkyl halide to dendrimer. These new hydrophobic dendrimers make suitable unimolecular phase transfer catalysts. The rates of decarboxylation of 6-nitrobenzisoxazole-3-carboxylate were measured at concentration of dendrimer cationic repeat units between 2.45 xX 10^{-5} and 3.28 x 10^{-2} M at 25 ^{o}C in water. The fastest rates (650 times that in water) were measured for TAM D8 quaternized with 8 dodecyl chains at a concentration of 2.4 mM in quaternary ammonium groups. These materials also showed surfactant properties with critical aggregation concentrations between 3.5 x 10^{-5} and 8.5 x 10^{-4} M in quaternary ammonium groups.

Introduction

Dendrimers are a class of hyperbranched polymers that are extremely monodisperse.[1-3] Dendrimers gain their monodispersity from the fact that they are synthesized using stepwise organic synthesis and are not formed by reactions that give statistical distributions of chain lengths. Using organic synthesis allows for complete branching at each branch point with very few defects. Several approaches have been utilized to form dendrimers including convergent and divergent synthesis. In divergent synthesis the dendrimer is grown stepwise from a core in successive generations, while in the convergent method dendrimer pieces are synthesized separately and later combined with a core or other sections to form the complete dendrimer.[1]

Due to their monodispersity and their large number of functional groups, dendrimers have been investigated for many applications including catalysts,[4-9] drug delivery materials and gene therapy,[10-12] antimicrobial agents[13-15] and polymeric templates.[16,17] Dendrimers are hyperbranched, spherical and symmetric with generations of repeat units grown around the central core as shown in Scheme 1, leading to, at higher generations, a hollow ball like structure.[1]

Scheme 1. Generation 4 PPI Dendrimer

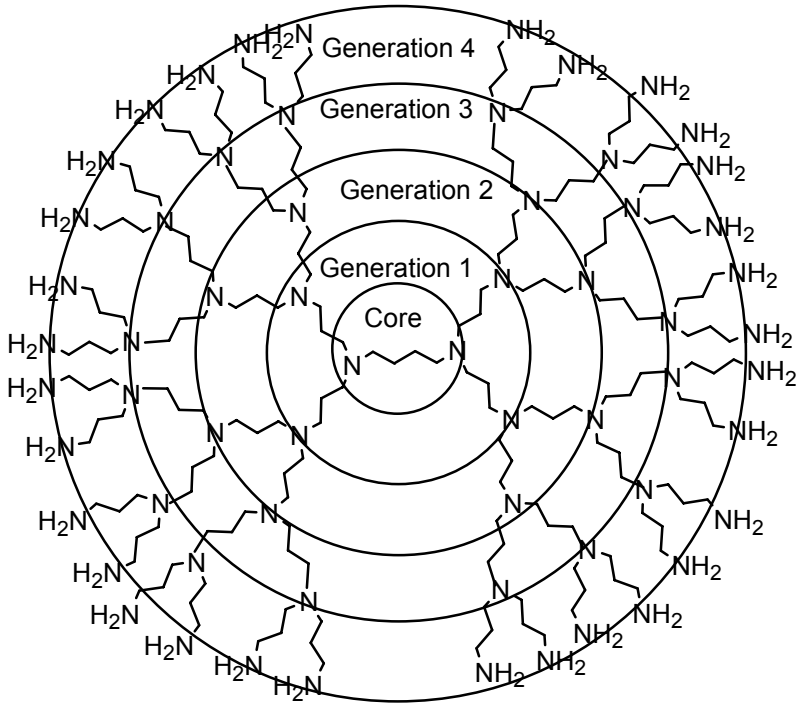

1

We have modified generation two, four and five poly(propyleneimine) dendrimers[1] (PPI), 8, 32 and 64 end group materials, which have the structure shown in Scheme 1, for use as catalysts. Poly(propyleneimine) dendrimers are commercially available materials that consist of n primary amines on the surface and (n-2) tertiary amines in the interior with trimethylene (propylene) groups as spacers. They are made from the Michael addition of acrylonitrile to 1,4-diaminobutane to give the tetracyano product. The cyano product is then reduced to give the external tetra primary amine material.[18] This growth is continued for successive generations, resulting in doubling the number of external amines with each generation. This nearly perfect balance of primary and tertiary amines allows for many useful functionalization reactions, including

selective quaternization of the interior and exterior[9] and alkylation and amidation of the exterior,[7,9] to produce structures such as those in Scheme 2.[7,9]

Scheme 2. Various Quaternary Ammonium Dendrimers

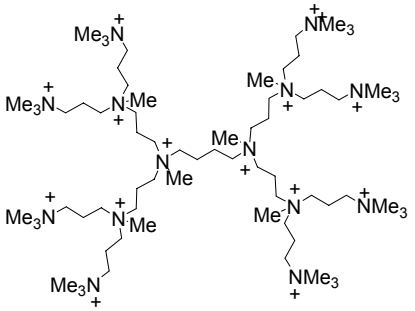

2

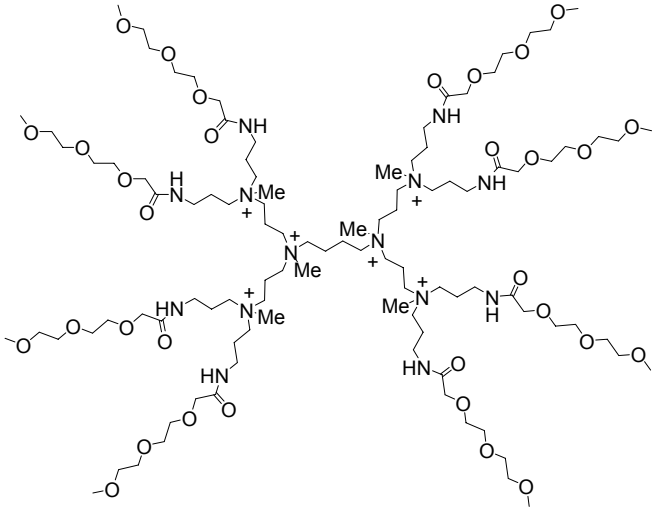

3

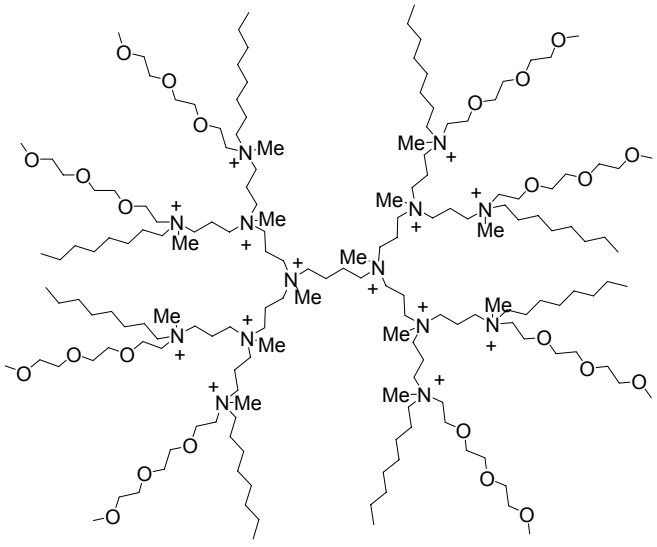

4

Aqueous dispersions of cationic polymers and aggregates of cationic molecules can act as catalysts for reactions of anions.[7,9,19-24] The catalytic activity for bimolecular

reactions is due to their ability to concentrate anionic reactants into a small volume of the aqueous solution.[4-9,19,20,25,26] This speeds up the rate of reaction by bringing reactants together and not by increasing the bimolecular rate constant. Typical materials that have been used as cationic catalysts of this type include: surfactant micelles,[19-21,25,27-31] microemulsions,[32-34] bilayer vesicles,[22,35-38] linear and branched polyelectrolytes[19,39-43] and latexes.[5,24,44-47] Of these materials, polymers have the advantage of activity at all concentrations while monomeric cations must be above a critical aggregation concentration.

Quaternary ammonium dendrimers with a balance of hydrophobic and hydrophilic groups have been shown to be good unimolecular phase transfer catalysts for the decarboxylation of 6-nitrobenzisoxazole-3-carboxylate[5,7,9] (**5**) as shown in Scheme 3. This is a good probe of the environment of the catalyst since, in a balanced hydrophobic/cationic environment, rates of decarboxylation are fast. The materials shown in Scheme 2 have been previously tested as catalysts for this reaction. From kinetic data it was found that the first two materials, permethylated 8 end group dendrimer[9] (**2**) and the internally quaternized MPEG amide[9] (**3**), were poor catalysts due to their highly hydrophilic nature. The last compound[7] (**4**), permethylated with octyl and MPEG amine chains, was found to be a much better catalyst. However, to be active, it had to be a higher generation 4 material with 32 end groups and not the 8 end group material that is shown. All of these materials except the permethylated material are very labor intensive to synthesize and synthetically inefficient.[7] This inefficiency, and relatively low kinetic rate compared to other quaternary ammonium catalysts such as

quaternary ammonium latexes,[24] has led us to investigate a simpler method for synthesis of catalysts with better hydrophobic/hydrophilic balance.

Scheme 3. Reaction of 6-Nitrobenzisoxazole-3-Carboxylate

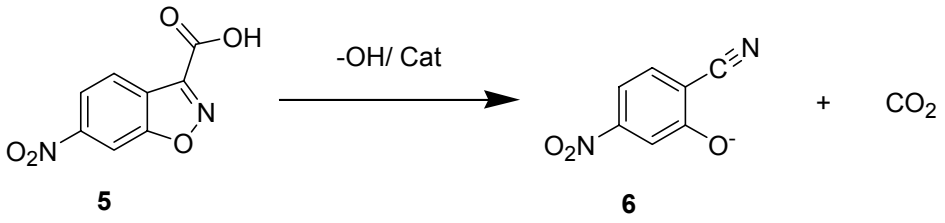

5 **6**

To improve the hydrophobic/hydrophilic balance of quaternary ammonium dendrimers and improve the synthetic methods previously used in this group, we have simplified the synthesis of quaternary ammonium dendrimers. Our approach is to efficiently synthesize tertiary amine dendrimers, then partially quaternize with long chain alkyl halides for hydrophobic/hydrophilic balance to produce new quaternary ammonium dendrimers.

Results and Discussion

Tertiary Amine Dendrimers. To produce quaternary ammonium dendrimers it was necessary to first produce tertiary amine materials. Poly(propylenimine) dendrimers (**7, 1, 8**) contain 8, 32 and 64 primary amine end groups respectively. Scheme 4 shows the synthesis of externally tertiary methylated amine dendrimers (TAM) using reductive methylation.[9,48] This method for synthesis was simple and cost efficient. However, full

methylation was never achieved, as previously reported by Kreider.[9] ^{13}C NMR analysis showed both the tertiary dimethylamine located at 45.5 ppm and the secondary monomethylamine at 42.2 ppm in a 6.3:1.7 ratio of dimethyl to monomethyl for 8 end groups (**9**), 25.6:6.4 for 32 end groups (**10**) and 44.8:19.2 for 64 end groups (**11**).

Scheme 4. Reductive Methylation of PPI Dendrimers

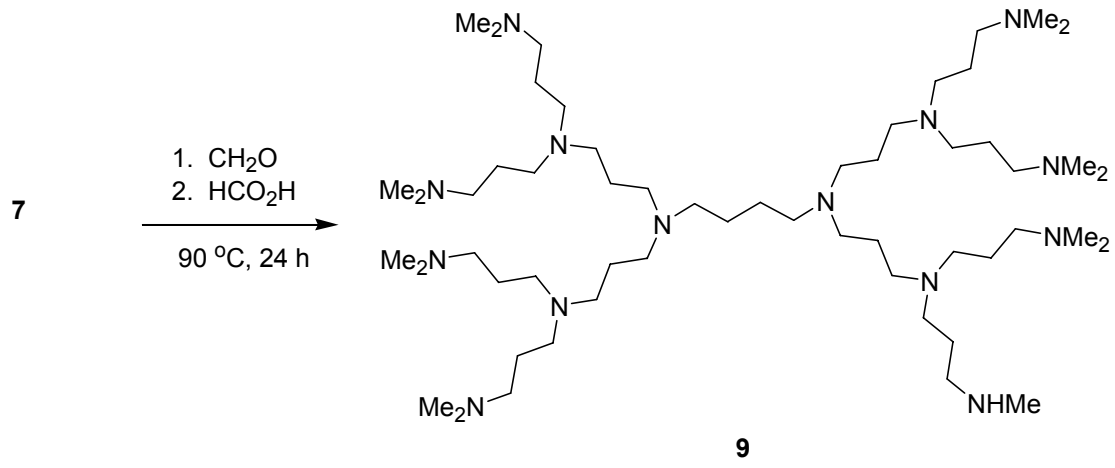

1 ⟶ **10**
8 ⟶ **11**

A second method to produce tertiary amines was reductive ethylation as shown in Scheme 5. This method allows for synthesis of fully tertiary ethylated (TAE) dendrimers (**12**). This method was originally developed by Young Hie Kim in our group.[49,50]

Scheme 5. Reductive Ethylation of PPI Dendrimer

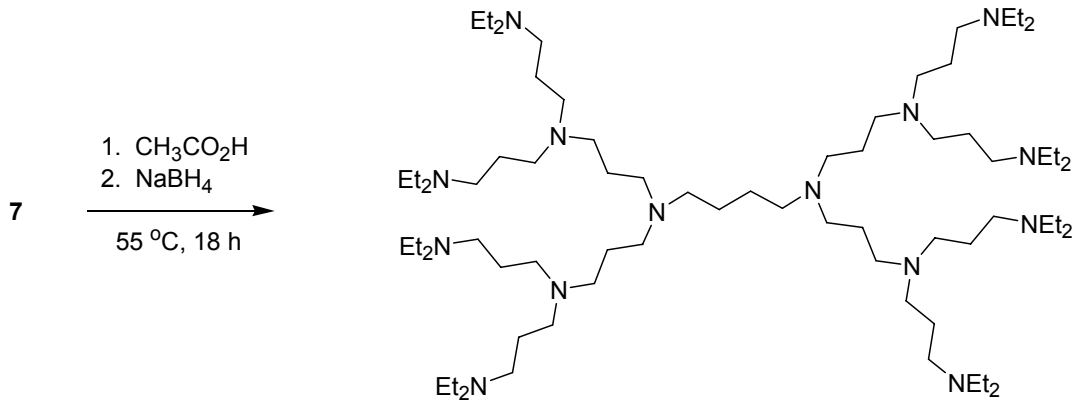

12

Quaternary Ammonium Dendrimers. Quaternization of tertiary amine dendrimers in our group was accomplished previously in methanol solution using alkyl iodides.[9] This method was found to be inefficient due to methanol being a poor solvent for the reactions kinetics. This led to the use of reaction temperatures above the boiling point of methanol (65 °C). Since temperatures above the boiling point of the solvent were used, sealed glass tubes were employed for carrying out the reaction. This was slightly dangerous due to the heating of sealed glass tubes. In the new research methanol was replaced with DMF solvent, alkyl bromides were substituted for alkyl iodides, where applicable, and reactions were carried out under inert atmosphere in round-bottomed flasks. Alkylation reactions of primary amine dendrimer **7** using alkyl halides are shown in Scheme 6. Schemes 7, 8, 9 and 10 show successful quaternization reactions using tertiary amine dendrimers **9, 10, 11,** and **12**. Quaternary ammonium iodides and bromides were converted to the chloride form soon after synthesis because of their higher stability compared to bromides and iodides, their higher solubility in aqueous solutions,

and lesser binding to quaternary ammonium groups in the catalysis experiments. Table 1 shows the degree of quaternization found from chloride analysis after ion exchange.

Scheme 6. Alkylation of Primary Amine Dendrimers

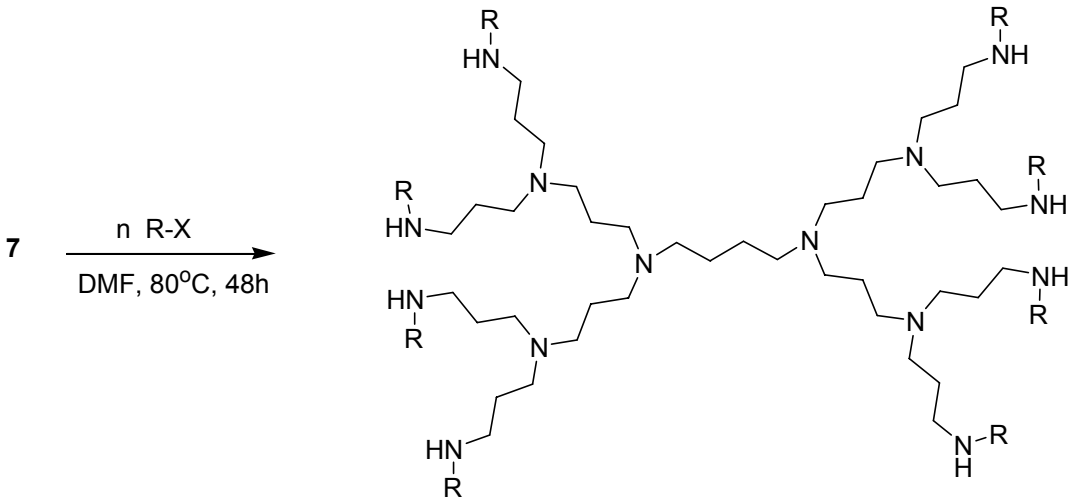

		n	R	X
7 →	**13**	8	n-C_4H_9	I
7 →	**14**	8	$CH_2C_6H_5$	Br
7 →	**15**	8	$CH_2CH(CH_2CH_3)C_4H_9$	Br

Scheme 7. Quaternization of 8 End-Group Tertiary Methylated Amine Dendrimer

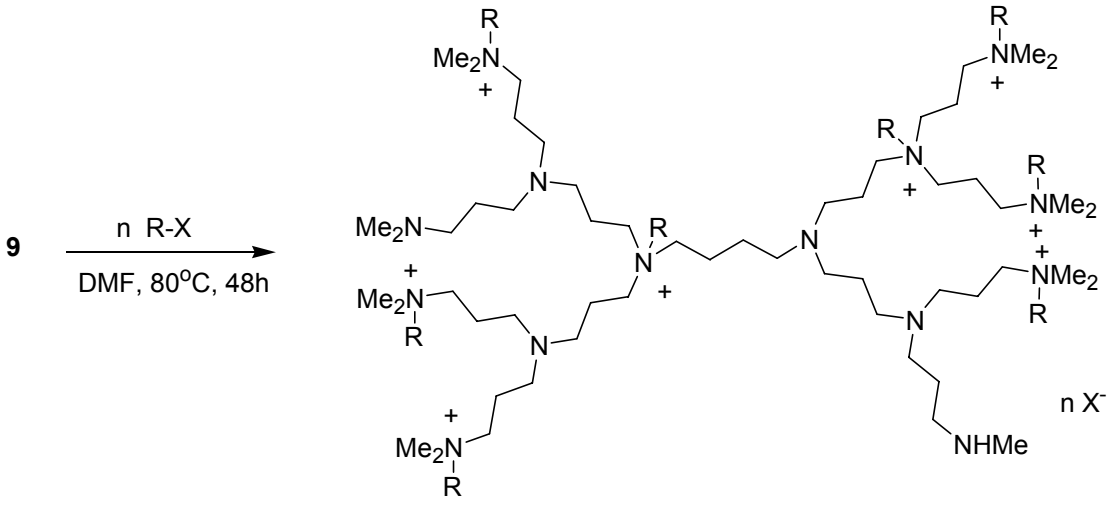

		n	R	X
9 →	**16-I**	8	n-C_4H_9	I
9 →	**17-Br**	8	$CH_2C_6H_5$	Br
9 →	**18-Br**	8	$CH_2CH(CH_2CH_3)C_4H_9$	Br
9 →	**19-Br**	5	n-C_8H_{17}	Br
9 →	**20-Br**	10	n-C_8H_{17}	Br
9 →	**21-Br**	4	n-$C_{12}H_{25}$	Br
9 →	**22-Br**	8	n-$C_{12}H_{25}$	Br
9 →	**23-Br**	17	n-$C_{12}H_{25}$	Br
9 →	**24-Br**	8	n-$C_{16}H_{33}$	Br

Scheme 8. Quaternization of 32 End-group Tertiary Methylated Amine Dendrimer

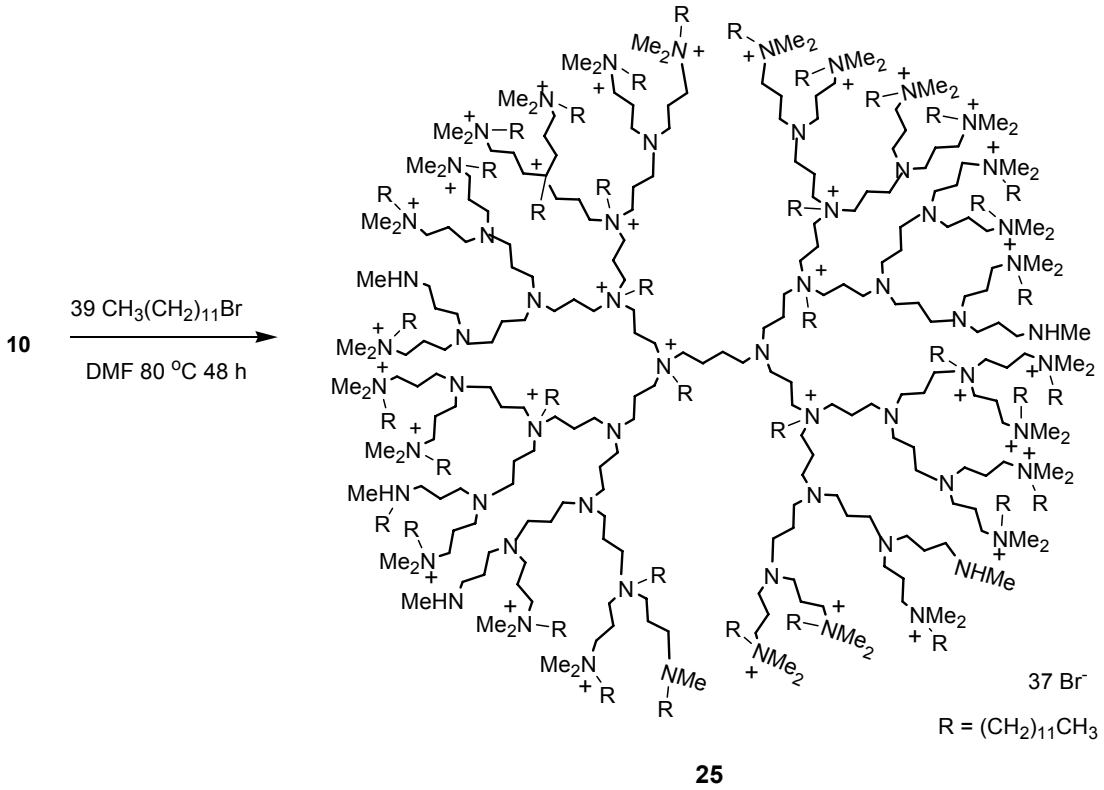

25

Scheme 9. Quaternization of 64 End-Group Tertiary Methylated Amine Dendrimer

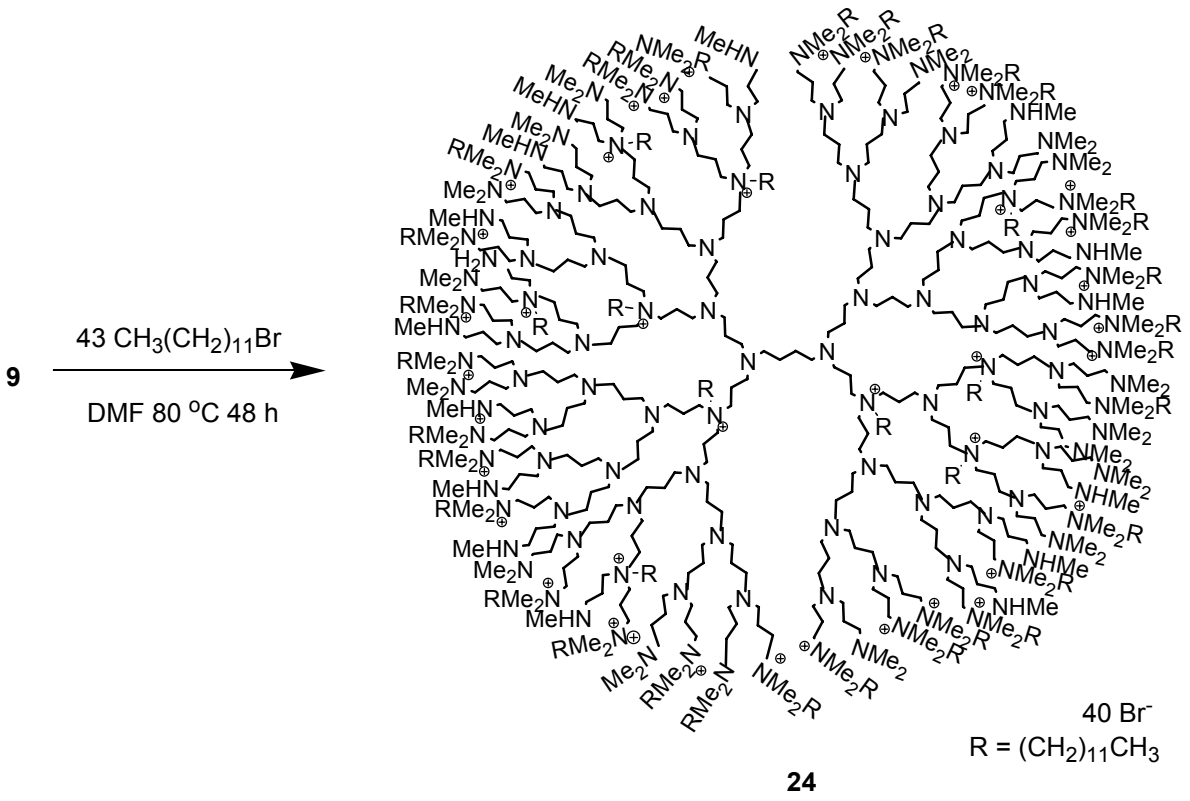

Scheme 10. Quaternization of 8 End-Group Tertiary Ethylated Amine Dendrimer

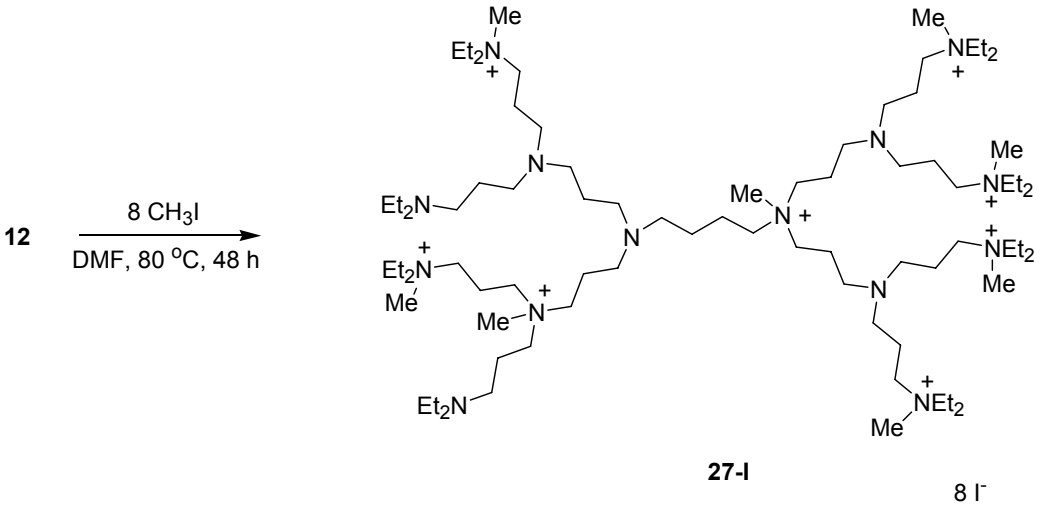

Table 1. Chloride Content of Quaternary Ammonium Dendrimers

sample	eq RX[a]	Cl^- titrated
13-Cl	8.0	0
14-Cl	8.0	0
15-Cl	8.0	0
16-Cl	8.2	7.1
17-Cl	8.2	8.0
18-Cl	8.2	8.0
19-Cl	5.2	4.8
20-Cl	10.4	9.7
21-Cl	4.0	4.0
22-Cl	8.0	7.7
23-Cl	17.3	12
24-Cl	8.0	8.1
25-Cl	39	37
26-Cl	43	40
27-Cl	8.0	8.0

[a]From reaction stiochometry

The degree of quaternization was determined by chloride titrations with $AgNO_3$ using a chloride ion specific electrode. These data were reinforced with ^{13}C NMR data which show a decrease in the $N(CH_3)_2$ peak at 45.5 ppm, an increase in CH_3 peaks next

to quaternary ammonium groups between 50 and 60 ppm, and an increase in the broad CH_2N^+ peaks between 60 and 70 ppm.[9] Finally ^1H NMR was used to show that quaternization reactions have occurred, as seen in very broad peaks in the quaternized polymer. When quaternization did not occur, sharp unchanged ^1H and ^{13}C NMR spectra of mixtures were produced, and the samples contained no halide ions.

Quaternization for samples with 8 quaternizing chains and higher occurs both at terminal amines and at branch points. This was determined by the retention of some dimethyl terminal amine peak at 45.5 ppm. This peak was present until higher degrees of quaternization were carried out. The same may also be said for the monomethyl terminal amine peak at 42.2 ppm. This group resists alkyation until an even higher degree of alkylation has occurred.

It was found that most of the samples **13-27** prepared from tertiary amine dendrimers **9, 10,** and **11** underwent quantitative or nearly quantitative quaternization, based on chloride titration. Samples **13, 14, 15, 16, 23, 25** and **26** did not have full quaternizaion based on alkyl halide stoichiometry. Samples **13, 14** and **15** were test materials with primary amine **7** being alkylated. These materials were used to show the effect on NMR chemical shifts and broadening of the peaks of the alkyl chains once attached to the large slowly tumbling dendrimer molecule. Since the parent amines were primary, no quaternization was seen, or expected, but small NMR chemical shifts and broadening was seen in the peaks of the alkylating chains. For **23,** not all 17 bromides from the alkyl bromide reagent were expected to be seen, since only 14 amines can be quaternized, with 2 additional chains for forming the tertiary terminal amine. For the higher generation dendrimers, **25** and **26,** a lower degree of quaternization was expected

due to the large number of secondary terminal amines that were available to react. Sample **16**'s lower conversion was the only result not easily explained. This could have been caused by the small butyl chain favoring the formation of the tertiary amine at the secondary amine site. It was also noticed in **16** that a Hoffman elimination reaction,[51] the decomposition of a quaternary ammonium group to a tertiary amine and an alkene, occurred. This reaction produced the vinyl groups seen in the ^{13}C NMR at 135 and 118 ppm, which could account for the reduced chloride content. One possible reason for this elimination could be that acetonitrile was used as solvent while DMF was used for all other reactions.

Tertiary ethylated materials did not quaternize as easily as the tertiary methylated materials. The tertiary ethylated dendrimer **12** failed to react with 1-bromo-2-ethylhexane, benzylbromide and 1-bromododecane, even at temperatures as high at 90 ^{o}C for 3 days. Only methyl iodide reacted with **12**. Addition of catalytic NaI was attempted in these reactions but no reaction occurred, as determined by chloride titration and NMR analysis. It is possible that higher temperatures could allow for quaternization but temperatures above 90 ^{o}C were not attempted due to discoloration of products at high temperatures.

Workup of shorter chain quaternary ammonium materials originally was achieved using extraction from aqueous NaOH into CH_2Cl_2, after removal of DMF by rotary evaporation. However as the chain length grew to 8 carbons and longer (samples **19-26**), the dendrimers became good emulsifying agents/surfactants. Attempted extraction resulted in nearly permanent emulsions of $NaOH_{(aq)}/CH_2Cl_2$ and dendrimer. When dendrimers were successfully isolated they usually contained large quantities of salt

(NaOH). Drying the CH_2Cl_2 solution, after extraction of dodecylated materials, especially **22,** resulted in aggregation and precipitation when $MgSO_4$ was used as drying agent. These results were also complicated because of the solubility of the dendrimers in both water and CH_2Cl_2, resulting in low recoveries, typically 40-60%. Alternate extraction methods using other solvents resulted in poorer yields. Because of these problems it was determined that using a weakly basic ion exchange resin (IRA 95), with aqueous methanol solvent, would be an efficient way of purifying and deprotonating the materials after quaternization since the only byproduct of the reaction would be protonated amines. This change in workup resulted in increased yields, 70-90%.

Surfactant Properties of Long Chain Quaternary Ammonium Dendrimers. After synthesizing quaternary ammonium dendrimers it was necessary to remove the DMF solvent. Total solvent removal was impossible using standard rotary evaporator conditions (i.e. 40 ^{o}C water bath and 10 Torr vacuum), based on NMR analysis. Drying using an Abderhalden apparatus at 56 ^{o}C for >24 h also did not remove all DMF. Removal of the final traces was done by dispersing the dried dendrimer in 100 mL of water and rotary evaporating the water from the solution. This further lead to the discovery that dodecylated and hexadecylated materials have surfactant like properties. Aqueous solutions of these dendrimers, **21-26**, foam when agitated, and have a soapy feel. This foaming can result in extreme loss of material when the entire rotary evaporator fills with dendridic foam. To prevent foaming, ethanol and water, typically 80:20 respectively, were added during rotary evaporation of **21-26** to prevent foaming and to remove the DMF.

Critical aggregation concentration (CAC) analysis was done to investigate the surfactant properties of these foaming agents. CAC nomenclature was used instead of CMC (critical micelle concentration) since the exact morphology of the aggregates is unknown. CAC analysis was done using conductivity measurements and surface tension analysis as shown in Figures 1 and 2. CAC was determined by the intersection of the two lines for conductivity and by the lowest point on the plot of surface tension. Table 2 shows the CAC of **20, 21, 22** and **24**. Octylated, dodecylated and hexadecylated materials were used because of their low solubility in water, compared to the shorter alkyl chain dendrimers, and **21, 22, 24** and to a lesser extent **20**'s ability to foam in aqueous solution. The CAC was found to decrease as the chain length increased (samples **20, 22** and **24**) and as the number of chains increases the CAC decreases (samples **21** and **22**).

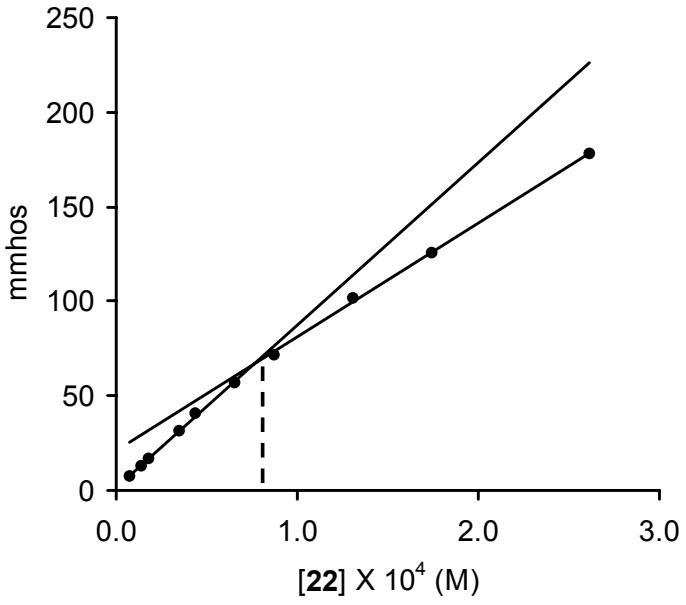

Figure 1. CAC determination for dendrimer **22** by conductivity measurements.

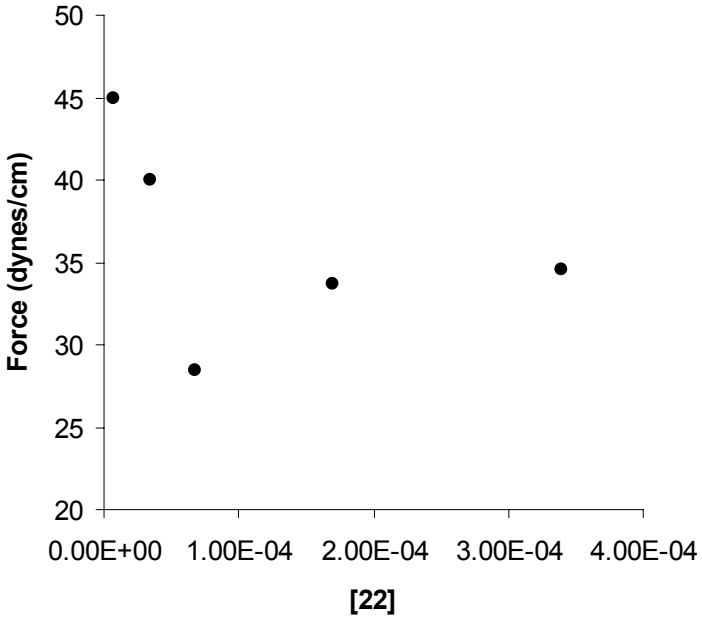

Figure 2. CAC determination for dendrimer **22** by surface tension analysis. The concentration at the minimum surface tension is taken as the CAC.

Table 2. CAC Results for Hydrophobic Dendrimers

sample	CAC [N^+] M
20 (TAM D8(C_8H_{17})$_{10}$)	8.5 x 10^{-4}
21 (TAM D8($C_{12}H_{25}$)$_4$)	3.8 x 10^{-4}
22 (TAM D8($C_{12}H_{25}$)$_8$)	9.0 x 10^{-5}
24 (TAM D8($C_{16}H_{33}$)$_8$)	3.5 x 10^{-5}
$C_{12}H_{25}N^+(CH_3)_3Br^-$ [52]	1.6 x 10^{-2}
$C_{12}H_{25}N^+(CH_3)_3Cl^-$ [53]	2.2 x 10^{-2}
$C_{16}H_{33}N^+(CH_3)_3Br^-$ [54]	1.0 x 10^{-3}
$C_{12}H_{25}N^+(CH_3)_2$-$(CH_2)_3$-$N^+(CH_3)_2C_{12}H_{25}2Br^-$ [55]	0.94 x 10^{-3}
$C_{16}H_{33}N^+(CH_3)_2$-$(CH_2)_2$-$N^+(CH_3)_2C_{16}H_{33}2Br^-$ [56]	3 x 10^{-6}
$C_8H_{17}N^+(CH_3)_2$-$(CH_2)_3$-$N^+(CH_3)_2C_8H_{17}2Br^-$ [57]	5.5 x 10^{-2}

One criterion for a good surfactant is a low CMC. Comparison of dendrimer CACs to cationic surfactants, dodecyltrimethylammonium bromide[52] and chloride[53] and hexadecyltrimethylammonium bromide[54] show that the quaternary ammonium dendrimers, even in the more soluble chloride form, have lower critical aggregation concentrations per cationic repeat unit than the monomeric surfactants.[58] Gemini surfactants,[58] didodecyl[55] and dioctyl[56] surfactants, also showed higher solubilities than the corresponding dendritic surfactants. The only material that had lower solubilities then the dendrimer surfactants was the dihexadecylated[57] gemini surfactant. The low CACs of the dendrimers **20, 21, 22** and **24** support the idea that these materials are good

surfactants. This is, however, limited by the overall solubility of these materials in water (only a few mg/mL).

Kinetic Study. Kinetic studies were carried out to determine the hydrophilic/hydrophobic balance of the dendrimers in aqueous solution.[26,59-61] The decarboxylation of 6-nitrobenzisoxazole-3-carboxylate (**5**) shown in Scheme 3 is very sensitive to the environment of the substrate and occurs fastest when in an environment balanced with both hydrophobic and quaternary ammonium sites.[26,59-63] The positive charge helps to bring reactants into the catalyst and the hydrophobic alkyl group helps to stabilize the transition state of the decarboxylation reaction.

Before kinetic studies could be carried out, substrate **5** had to be synthesized.[64-66] In the past, **5** was synthesized from **30** which was a commercially available material as shown in Scheme 11. However, during the past 10 years, **30** was discontinued from sale. Therefore **30** had to be synthesized using a literature method, as shown in Scheme 11.[64-66]

Scheme 11. Synthesis of 6-Nitrobenzisoxazole-3-carboxylate

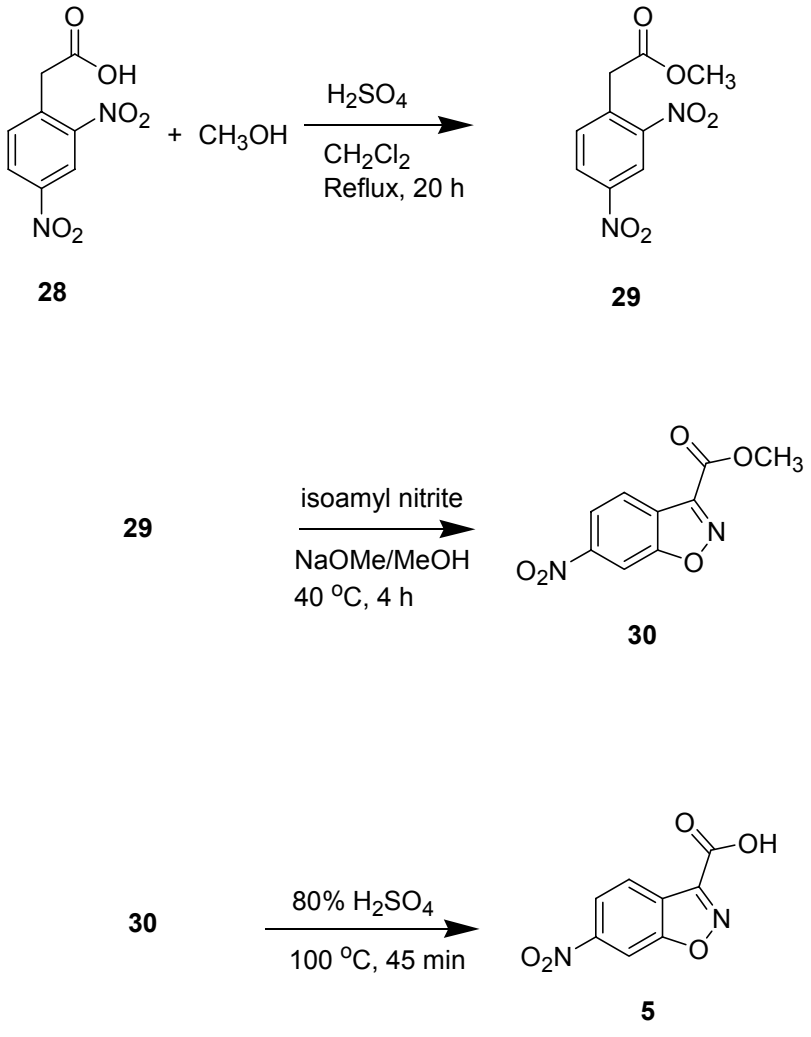

The methyl ester **30** was synthesized from commercially available 2,4-dinitrophenyl acetic acid (**28**).[66] The acid **28** was first protected as the methyl ester via an acid catalyzed esterification reaction to give methyl ester **29**. The methyl ester then underwent a cyclization reaction to the benzisoxazole **30** using isoamyl nitrite.[64] This sample had the same ^{1}H and ^{13}C NMR spectra as the previous commercially available material. This material could then be stored until **5** was needed for kinetic studies.

The first order kinetics for the decomposition of **5** into the phenoxide **6**, shown in Scheme 3, was measured colorimetrically using Hewlett Packard UV/Vis kinetics software. The appearance of the bright yellow phenoxide was observed in 1 cm cuvets at 25.0 ^{o}C as described in the experimental.

Kinetic results in Table 3 reveal that a more hydrophobic dendrimer was necessary for fast decarboxylation of **5**. Slow rates were found for dendrimers **17-20,** with benzyl, 2-ethylhexyl and octyl chains respectively, even at concentrations as high as 32 mM in quaternary ammonium repeat units for **19** and **20.** When longer, hydrophobic, dodecyl and hexadecyl chains were used, faster rates were observed. For docecylated 8-ended materials **21, 22** and **23** the fastest rates were seen. Using **22** at 0.024 mM concentration the rate was three times faster than using the octylated materials at 11 mM and nearly as fast as using **20** at 33 mM. Dodecylated sample **22** at 2.4 mM gave an observed rate constant 650 times greater than in water (k_{obsd}/k_w = 650). This is the fastest rate reported in the literature for decarboxylation of **5** using a dendrimer catalyst. Samples **22**^{b} and **22**^{c} were tested by two different individuals nearly 3 years apart. These results were very similar to one another, considering that **20**^{b} was only a trial run using a day-old solution of **5**, which is not recommended since it was later found that the

reproducibility of the experiment reduces as solutions of **5** age. The hexadecylated material **24** showed very fast rates, but the catalyst did not form a homogeneous solution and was cloudy. The decarboxylation reaction was probably being carried out on/in large dendrimer aggregates. Dendrimers **25** and **26** with 32 and 64 dodecylated end groups, both showed fast rates but not as fast as the 8 end group materials. This was not expected and may be a function of CAC or the relatively small number of quaternary ammonium groups for the given volume of the dendrimer or the low solubility of the larger dendrimers.

Table 3. Kinetic Results for Decarboxylation of 29.

dendrimer	structure	10^3 [N+] (M)	k_{obsd} (s^{-1})	k_{obsd}/k_w [a]
17[b]	TAM D8($CH_2C_6H_5$)$_8$	2.4	1.10 x 10^{-5}	3.5
18[b]	TAM D8($CH_2CH(C_2H_5)C_6H_{13}$)$_8$	2.4	2.5 x 10^{-6}	0.8
19[c]	TAM D8(C_8H_{17})$_5$	32.2	1.36 x 10^{-4}	43.7
		10.7	3.43 x 10^{-5}	11.0
20[c]	TAM D8(C_8H_{17})$_{10}$	32.8	2.09 x 10^{-4}	67.5
		10.9	2.98 x 10^{-5}	9.6
21[c]	TAM D8($C_{12}H_{25}$)$_4$	2.45	1.24 x 10^{-3}	401
		0.0245	3.04 x 10^{-5}	9.8
22[c]	TAM D8($C_{12}H_{25}$)$_8$	2.45	2.02 x 10^{-3}	650
		0.0245	1.01 x 10^{-4}	32.7
22[b]		2.4	2.55 x 10^{-3}	821
23[b]	TAM D8($C_{12}H_{25}$)$_{12}$	0.72	1.09 x 10^{-3}	351
24[b]	TAM D8($C_{16}H_{33}$)$_8$	2.05	2.08 x 10^{-3}	669
25[b]	TAM D32($C_{12}H_{25}$)$_{37}$	0.95	1.05 x 10^{-3}	339
26[b]	TAM D64($C_{12}H_{25}$)$_{40}$	2.4	5.65 x 10^{-4}	182
31[d]		24.0	2.58 x 10^{-5}	8.32
		2.40	1.36 x 10^{-5}	4.39
32[e]		2.45	1.55 x 10^{-4}	487

[a] k_w = 3.1 x 10^{-6} s^{-1}. [b]Measured by Robert Sherman. [c]Measured by Egambaram Murugan. [d]Reference[9]. See text for dendrimer description. [e]Reference[7]. See text for dendrimer description.

Comparing our new simpler hydrophobic dendrimers to previous dendrimers from this group emphasizes the increased efficiency of our new catalysts. Compared to sample

31[9] (TAM D32(CH_3)$_{62}$) our dendrimers are much more efficient catalytically, and have smaller generation size. Compared to our group's previous most active dendrimer **32**[7] (permethylated with octyl and MPEG chains and 32 end groups) our new dendrimers, especially **22**, are more active, smaller in generation, and much more efficient to synthesize.

Conclusions

We have improved both the ease of synthesis and the degree of alkylation of quaternary ammonium dendrimers quaternized with alkyl chains longer than butyl. It was found that tertiary methylated 8 end group materials quaternized with octyl, dodecyl and hexadecyl groups are surface active with CACs varying from 8.5 x 10^{-4} M to 3.5 x 10^{-5} respectively. These materials were examined as catalysts for the decarboxylation of 6-nitrobenzisoxazole-3-carboxylate. Increasing the number of carbons in the alkyl chain dramatically increased the rate of decarboxylation, and increasing the number of long chains also increased the rate. These dendrimers, especially 8 end group materials quaternized with 8 dodecyl chains, were found to have the fastest catalytic rates, 650 times that in water at 2.4 mM in quaternary repeat units, that have been reported for dendrimer catalysts for this reaction.[67]

Future Work

These new quaternary ammonium PPI dendrimers are some of the most promising PPI dendrimer catalysts produced. Many new questions have arisen from this research,

most importantly the importance of CAC in hydrophobic dendrimers. Several experiments need to be attempted in order to better understand these phenomena.

First, TAM D8 dendrimers need to be quaternized with 8 decyl and 8 tetradecyl chains. This is important because TAM D8 $(C_8H_{17})_{10}$ does not have surfactant character, i.e. does not foam well when aqueous solutions are agitated and have high CAC. The TAM D8 $(C_{12}H_{25})_x$ are good surfactants, and TAM D8 $(C_{16}H_{33})_8$ is too insoluble to be a good catalyst. It is also interesting how TAM D8 $(C_{12}H_{25})_x$ materials have much faster kinetic results than the TAM D8 $(C_8H_{17})_x$ materials. This series of experiments would bridge the gaps between octylated, dodecylated and hexadecylated materials and optimize surfactant chains with kinetic results.

Second, form tertiary dioctylated materials need to be formed and then quaternized with methyl iodide. This would mimic the number of carbons in the TAM D8$(C_{12}H_{25})$x materials but would be divided into two more compact segments. CMC and kinetic data could then be correlated to the data in Table 2 and 3.

Third, it may be wise to determine the kinetics and CAC with 4 and 16 end group analogues of **22**. This would allow one to compare the importance of chain length, the importance of the number of quaternizing chains and the dendrimer generation.

The relation of the CAC to kinetics also needs to be better understood. A series of kinetic experiments on sample **22** with several concentrations below, at and above the CAC would show if the aggregation of these dendrimers has any direct effect on the kinetics of 6-NBS decarboxylation. Also Cryo TEM could be used to determine the morphology of the aggregates above CAC. This could be important in classifying these

materials as surfactants and could help explain catalytic differences above the CAC if applicable.

Other important uses for these materials, other than surfactants or catalysts, should be investigated. Antimicrobial activity of our TAM D8 $(C_{12}H_{25})x$ dendrimers should be studied. Previous research by other groups using toxic/expensive reagents have shown that long chain quaternary ammonium dendrimers make good antimicrobial agents.[13-15]

Finally, starved seeded semi-continuous emulsion polymerization (Chapter IV) should be carried out on 64 end group dodecylated or benzylated materials below the CAC. These materials, which are approximately 10 nm in diameter, could act as a high surface area monodisperse template for the formation of cationic latexes with only one dendrimer per latex particle.

Experimental

Materials. All materials were purchased from Aldrich or Fisher and used without purification. Amberlite IRA 95 and IRA 402 were conditioned using previously described methods.[9] UV/Vis results were obtained on a Hewlett Packard 8452A diode array spectrophotometer using HP 89532K UV/Vis kinetics software and a VWR Scientific model 1141 constant temperature bath that circulated water through the cell block of the spectrophotometer. Conductivity was measured on a YSI model 31 conductivity bridge using a 1 cm^2 platinum electrode. NMR spectra were obtained on a Varian Gemini instrument at 300 MHz for ^1H and 75 MHz for ^{13}C. Chloride

determination was done using an Orion Model 96-17B chloride selective electrode and a Fisher Scientific Accumet pH Meter 25 using methods previously described.[9]

Polypropylenimine Octamine Dendrimer (D_8) (7). ^{1}H NMR (300 MHz, $CDCl_3$, δ): 2.5–2.4 (t), 2.2-2.0 (br), 1.5-1.4 (br), 1.4-1.1 (br). ^{13}C NMR (75 MHz, $CDCl_3$, δ): 54.1, 52.2, 52.1, 51.7, 40.6, 29.8, 25.0, 24.5.

Polypropylenimine Dotriacontamine Dendrimer (D_{32}) (1). ^{1}H NMR (300 MHz, $CDCl_3$, δ): 2.8–2.6 (br), 2.6-2.4 (br), 1.7-1.4 (br), 1.4-1.1 (br). ^{13}C NMR (75 MHz, $CDCl_3$, δ): 53.2, 52.5, 52.0, 51.7, 40.6, 29.9, 24.3, 24.5.

Polypropylenimine Tetrahexacontamine Dendrimer (D_{64}) (8). ^{1}H NMR (300 MHz, $CDCl_3$, δ): 2.9–2.6 (br), 2.6-2.3 (br), 2.2-1.6 (br), 1.6-1.1 (br). ^{13}C NMR (75 MHz, $CDCl_3$, δ): 52.9, 52.5, 52.0, 51.7, 49.2, 40.6, 30.9, 24.4, 17.5.

Tertiary Methylated D_8 (TAM D_8) (9).[9] In a 100-mL round-bottomed flask equipped with a reflux condenser and nitrogen atmosphere 10.00 g (12.9 mmol) of **5** was reacted with 30 g (370 mmol) of 37% formaldehyde to form a solid. Then, 60 g (2.18 mol) of 88% formic acid was added. The solid dissolved and began to evolve CO_2. The mixture was heated at 90 ^{o}C for 24 h. Once the reaction was complete the mixture was placed in an ice bath and rendered basic with 50% aqueous NaOH. The cloudy mixture was extracted 3 times with 50 mL of CH_2Cl_2 and the combined organic extracts were dried with Na_2SO_4. Solvent was removed under vacuum, and the product was dried overnight using an Abderhalden apparatus at 56 ^{o}C to yield 8.40 g (67% recovery) of a thick light yellow oil. ^{1}H NMR (300 MHz, $CDCl_3$, δ): 2.5-2.3 (br), 2.2-2.1 (s), 1.7-1.5 (br), 1.5-1.4 (br). ^{13}C NMR (75 MHz, $CDCl_3$, δ): 58.0, 55.9, 52.4, 52.3, 52.0, 45.5 (6.3 $N(CH_3)_2$), 42.2 (1.7 $NHCH_3$), 25.6, 25.3, 24.5.

Dendrimer Handling Procedures. After solvent removal by rotary evaporation, the dendrimers were stored in 20 mL scintillation vials, purged with nitrogen and protected from light. The dendrimers are hygroscopic, and they decompose in light after long periods of time in chloride ion form and in a few days in iodide ion form.

To the round-bottomed flask containing the dendrimer dried using water and ethanol rotary evaporation, a minimal amount of CH_2Cl_2 was added to markedly decrease the viscosity of the dendrimer. The dendrimer was then transferred to 20 mL scintillation vials, so that no more that 2 g of dry dendrimer was present after solvent removal. No more than 2 g was used due to foaming and splattering during vacuum drying. The CH_2Cl_2 was then removed from the scintillation vial using an inverted 14/20 rubber septum over the mouth of the vial. The septum was pierced with an 18 gauge needle and the bottom of the septum was placed into a 19/22 bump-trap and rotary evaporated. After rotary evaporation the sample was loosely capped and further dried using an Abderhalden device at 56 ^{o}C and <10 Torr pressure. Samples were weighed on analytical balances.

Highly viscous, waxy or solid materials were transferred using a spatula and wiping the dendrimer into a tared container. Liquid or lightly viscous materials were transferred using Pasteur pipets with the tapered end broken off. All measurements must be done quickly due to the hygroscopic nature of the dendrimers.

Tertiary Methylated D_{32} (TAM D_{32}) (10). Using the method of **9**, 0.500 g (0.142 mmol) of **1**, 5.46 g (67 mmol) of 37% formaldehyde and 8.38 g (160 mmol) of 88% formic acid gave a yield of 0.357 g (58 % recovery) of **10** as a thick yellow oil. ^{13}C NMR (75 MHz, $CDCl_3$,δ):57.5, 55.6, 52.3, 52.0, 51.8, 50.5, 45.4 (25.6 $N(CH_3)_2$), 42.1 (6.4 $NHCH_3$), 25.3, 25.1, 24.6, 24.2.

Tertiary Methylated D_{64} (TAM D_{64}) (11). Using the method of **9**, 1.046 g (0.146 mmol) of **8**, 4.972 g (61 mmol) of 37% formaldehyde and 2.44 g (47 mmol) of 88% formic acid gave a thick light yellow oil. The majority of the sample was given to Jason Krieder for use and therefore no yield was reported. ^{13}C NMR (75 MHz, $CDCl_3$, δ): 65.9, 58.0, 56.2, 55.9, 53.4, 52.5, 52.1, 50.1, 45.6 (44.8 $N(CH_3)_2$), 42.3 (19.2 $NHCH_3$), 26.0, 25.6, 25.3, 25.1, 24.8, 24.4.

Tertiary Ethylated D_8 (TAE D_8) (12). In a 100-mL round-bottomed flask equipped for reflux under nitrogen 2.000 g (2.59 mmol) of dendrimer **7** and 71 mL (1.2 mol) of acetic acid were mixed at 55 ^{o}C. Once all the dendrimer had dissolved 7.8 g (0.22 mol) of $NaBH_4$ was added slowly over a 3 h period, (Caution: severe foaming). Once the reaction had stirred overnight it was rendered basic with 50% NaOH and extracted three times with 75 mL of CH_2Cl_2 and dried with Na_2SO_4 before vacuum drying. The product was dried in an Abderhalden device overnight at 56 ^{o}C to obtain a thick yellow oil with a weight of 1.432 g (41% recovery). ^{1}H NMR (300 MHz, $CDCl_3$, δ): 3.4-3.3 (br), 2.8-2.7 (br), 2.6-2.3 (br), 1.7-1.5 (br), 1.4-1.3 (br), 1.1-0.9 (t). ^{13}C NMR (75 MHz, $CDCl_3$, δ): 54.2, 52.1, 51.1, 46.8, 25.1, 24.5, 24.4, 23.3, 11.7.

D_8 $(C_4H_9)_8$ (12). In a thick-walled glass tube, 0.259g (0.335 mmol) of **7** was dissolved in 20 mL of DMF and 0.510 g (2.77 mmol) of 1-iodobutane was added. The mixture was frozen in liquid nitrogen and sealed with a torch. The solution was heated in a 70 ^{o}C oil bath for 72 h. After opening, the solvent was removed under vacuum. The oil was dissolved in 10 mL of water and made basic with 50% NaOH to a pH of 14. The aqueous solution was extracted 3 times with 20 mL of CH_2Cl_2. The combined organic layers were dried with $MgSO_4$ and then evaporated using a rotary evaporator. After

solvent removal, the product was dried in a heated vacuum desicator to obtain a reddish colored oil. ^{1}H NMR (300 MHz, $CDCl_3$, δ): 3.4-3.3 (br), 2.8-2.5 (br), 1.8-1.5 (br), 1.5-1.2 (br), 1.0-0.8 (br). ^{13}C NMR (75 MHz, $CDCl_3$, δ): 54.0, 53.7, 52.1, 51.6, 49.7, 48.4, 40.5, 32.2, 30.0, 29.1, 27.3, 25.0, 24.6, 20.8, 20.7, 14.3, 14.2.

D_8 ($CH_2C_6H_5$)$_8$ (14). Using the method of **13**, 0.314 g (0.406 mmol) of **7**, 20 mL of DMF and 0.585 g (3.42 mmol) of benzylbromide produced a reddish colored oil. ^{1}H NMR (300 MHz, $CDCl_3$, δ): 7.4-7.1 (br), 3.8-3.7 (br), 3.7-3.4 (br), 3.4-3.0 (br), 2.7-2 (br), 1.8-1.2 (br). ^{13}C NMR (75 MHz, $CDCl_3$, δ): 140.2, 139.6, 139.0, 129.2, 128.6, 128.2, 128.0, 126.6, 58.5, 58.1, 57.5, 54.0, 51.8, 51.2, 50.5, 47.8, 40.7, 30.6, 27.2, 24.8, 24.6, 24.4.

D_8 ($CH_2CH(C_2H_5)C_6H_{13}$)$_8$ (15). Using the method of **13**, 0.280g (0.362 mmol) of **7**, 20 mL of DMF and 0.561 g (2.91 mmol) of 2-ethylhexylbromide produced a pinkish/red colored oil. ^{1}H NMR (300 MHz, $CDCl_3$, δ): 3.4-3.2 (br), 2.8-2.7 (br), 2.7-2.2 (br), 2.1 (br), 1.7-1.2 (br), 1.0-0.8(br). ^{13}C NMR (75 MHz, $CDCl_3$, δ): 59.6, 54.1, 53.3, 51.9, 51.7, 51.3, 48.9, 40.6, 39.4, 37.4, 34.2, 33.0, 31.4, 28.9, 28.5, 27.3, 26.4, 25.1, 24.5, 24.1, 14.2, 10.8.

TAM D_8 (C_4H_9)$_8$ (16). In a thick-walled glass tube, 0.312 g (0.313 mmol) of **9** was dissolved in 20 mL of acetonitrile and 0.461 g (2.51 mmol) of 1-iodobutane was added before freezing in liquid nitrogen under vacuum and sealing with a torch. The solution was heated in a 70 ^{o}C oil bath for 72 h. After opening, the solvent was removed under vacuum. The oil was dissolved in 10 mL of water and made basic to a pH of 14. The aqueous solution was extracted 3 times with 20 mL of CH_2Cl_2 and the combined organic layers were dried with $MgSO_4$ and then dried using a rotary evaporator. The

product was then dissolved in 5 mL water and passed through a strongly basic ion exchange column to exchange iodide for chloride. After solvent removal the product was dried in a heated vacuum desiccator to obtain a yellow oil weighing 0.297 g (55% recovery). ^{13}C NMR (75 MHz, $CDCl_3$, δ): 135.0, 118.0, 63.7, 63.4, 62.5, 62.0, 61.0, 57.5, 56.8, 55.8, 55.6, 54.0, 53.7 53.2, 51.4, 51.2, 51.0, 50.2, 49.5, 45.5, 42.13, 42.1, 41.9, 29.4, 29.2, 24.5, 20.7, 20.4, 10.6, 14.1, 13.8, 13.7.

TAM D_8 ($CH_2C_6H_5)_8$ (17). Using the method of **16** 0.440 g (0.530 mmol) of **9,** 20 mL of DMF and 0.450 g (2.49 mmol) of benzyl bromide produced a reddish colored oil. ^{13}C NMR (75 MHz, $CDCl_3$, δ): 133.4, 130.4, 129.0, 127.9, 67.1, 64.0, 62.5, 54.1, 52.0, 51.5, 50.6, 49.4, 49.1, 45.5, 42.2, 25.2, 25.0, 24.0, 20.9.

TAM D_8 ($CH_2CH(C_2H_5)C_6H_{13})_8$ (18). Using the method of **16**, 0.512 g (0.530 mmol) of **9**, 20 mL DMF and 0.816 g (4.23 mmol) of 2-ethylhexylbromide produced 0.635 g (91% recovery) of a light yellow colored oil. ^{13}C NMR (75 MHz, $CDCl_3$, δ): 68.0, 63.8, 63.0, 54.8, 53.1, 49.5, 48.8, 42.2, 35.7, 33.2, 30.9, 29.0, 27.6, 25.4, 22.4, 22.1, 21.9, 19.8, 13.2, 9.8.

TAM D_8 ($C_8H_{17})_5$ (19). In a 100-ml round-bottomed flask equipped with a reflux condenser and nitrogen atmosphere 1.074 g (1.11 mmol) of **9** was dissolved in 50 mL of DMF and 1.105 g (5.76 mmol) of 1-bromooctane was added. The solution was stirred in an 80 ^{o}C oil bath for 48 h. The DMF solvent was removed under vacuum. Final traces of DMF were removed by adding 100 mL of water to the flask, evaporating the water under vacuum, adding 100 mL of ethanol and removing it via vacuum. The oil was dissolved in 10 mL of water and passed through a weakly basic ion exchange resin and then through a strongly basic ion exchange column to exchange bromide for chloride. After solvent

removal the product was dried in an Abderhalden device overnight at 56 ^{o}C to obtain 1.018 g (52.9% recovery, low due to spillage) of a tarry yellow/orange oil. ^{1}H NMR (300 MHz, $CDCl_3$, δ): 3.9-3.7 (br), 3.7-3.6 (br), 3.4-3.0 (br), 2.5-2.0 (br), 1.9-1.6 (br), 1.6-1.3 (br), 1.3-1.0 (br), 0.7 (t). ^{13}C NMR (75 MHz, $CDCl_3$, δ): 63.9, 62.3, 57.5, 57.2, 55.5, 54.0, 51.8, 50.8, 50.4, 45.4, 42.1, 31.8, 29.4, 29.2, 26.2, 25.1, 24.4, 22.7, 22.4, 20.6, 13.9.

TAM D_8 (C_8H_{17})$_{10}$ (20). Using the method of **19**, 2.000 g (2.06 mmol) of **9,** 50 mL of DMF and 4.115 g (21.4 mmol) of 1-bromooctane produced a viscous yellow/orange oil 3.512 g (68% recovery). ^{1}H NMR (300 MHz, $CDCl_3$, δ): 3.9-3.7 (br), 3.7-3.6 (br), 3.4-3.0 (br), 2.5-2.0 (br), 1.9-1.6 (br), 1.6-1.3 (br), 1.3-1.0 (br), 0.7 (t). ^{13}C NMR (75 MHz, $CDCl_3$, δ): 64.0, 63.2, 57.2, 52.0, 51.2, 50.6, 50.4, 31.5, 29.0, 28.9, 28.8, 26.2, 26.0, 22.7, 22.5, 22.4, 20.5, 13.9.

TAM D_8 ($C_{12}H_{25}$)$_4$ (21). Using the method of **19**, 3.000 g (3.10 mmol) of **9,** 50 mL of DMF and 3.086 g (12.4 mmol) of 1-bromododecane produce a thick yellow oil 4.102 g (72.5% recovery). ^{1}H NMR (300 MHz, $CDCl_3$, δ): 4.0-3.8 (br), 3.8-3.6 (br), 3.5-3.1 (br), 2.6-2 (br), 2.0-1.7 (br), 1.7-1.4 (br), 1.4-0.9 (br), 0.7 (t). ^{13}C NMR (75 MHz, $CDCl_3$, δ): 63.7, 62.3, 57.8, 57.4, 55.6, 53.7, 51.8, 51.1, 50.4, 45.5 42.1, 31.7, 29.4, 29.3, 29.1, 26.2, 25.1, 24.9, 22.7, 22.4, 20.6, 13.9.

TAM D_8 ($C_{12}H_{25}$)$_8$ (22). In a 100-ml round-bottomed flask equipped with a reflux condenser and a nitrogen atmosphere 3.000 g (3.10 mmol) of **9** was dissolved in 50 mL of DMF and 6.170 g (24.7 mmol) of bromododecane was added. The solution was stirred in an 80 ^{o}C oil bath for 48 h. The DMF solvent was removed under vacuum. Final traces of DMF were removed by adding 100 mL of water to the flask and evaporating the water and then adding 100 mL of ethanol and removing it via vacuum.

The oil was dissolved in 5 mL of water and 10 mL of methanol and passed through a weakly basic ion exchange resin using 70% aqueous methanol as solvent to deprotonate any protonated amines. (Note: No extraction was attempted as the sample precipitated with $MgSO_4$ drying agent; additionally **19** acts as an emulsifying agent for $NaOH_{(aq)}$ and CH_2Cl_2.) The product was then passed through a strongly basic ion exchange column, using the same method as the weakly basic resin, to exchange bromide for chloride. After solvent removal under vacuum, (Note: Extreme foaming occurs during rotary evaporation. Ethanol cosolvent reduces foaming), the product was dried in an Abderhalden device overnight at 56 ^oC to obtain 7.012 g (87% recovery) of a fluffy/crunchy yellow solid (which becomes sticky after exposure to air). ^1H NMR (300 MHz, $CDCl_3$, δ): 4.0-3.7 (br), 3.7-3.5 (br), 3.5-3.1 (br), 2.6-2.0 (br), 2.0-1.7 (br), 1.7-1.4 (br), 1.4-1.0 (br), 0.7 (t). ^{13}C NMR (75 MHz, $CDCl_3$, δ): 64.2, 63.6, 62.3, 53.7, 51.8, 51.1, 50.4, 45.4, 31.7, 29.4, 29.3, 29.1, 26.2, 25.1, 22.7, 22.5, 20.7, 13.9.

TAM D_8 ($C_{12}H_{25}$)$_{14}$ (23). Using the method of **16**, 0.334 g (0.345 mmol) of **9** 20 mL of DMF and 1.483 g (5.96 mmol) of 1-bromododecane were reacted. The product was then dissolved in 5 mL water and 10 mL methanol and passed through a strongly basic ion exchange column to exchange bromide. A yellow colored solid was recovered with a weight of 1.075 g (69% recovery). ^{13}C NMR (75 MHz, $CDCl_3$,δ): 63.5, 62.5, 51.0, 50.4, 32.7, 31.7, 29.5, 29.5, 29.4, 29.4, 29.1, 26.3, 26.1, 25.7, 22.7, 22.5, 14.0.

TAM D_8 ($C_{16}H_{33}$)$_8$ (24). Using the method of **23**, 0.250 g (0.258 mmol) of **9,** 20 mL of DMF and 0.776 g (2.56 mmol) of 1-bromohexadecane produced a yellow waxy solid with a weight of 0.388 g (42% recovery). ^{13}C NMR (75 MHz, $CDCl_3$, δ): 64.0,

63.3, 62.5, 59.8, 51.2, 50.5, 45.3, 32.8, 31.8, 29.6, 29.4, 29.2, 27.4, 26.3, 26.1, 25.7, 22.8, 22.6, 20.7, 14.0.

TAM D_{32} $(C_{12}H_{25})_{37}$ (25). Using the method of **23**, 0.109 g (0.025 mmol) of **10,** 20 mL of DMF and 0.246 g (0.99 mmol) of 1-bromododecane produced a yellow colored solid that weighed 0.190 g (61% recovery). ^{13}C NMR (75 MHz, $CDCl_3$, δ): 64.2, 63.5, 62.1, 52.8, 50.8, 50.2, 49.4, 42.2, 34.4, 32.3, 31.5, 29.2, 29.1, 29.0, 28.9, 28.7, 26.1, 25.9, 25.5, 22.2, 13.7.

TAM D_{64} $(C_{12}H_{25})_{40}$ (26). Using the method of **23**, 0.536g (0.069 mmol) of **11,** 20 mL of DMF and 0.782 g (3.14 mmol) of 1-bromododecane were reacted. After solvent removal. (Caution: foaming) The product was dried in a heated vacuum desicator to obtain a reddish colored oil that weighed 0.21 g (18% recovery due to severe foaming and subsequent loss of material). ^{13}C NMR (75 MHz, $CDCl_3$, δ): 66.8, 62.8, 57.9, 53.2, 52.0, 51.9, 45.5, 32.8, 31.8, 29.6, 29.5, 29.4, 29.3, 26.1, 25.7, 23.1, 22.6, 14.0.

TAE D_8 $(CH_3)_8$ (27). In a thick-walled tube 0.547 g (0.45 mmol) of **12** and 30 mL of DMF were mixed. To the mixture, 0.509 g (3.6 mmol) of iodomethane was added and the solution was frozen with $N_{2(l)}$ and degassed under vacuum before sealing the tube with a torch. The mixture was allowed to react at 80 ^oC for 48 h in an oil bath. Once the tube was opened the DMF solvent was removed under vacuum, the final traces of DMF were removed by adding 100 mL of water to the flask and evaporating the water and then adding 100 mL of ethanol and removing it via vacuum. The oil was dissolved in 10 mL of water and passed through a weakly basic ion exchange resin to deprotonate any protonated amines. The product was then passed through a strongly basic ion exchange column to exchange bromide for chloride. After solvent removal, the product was dried

in an Abderhalden device overnight at 56 ^{o}C to obtain a thick yellow/orange oil that weighed 0.851 g (117% recovery). ^{1}H NMR (300 MHz, D_2O, δ): 4.0-3.0 (br), 3.0-2.7 (br), 2.7-2.2 (br), 2.1-1.4 (br), 1.4-1.1 (br), 1.1-0.9 (m). ^{13}C NMR (75 MHz, D_2O, δ): 60.2, 58.6, 57.3, 57.2, 56.8, 51.0, 49.5, 48.1, 47.2, 46.6, 37.9, 37.0, 22.3, 19.1, 18.9, 10.3, 9.8, 7.5.

Conditioning of Ion Exchange Resin.[9] The quaternary ammonium chloride resin IRA-402 was rinsed with 5 bed volumes of each, water, methanol, and water, 1 bed volume of 2 M HCl, 10 bed volumes of water, 5 bed volumes of methanol, and water until the pH was neutral. IRA 95 used 2 M NaOH in place of 2 M HCl. Since most of the quaternary ammonium dendrimers used are not readily soluble in small volumes of pure water several bed volumes of 30%-50% methanol were passed down the column to prepare it for dendrimer passage.

Chloride Determination. Known masses of ion exchanged quaternary ammonium dendrimers were dissolved in 25 mL of purified water. To this dendrimer solution, 0.5 mL of 5 M sodium nitrate was added, and the resulting solution was titrated with 0.025 M silver nitrate using a chloride selective electrode. The concentration of chloride was determined by the amount of silver nitrate necessary to react all chloride in the system.

Moisture Absorption. A 0.25 g sample of **22** was weighed in a tared vial after all kinetic experiments had been carried out. The vial was allowed to sit on the bench top covered with a beaker. The vial was weighed periodically, with initial weight gains of 2 mg/h. After 2 days the sample was dried using an Abderhalden device at 56 ^{o}C, and a

final dry weight was obtained. A total of 13% by weight of water was absorbed during a 48 hr period in which the dendrimer changed from a dry solid to a viscous oil.

Conductivity Measurement of Critical Aggregation Concentration. CAC values were determined using conductance measurements for a series of 12 samples with concentrations based on a 100-mL master solution diluted into 50 mL solutions of: 1/2, 1/5, 1/25 and 3/4 concentration. These samples were then further diluted by half and then by half again. In sample **22** concentrations were varied from 6.97×10^{-6} M to 3.48×10^{-4} M in dendrimer. A plot of concentration vs. conductivity produced a plot with two intersecting lines. The intersection of these lines corresponds to the CAC.

Surface Tension Analysis of Critical Aggregation Concentration. CAC for sample **22** was determined using 5 samples with concentrations varying from 3.4×10^{-4} to 6.8×10^{-6} M in dendrimer. These samples were tested using the Wilhelmy Plate method by Dr. Dale Teeters at the University of Tulsa. A plot of force vs. concentration produced a plot where the lowest point was equal to the CAC.

Methyl 2,4-dinitrophenylacetate (29).[66] In a 100 mL round-bottom flask equipped for reflux under nitrogen, 10.000 g (44 mmol) of 2,4-dinitrophenylacetic acid (**28**) react with 5.30 mL (132 mmol) of methanol in 13.0 mL of CH_2Cl_2 with 0.66 mL H_2SO_4 as catalyst. The mixture was refluxed in a 50 ^oC oil bath for 20 h, the reaction was accompanied by a color change from pink to yellow. The product was extracted with 20 mL of H_2O, 20 mL of $NaHCO_3$(sat), and 20 mL of H_2O, dried over $MgSO_4$ and rotary evaporated. The product was initially a yellow oil but eventually solidified after recrystallization from ethanol into light creamy yellow crystals weighing 7.100 g (68% yield). The product had a mp of 81-82 ^oC (lit 82-83 ^oC);[66] ^1H NMR ($CDCl_3$) δ 3.82 (s,

3H), 4.17 (s, 2H), 7.64 (dd, 1H, J = 8.1, 0.3 Hz), 8.47 (dd,1H, J = , 4.2, 2.4 Hz), 8.96 (d, 1H, J = 2.4 Hz); ^{13}C NMR ($CDCl_3$) δ 169.0, 149.4, 147.4, 136.2, 134.6, 127.5, 120.7, 52.6, 39.4.

Methyl 6-nitrobenzisoxazole-3-carboxylate (30).[64] In a three-neck round-bottomed flask equipped with a condenser and an addition funnel under nitrogen 3.500 g (14.6 mmol) of methyl ester **29** was dissolved in 50 mL methanol at 40 ^{o}C. To the solution 2.1 g (18 mmol) of freshly distilled isoamyl nitrite was added and the addition funnel was charged with 10 mL of methanol and 0.33 g of sodium metal. Once all of the sodium had reacted with the methanol, the sodium methoxide was added slowly with vigorous stirring. The reaction mixture immediately turned from yellow to black upon addition of the methoxide and within 1 h became reddish/brown. This color then faded and a yellow ppt with a red/brown solution was produced. After 4 h of reacting the suspension was cooled in an ice bath and vacuum filtered to produce yellow crystals. The crystals were recrystallized from 50 mL of methanol to give 2.00 g (63% yield) of dry blonde needle crystals. The product; ^{1}H NMR ($CDCl_3$) δ 8.55(dd, 1H, J = 1.5, 0.8 Hz), 8.32 (d, 1H, J = 1.62 Hz), 8.31 (d, 1H, J = 1.0 Hz), 4.11 (s, 3H).; ^{12}C NMR ($CDCl_3$) δ 163.2, 159.5, 150.3, 149.4, 124.2, 120.3, 106.4, 54.5.

6-Nitrobenzisoxazole-3-carboxylic acid (5). In a 50 mL flask in a steam bath, 1.000 g (4.5 mmol) of **30** was dissolved in 20 mL of 80% sulfuric acid and heated for 40 min. After reacting the mixture was dumped into 10 mL of ice and allowed to cool in an ice bath before vacuum filtering. The impure crystals were recrystallized from 3-4 mL of acetone/heptane. The purified crystals, 0.345 g (37% yield) were then subjected to ^{1}H NMR for a purity determination of 90% carboxylic acid and 10% methyl ester; ^{1}H NMR

($CDCl_3$) δ 8.55 (dd, 1H, J = 1.5, 0.8 Hz), 8.32 (d, 1H, J = 1.62 Hz), 8.31 (d, 1H, J = 1.0 Hz), 4.11 (s, 3H,).

Decarboxylation Kinetics. Kinetic experiments were carried out in 1 cm polystyrene cells at a constant temperature of 25.0 $\pm$ 0.1 ^{o}C. Solutions of dendrimer of known concentration were prepared in nitrogenated aqueous NaOH solution with a pH of 11.4. To a polystyrene cuvette 2.98 mL of aqueous dendrimer solution was added. The cuvette was then allowed to equilibrate to 25 ^{o}C in the spectrometer for at least 20 minutes. Background spectra were then taken of the solution at 390-410 nm, and 22 μL of a 10.6 mmol ethanolic solution of **5** was added. (Note: The ethanolic solution can only be stored for 1-2 days under nitrogen at 5 ^{o}C in the dark. The decarboxylation reaction is not detectable until base is added as the decarboxylated phenol is colorless; only the phenoxide **6** is colored.) The solution was inverted several times and the experiment was observed over the first 10% of conversion. The first order rate constant was determined using the first order rate equation, $k_{obsd} = \ln[(A_{inf} - A_o)/(A_{inf} - A_t)]/t$, where t is the time of the reaction and A_o, A_t, and A_{inf} are the absorbance at time 0, t, and infinity.[1,2,3]

References

(1) Newkome, G. R.; Moorefield, C. N.; Vogtle, F. *Dendrimers, 2nd Edition*, 2001.

(2) Tomalia, D. A.; Dewald, J. R. In *PCT Int. Appl.*; (Dow Chemical Co., USA). Wo, 1984, p 40 pp.

(3) Tomalia, D. A.; Baker, H.; Dewald, J.; Hall, M.; Kallos, G.; Martin, S.; Roeck, J.; Ryder, J.; Smith, P. *Polymer Journal (Tokyo, Japan)* **1985**, *17*, 117-132.

(4) Cherestes, A.; Engel, R. *Polymer* **1994**, *35*, 3343-3344.

(5) Lee, J.-J.; Ford, W. T.; Moore, J. A.; Li, Y. *Macromolecules* **1994**, *27*, 4632-4634.

(6) Piotti, M. E.; Rivera, F., Jr.; Bond, R.; Hawker, C. J.; Frechet, J. M. J. *J. Am. Chem. Soc.* **1999**, *121*, 9471-9472.

(7) Pan, Y.; Ford, W. T. *Macromolecules* **2000**, *33*, 3731-3738.

(8) Goetheer, E. L. V.; Baars, M. W. P. L.; van den Broeke, L. J. P.; Meijer, E. W.; Keurentjes, J. T. F. *Ind. Eng. Chem. Res.* **2000**, *39*, 4634-4640.

(9) Kreider, J. L.; Ford, W. T. *J. Polym. Sci., Part A: Polym. Chem.* **2001**, *39*, 821-832.

(10) Baker, J. R., Jr.; Quintana, A.; Piehler, L.; Banazak-Holl, M.; Tomalia, D.; Raczka, E. *Biomedical Microdevices* **2001**, *3*, 61-69.

(11) Esfand, R.; Tomalia, D. A. *Drug Discovery Today* **2001**, *6*, 427-436.

(12) Liu, M.; Kono, K.; Frechet, J. M. J. *J. Controlled Release* **2000**, *65*, 121-131.

(13) Chen, C. Z.; Cooper, S. L. *Polym. Mater. Sci. Eng.* **1999**, *81*, 483-484.

(14) Chen, C. Z.; Beck-Tan, N. C.; Dhurjati, P.; Van Dyk, T. K.; LaRossa, R. A.; Cooper, S. L. *Biomacromolecules* **2000**, *1*, 473-480.

(15) Chen, C. Z.; Cooper, S. L. *Adv. Mater.* **2000**, *12*, 843-846.

(16) Xu, Z.; Ford, W. T. *J. Polym. Sci., Part A: Polym. Chem.* **2003**, *41*, 597-605.

(17) Xu, Z.; Ford, W. T. *Macromolecules* **2002**, *35*, 7662-7668.

(18) de Brabander-van den Berg, E. M. M.; Meijer, E. W. *Angew. Chem.* **1993**, *105*, 1370-1372 .

(19) Fendler, J. H.; Fendler, E. J. *Catalysis in Micellar and Macromolecular Systems*, 1975.

(20) Bunton, C. A.; Savelli, G. *Adv. Phys. Org. Chem.* **1986**, *22*, 213-309.

(21) Bunton, C. A. *Surfactant Sci. Ser.* **1991**, *38*, 13-47.

(22) Kunitake, T.; Okahata, Y.; Ando, R.; Shinkai, S.; Hirakawa, S. *J. Am. Chem. Soc.* **1980**, *102*, 7877-7881.

(23) Ford, W. T.; Tomoi, M. *Advances in Polymer Science* **1984**, *55*, 49-104.

(24) Ford, W. T.; Miller, P. D. *Microspheres, Microcapsules & Liposomes* **2002**, *4*, 171-202.

(25) Bunton, C. A. *Surfactant Sci. Ser.* **1991**, *37*, 323-405.

(26) Newkome, G. R.; Yao, Z.; Baker, G. R.; Gupta, V. K. *J. Org. Chem.* **1985**, *50*, 2003-2004.

(27) Romsted, L. S.; Bunton, C. A.; Yao, J. *Curr. Opin. Colloid Interface Sci.* **1997**, *2*, 622-628.

(28) Bunton, C. A.; Minch, M. J. *Tetrahedron Lett.* **1970**, 3881-3884.

(29) Bunton, C. A.; Minch, M. J.; Hidalgo, J.; Sepulveda, L. *J. Am. Chem. Soc.* **1973**, *95*, 3262-3272.

(30) Rupert, L. A. M.; Engberts, J. B. F. N. *J. Org. Chem.* **1982**, *47*, 5015-5017.

(31) Nusselder, J. J. H.; Engberts, J. B. F. N. *Langmuir* **1991**, *7*, 2089-2096.

(32) Mackay, R. A. *J. Phys. Chem.* **1982**, *86*, 4756-4758.

(33) Menger, F. M.; Elrington, A. R. *J. Am. Chem. Soc.* **1991**, *113*, 9621-9624.

(34) Wang, G.-J.; Engberts, J. B. F. N. *J. Org. Chem.* **1994**, *59*, 4076-4081.

(35) Chaimovich, H.; Cuccovia, I. M. *Prog. Colloid Polym. Sci.* **1997**, *103*, 67-77.

(36) Kunitake, T.; Shinkai, S. *Adv. Phys. Org. Chem.* **1980**, *17*, 435-487.

(37) Germani, R.; Ponti, P. P.; Savelli, G.; Spreti, N.; Cipiciani, A.; Cerichelli, G.; Bunton, C. A. *J. Chem. Soc., Perkin Trans. 2* **1989**, 1767-1771.

(38) Scarpa, M. V.; Araujo, P. S.; Schreier, S.; Sesso, A.; Oliveira, A. G.; Chaimovich, H.; Cuccovia, I. M. *Langmuir* **2000**, *16*, 993-999.

(39) Klotz, I. M. *Ann. N. Y. Acad. Sci.* **1984**, *434*, 302-320.

(40) Fife, W. K. *Trends in Polym. Sci.* **1995**, *3*, 214-221.

(41) Yamazaki, N.; Nakahama, S.; Hirao, A.; Kawabata, J. *Polymer Journal (Tokyo, Japan)* **1980**, *12*, 231-238.

(42) Kunitake, T.; Shinkai, S.; Hirotsu, S. *J. Org. Chem.* **1977**, *42*, 306-312.

(43) Shah, S. C.; Smid, J. *J. Am. Chem. Soc.* **1978**, *100*, 1426-1432.

(44) Ford, W. T.; Yu, H.; Lee, J. J.; El-Hamshary, H. *Langmuir* **1993**, *9*, 1698-1703.

(45) Lee, J. J.; Ford, W. T. *J. Org. Chem.* **1993**, *58*, 4070-4077.

(46) Ford, W. T. *React. Funct. Polym.* **2001**, *48*, 3-13.

(47) Miller, P. D.; Ford, W. T. *Langmuir* **2000**, *16*, 592-596.

(48) Pine, S. H.; Sanchez, B. L. *J. Org. Chem.* **1971**, *36*, 829-832.

(49) Gribble, G. W. *Chem. Soc. Rev.* **1998**, *27*, 395-404.

(50) Gribble, G. W.; Jasinski, J. M.; Pellicone, J. T.; Panetta, J. A. *Synthesis* **1978**, 766-768.

(51) March, J. *Advanced Organic Chemistry 4th Edition*; 4th ed.; Wiley Interscience: New York, 1992.

(52) Rosen, M. J.; Tracy, D. J. *Surfactants Deterg.* **1998**, *1*, 547-554.

(53) Zana, R.; Levy, H.; Papoutsi, D.; Beinert, G. *Langmuir* **1995**, *11*, 3694-3698.

(54) Dam, T.; Engberts, J. B. F. N.; Karthauser, J.; Karaborni, S.; van Os, N. M. *Colloids Surf., A: Physicochemical and Engineering Aspects* **1996**, *118*, 41-49.

(55) Alami, E.; Beinert, G.; Marie, P.; Zana, R. *Langmuir* **1993**, *9*, 1465-1467.

(56) Frindi, M.; Michels, B.; Levy, H.; Zana, R. *Langmuir* **1994**, *10*, 1140-1145.

(57) Zhao, J.; Christian, S. D.; Fung, B. M. *J. Phys. Chem. B* **1998**, *102*, 7613-7618.

(58) Menger, F. M.; Keiper, J. S. *Angew. Chem., Int. Ed. Engl.* **2000**, *39*, 1907-1920.

(59) Newkome, G. R.; Lin, X.; Weis, C. D. *Tetrahedron: Asymmetry* **1991**, *2*, 957-960.

(60) Tomalia, D. A.; Berry, V.; Hall, M.; Hedstrand, D. M. *Macromolecules* **1987**, *20*, 1164-1167.

(61) Hawker, C. J.; Wooley, K. L.; Frechet, J. M. J. *J. Chem. Soc., Perkin Trans. 1* **1993**, 1287-1297.

(62) Kemp, D. S.; Cox, D. D.; Paul, K. G. *J. Am. Chem. Soc.* **1975**, *97*, 7312-7318.

(63) Kemp, D. S.; Paul, K. G. *J. Am. Chem. Soc.* **1975**, *97*, 7305-7312.

(64) Borsche, W. *Ber.* **1909**, *42*, 1310-1318.

(65) Clinton, R. O.; Laskowski, S. C. *J. Am. Chem. Soc.* **1952**, *74*, 2226-2237.

(66) Clinton, R. O.; Laskowski, S. C. *J. Am. Chem. Soc.* **1948**, *70*, 3135-3136.

(67) Murugan, E.; Sherman, R. L., Jr.; Spivey, H. O.; Ford, W. T. *Langmuir* **2004**, *20*, 8307-8312.

Chapter VI

Concluding Remarks

Various nanomaterials have been created using polymers as a unifying theme. These polymers have allowed for dispersion, stability and structure of nanomaterials and they have acted as catalysts.

Semiconductor nanoparticles were stabilized using polymeric thiol ligands. The resulting polymer coated nanoparticles were dispersable in aqueous solvent and due to the attachment of polymeric thiol ligands on the surface, these materials were highly stable after purification. These highly fluorescent nanomaterials showed tunable absorption and emission and were stable at pH ranges of 3-10. The use of poly(cysteine acrylamide) as a ligand for nanoparticle dispersion and stabilization was extremely successful and has potential for stabilization of other nanoparticles.

Nanoparticle/polystyrene latex composites were synthesized in three different ways. Each of these methods has many advantages and disadvantages. Depending on the experimental conditions necessary the correct composite may be chosen.

Core/shell polystyrene/poly(methyl methacrylate) core/shell latexes were formed with a 1:7.5 core shell ratio. This size difference allows for the potential use in dynamic light scattering experiments. The synthesis of these materials was achieved using a starved semi-batch emulsion polymerization. Growth above 800 nm was found to be

impossible due to the low surface area of large latexes. Since growth of massive shells was not possible, a smaller core was chosen to achieve the high core:shell diameter ratio.

Hydrophobic/hydrophilic quaternary ammonium dendrimers were synthesized for use as unimolecular micelles during decarboxylation reactions in water. When dendrimers were quaternized with long dodecyl chains, highly catalytic materials were made. As the chain length grew shorter catalytic rates decreased. It was also found that these amphiphilic quaternary ammonium materials were surface active. The surface activity of these materials was as low as that of Gemini surfactant materials.

VITA

Robert Lee Sherman Jr.

Candidate for the Degree of

Doctor of Philosophy

Thesis: POLYMERIC NANOMATERIALS

Major Field: Chemistry

Biographical:

Personal Data: Born in Mt. Carmel, Illinois on December 24, 1974, son of Robert and Nancy Sherman. Married to Crystal Kirby on July 26, 1997.

Education: Received Bachelor of Science Degree in Chemistry at Southern Illinois University, Carbondale, Illinois in May 1997. Received Masters of Science Degree in Chemistry at Southern Illinois University, Carbondale, Illinois in December 2000. Completed the requirements for the Doctor of Philosophy with a major in Chemistry at Oklahoma State University, Stillwater, Oklahoma in December 2004.

Experience: Laboratory Technician, Central States Analytical, Evansville, Indiana. 1996 and 1997. Teaching Assistant, Southern Illinois University, Carbondale, Illinois 1997-2000. Instructor, Southern Illinois University, Carbondale, Illinois 2000. Teaching Assistant, Oklahoma State University, Stillwater, Oklahoma 2000-2002. Research Assistant, Oklahoma State University, Stillwater, Oklahoma 2000-2004.

Professional Memberships: American Chemical Society, International Union of Pure and Applied Chemistry, Association for the Advancement of Science, Phi Lambda Upsilon Honorary Chemical Society.